# DISSOLVED INORGANIC CARBON IN SOIL AND SHALLOW GROUNDWATER, KONZA PRAIRIE LTER SITE, NE KANSAS, USA

BY

MIKHAIL TSYPIN
B.S., St. Petersburg State University (Russia), 2009

Submitted to the Department of Geology
and the Graduate Faculty of the University of Kansas
in partial fulfillment of the requirements for
the degree of Master of Science
2011

Advisory committee:

_____
Chairperson Gwendolyn L. Macpherson

_____
Luis González

_____
David A. Fowle

Date Defended: 12/02/2011

The Thesis Committee for Mikhail Tsypin
certifies that this is the approved version of the following thesis:

DISSOLVED INORGANIC CARBON IN SOIL AND SHALLOW GROUNDWATER, KONZA PRAIRIE LTER SITE, NE KANSAS, USA

Advisory committee:

_____
Chairperson Gwendolyn L. Macpherson

_____
Luis González

_____
David A. Fowle

Date approved: 12/15/2011

## ABSTRACT

Sources and seasonal trends of dissolved inorganic carbon (DIC) in a shallow limestone aquifer were studied for 1 year at the Konza Prairie LTER (Long-Term Ecological Research) Site in northeastern Kansas, from spring 2010 to spring 2011. Annual cycles of soil air $CO_2$, groundwater DIC, and isotope characteristics showed a strong dependency on weather conditions and soil respiration.

Soil air $CO_2$ reached its annual maximum in the middle of the growing season, when moisture was not limiting to soil respiration. Following the maximum, the $CO_2$ decreased because of moisture deficiency in the late summer and temperature decline in the fall and winter. The decrease began first in the shallowest part of the soil and last in the deepest part. Groundwater $CO_2$ reached its annual maximum in October; this lag-time between the soil and groundwater $CO_2$ maxima of 2–3 months may correspond to the travel time of soil-generated $CO_2$ to the water table.

The time-variable $CO_2$ caused an annual carbonate-mineral saturation cycle, intensifying limestone dissolution, thus soil $CO_2$ and carbonate minerals are the two main sources of DIC in soil and groundwater. The stable carbon isotope composition of soil air $CO_2$ and DIC exhibited primarily $C_4$ plant signature and were similar to that of soil organic matter, suggesting that both root and bacterial respiration are sources of $CO_2$. DIC was enriched in 7–10‰ PDB relative to the $CO_2$ source due to isotope fractionation in a system open to soil $CO_2$; the enrichment was smallest under highest $pCO_2$. For this reason, $\delta^{13}C_{DIC}$ was out of phase with DIC, the lightest in the late growing season.

The carbon flux from the unsaturated zone to the unconfined aquifer during the year was variable depending on respiration and precipitation regimes, and had two main pathways. Transport of soil $CO_2$ in the dissolved form with diffuse flow of recharge water was the most effective during the entire growing season. Downward movement of gaseous $CO_2$ and equilibration with groundwater at the water table was possible in July to August. Storm rainfall events rapidly recharged the aquifer through preferential flow and stream-groundwater interaction. Rather than forcing soil gases downward because of water-saturated pores, the main effect of these events was dilution of groundwater. The calculated flux was about 0.3 $M/m^2/yr$ of C, which is less than 1% of the $CO_2$ that is released by soil to the atmosphere via efflux. However, the climate prediction of increased respiration rates, temperature, and frequency of

extreme rainfall events has the potential to cause higher carbon flux to the saturated zone, intensifying weathering and groundwater acidification.

## ACKNOWLEDGEMENTS

My greatest appreciation is to the scientific advisor and the chairman Dr. Gwendolyn L. Macpherson for patiently guiding me through the fundamentals of geochemistry and secrets of the Prairie, and providing me an access to the research site, lab facilities, and the long-term data record. I would also like to thank the University of Kansas (KU) geology faculty Dr. Luis Gonzales, Dr. David Fowle, and Dr. Randy Stotler for valuable consultations, Greg Cane for the assistance with the lab work and students Rachelle Warren, Michael Robbins, and Carol Fittell for their help with the field work.

The project was supported by KU Department of Geology research grant, KU Field Station grant program, Leo M. and Robert M. Orth Water Resources Grant, and the Konza Prairie LTER Program. Data for AGW01 (groundwater chemistry), APT01 (Konza Prairie precipitation), ASD01 (King's Creek discharge), ASM01 (soil moisture) are supported by the NSF Long Term Ecological Research Program at the Konza Prairie Biological Station.

# TABLE OF CONTENTS

# CHAPTER 1. GENERAL INTRODUCTION

This master thesis is based on the field data collected between March of 2010 and March of 2011 in the Konza Prairie LTER Site, parallel to the long-term monitoring of groundwater at the N04d watershed for the past 20 years. Laboratory analyses were performed in the KU facilities in collaboration with the faculty and staff of the Department of Geology.

This study expands the findings of Macpherson et al., (2008), who reported contentious increasing shallow groundwater $CO_2$ at the Konza Prairie and proposed multiple hypothesis explaining such trend. The purpose of my work was to incorporate measurements of soil air $CO_2$ and use stable isotopes to investigate sources of $CO_2$ and processes affecting its transport. Soil air $CO_2$ could potentially explain the documented seasonal carbonate saturation cycle in groundwater and be a driving force for $pCO_2$ increase in the aquifer. Carbon isotopes could provide insight into the origin of dissolved inorganic carbon (DIC) in the aquifer. In particular this work evaluates the portion of soil-respired $CO_2$ that does not escape to the atmosphere as gas efflux, but moves down to the underlying aquifer, contributing to the groundwater DIC. If downward transport of soil $CO_2$ is significant, then increase of $pCO_2$ in soils due to seasonal elevation of soil respiration rates could result in the same temporal trends in groundwater.

Chapters 2 and 3 describe two different aspects of the thesis work, and appendices provide details and additional data not included in those chapters. Each of chapters 2 and 3 formulates a particular goal and consists of introduction, details on the study site, methods, results, discussion, and conclusions.

Chapter 2 discusses the effect of large precipitation events on $CO_2$ transport from soil to the aquifer. It characterizes the behavior of water level, soil $CO_2$ and soil water and groundwater chemistry following rainfall events, contrasting it with the annual trends. The main mechanisms of downward carbon flux are proposed. An annual flux of carbon from the unsaturated zone to the shallowest aquifer is estimated.

Chapter 3 focuses on variations in sources of shallow groundwater DIC over the sampling year. It shows inorganic carbon transformations in a prairie environment with carbonate bedrock based on year-round sampling of stream, soil, and ground water, and soil gas. Stable carbon isotopes are used to estimate the contribution of carbonates, plants, and SOM to the DIC. Soil air $CO_2$ and DIC isotopic composition variations in time and with belowground depth are characterized. The effect of soil conditions, such as $pCO_2$, temperature, and moisture content, on concentration and isotopic composition of DIC is investigated. The theoretical stable

isotope composition of DIC is modeled using fractionation factors and initial conditions and compared with the measured values to better understand calcite saturation and isotopic equilibration.

The appendices contain details on geology of the site, an expanded description of the methods, tables with the results of the chemical and isotopic analyses, and supplementary materials related to the data interpretation on topics discussed in the chapters.

The results of this study have implications to carbon cycling in prairies with shallow water level and carbonate bedrock, and suggest a prediction of groundwater acidification due to elevated $CO_2$. This study shows additional reasons to consider groundwater as one of the missing sinks for carbon in the global carbon budget.

# CHAPTER 2. THE EFFECT OF LARGE PRECIPITATION EVENTS ON INORGANIC CARBON IN SOIL AND SHALLOW GROUNDWATER, KONZA PRAIRIE LTER SITE, NE KANSAS, USA

## Chapter summary

A 1-year study at the Konza Prairie LTER (Long-Term Ecological Research) Site in northeastern Kansas shows a connection between the annual cycles of $CO_2$ in soil gas and shallow groundwater DIC. Soil air $CO_2$ reached its annual maximum in July to mid-August, when moisture was not limiting to soil respiration. Following the maximum was a sequential decrease in $CO_2$ with soil depth because of moisture deficiency in the late summer and temperature decline in the fall and winter. Groundwater $CO_2$ reached its annual maximum in October; the lag-time of 2–3 months may correspond to the travel time of soil-generated $CO_2$ to the water table. The time-variable $CO_2$ caused an annual carbonate-mineral saturation cycle, intensifying limestone dissolution when $CO_2$ content was high and thus creating an additional source of DIC.

The carbon flux during the year was variable depending on respiration and precipitation regimes, and had two main pathways. Transport of soil $CO_2$ in the dissolved form with diffuse flow of recharge water was the most effective during the entire growing season. Downward movement of gaseous $CO_2$ and equilibration with groundwater at the water table was favorable in July to August. Storm rainfall events rapidly recharged the aquifer through preferential flow and stream-groundwater interaction. Rather than forcing soil gases downward (entrapping $CO_2$) because of water-saturated pores, the main effect of these events was dilution of groundwater.

Calculated carbon flux from the unsaturated zone to the unconfined aquifer was $0.26\pm0.03$ $M/m^2/yr$ of C, which is less than 1% of the $CO_2$ that is released by soil to the atmosphere via efflux. However, increased respiration rates due to warming of the atmosphere have the potential to cause higher carbon flux to the saturated zone, intensifying weathering and groundwater acidification.

# 1. Introduction

The global carbon cycle is one of the most important biogeochemical cycles involving the lithosphere, atmosphere, hydrosphere, and biosphere. Carbon is present in the atmosphere mainly in the form of carbon dioxide and has two major sinks: terrestrial ecosystems (soils and plants) and marine ecosystems (oceans) (White et al., 2000; Fung et. al., 2005). The fundamental problem in estimation of carbon fluxes is an imbalance in atmospheric inputs and outputs of carbon, suggesting that there is an additional unidentified $CO_2$ sink (Sundquist, 1993; Houghton, 2007).

Recent research proposed that there is a possible sink in the global water cycle where carbon is in the form of dissolved inorganic carbon (DIC) (Liu and Zhao, 2000). If assumptions are correct, the water cycle may sequester up to 0.8013 Pg C/yr (28.6% of the missing carbon sink) (Liu et al., 2008). As $CO_2$ dissolves in water, carbonic acid is formed that can dissolve carbonate minerals (e.g. calcite, dolomite) as well as weather aluminosilicate minerals. Weathering of carbonate rocks releases additional carbon into the solution (Cole et al., 2007).

Soils are one of the possible carbon reservoirs in terrestrial environment where $CO_2$ can be involved in the water cycle. Although most of $CO_2$ that is produced in soil escapes to the atmosphere as gas efflux, some $CO_2$ will dissolve in soil water and potentially recharge the underlying aquifer through a flux downward in the unsaturated zone.

Konza Prairie Long-Term Ecological Research (LTER) Site, situated in the northeastern Kansas (Fig. 2.1), is characterized by shallow water-table depth and relatively thick soil, suggesting an important influence of soil gas, moisture, and matrix on groundwater chemistry, while remoteness from croplands limits the impact of agricultural contaminants. Long-term events such as karst processes, erosion, expansion of woody vegetation and short-period perturbations such as extreme storm events or drought are the factors that would significantly affect carbon redistribution belowground. Moreover, 30 years of intensive studies on Konza Prairie LTER project addressed the affects of multiple global change phenomena on the sustainability and dynamics of the grassland ecosystems and created a complex picture of interaction within ecosystems. Water chemistry monitoring of a shallow limestone aquifer at Konza Prairie over a 15-year study period (1991-2005) showed that $pCO_2$ increases in groundwater from two wells, 6 and 12 m deep, are higher (18–36%) than the increase of atmospheric $CO_2$, which was around 7% (Macpherson et al., 2008). At the same time,

groundwater $pCO_2$ cycles annually with maxima during the fall even though soil respiration rates are at a maximum during the growing season (Harper et al., 2005; Hendry et al., 1999). This suggests that there is an indirect link and a lag time between the extrema of $CO_2$ concentrations in soil air and in groundwater that is depth dependent (Macpherson et al., 2008).

Several hypotheses have been proposed to explain increasing belowground $CO_2$ (Table G.1), such as an increasing groundwater residence time, increased atmospheric nitrogen loading (Macpherson et al., 2008), reforestation of prairie areas (Liu et al., 2008), or higher rates of organic matter decomposition (Bond-Lamberty and Thomson, 2010). Most of them consider the importance of increased soil respiration rates. In order to clarify the mechanism of groundwater response on soil $CO_2$ dynamics, details on carbon flux from the unsaturated zone to an aquifer, especially during groundwater recharge, have to be examined.

So far, most estimates show that downward carbon export out of the soil is insignificant: only from 2% (Hendry et al., 1993) to around 4% (Solomon and Cerling, 1987) of the $CO_2$ produced in the vadose zone or 1% of DIC (Andrews and Schlesinger, 2001), 0.17 GtC/y as global flux of DIC (Kessler and Harvey, 2001), was removed by recharge to groundwater. However, according to climate prediction models (McCarthy et al., 2001), the midcontinent temperate climate region of the U.S. may experience increased intensity of precipitation events and larger intervals between events. More extreme rainfall regimes are expected to increase the duration and severity of soil water stress in mesic ecosystems which will affect net primary productivity and soil respiration (Knapp et al., 2008; Fay et al., 2008). In addition, we hypothesize that during extreme precipitation events at Konza Prairie, soil-generated $CO_2$ that dissolves in percolating meteoric water flushing the soil zone will be a part of the recharge to the shallow aquifer. Assuming this mechanism of $CO_2$ transport into the aquifer, increase of $pCO_2$ in soil air due to seasonal elevation of soil respiration rates could result in the same temporal trends in groundwater.

The characterization of variations in $CO_2$ transport with recharge from the soil to the aquifer required a study of water level, soil air $CO_2$ and soil water and groundwater chemistry behavior following rainfall events and contrasting it with the annual trends. It is shown here that extreme precipitation events could initiate downward transport of $CO_2$ via focused flow, diffuse flow, stream-aquifer interactions, or direct gas flux.

# 2. Research site

## 2.1. Location

Konza Prairie LTER Site is situated in NE Kansas, approximately 13 km south the city of Manhattan (39°05'N and 96°35'W) (Fig. 2.1), occupying part of Riley and Geary Counties. The site includes 34 $km^2$ of the northern part of the Flint Hills physiographic province, consisting of more than 60 watersheds. Detailed monitoring of groundwater chemistry and water-table elevation started in 1990 at the 1.2–$km^2$ upland watershed called N04d. It is located on the watershed divide between Deep Creek to the east and the southern portion of McDowell Creek to the south, and Kings Creek, the main stream draining the Konza Prairie LTER Site. Kings Creek empties into McDowell Creek north of the Konza Prairie LTER Site, and is a tributary to the Kansas River.

The South Fork of Kings Creek drains the study watershed. Kings Creek above USGS gauging station 0679650 is entirely contained within the Konza LTER Site, so is minimally affected by humans. The nearest agricultural region, located 5 km away, is separated by a local watershed divide, so contamination of groundwater at the N04d site by agricultural chemicals is highly unlikely (Fig. 2.2). The absolute elevation of the ground surface within the watershed ranges from 427 m on the tops of hills to 364 m at the weir. Hillslopes have gradients of 10-20% and hilltops are flat. Hilltops and hillside benches are formed by more resistant limestone and cherty limestone; shales form slopes.

## 2.2. Climate and vegetation

In this region the variability in both precipitation and temperature is high within and between the years, which is typical for temperate, mid-continental climate (Hayden, 1998). Summer is usually wet and warm, while winter is dry and cold. The average annual air temperature is 13°C with mean January and July ranging between -9 to 3°C and 20 to 33°C, respectively (Nippert and Knapp, 2007a). Average annual total precipitation is 835 mm with 75% falling during the growing season (Hayden, 1998). May and June are the wettest months, although storms can occur almost at any time of year. Annually, Konza Prairie has about 200-300 hours with intense-rainfall thunderstorms (>56 mm/hr) (Hayden, 1998). During the growing season Gulf-of-Mexico-derived moist maritime tropical air coming from the south and southeast

is the dominant source of the precipitation. Non-growing season is characterized by Arctic and continental polar air masses coming from the north and west. Summer rainfall typically arises from thunderstorms associated with fronts and squall lines in the region (Hayden, 1998).

Konza Prairie is located on the western edge of the Midwest tallgrass prairie that extended from Saskatchewan to Texas prior to European settlement (Lauenroth et al., 1994). The vegetation at the site is mesic native tallgrass prairie, dominated by perennial grasses with woody riparian zones. The tallgrass canopy reaches over 2.5 m in height in the most productive years. $C_4$ species are dominant, although the community of $C_3$ species is more diverse (300 species) (Towne, 2002). The most common perennial, warm-season grasses are big bluestem (*Andropogon gerardii*), little bluestem (*A. scoparius*), Indian grass, and switchgrass (*Panicum virgatum*). A highly diverse mixture of other species includes cool-season grasses, composites, legumes, and other forbs. Buckbrush and smooth sumac are the examples of woody species (Freeman, 1998).

## 2.3. Geological setting

Geologic strata are horizontal or dip slightly (about 0.1–0.21° NW) (Smith, 1991). At the N04d watershed, bedrock exposed at the surface and covered by thin Quaternary deposits is composed of Lower Permian couplets of limestone and shale from the Council Grove Group of the Wolfcampian Series (Fig. A.1). The Beattie Limestone is a formation within this group that includes the Morrill Limestone Member (Morrill), the aquifer of interest in the present study. The Morrill is a brownish gray shallow marine limestone with a sharp base and transitional top (Twiss, 1988). It weathers into a mass of irregularly pitted, granular brown limestone without apparent bedding, and the openings that produce the pitted appearance are partly filled with crystalline calcite. This limestone is about 1.2-m thick within the N04d watershed, with the reduced thickness caused by leaching or erosion. The unit, truncated by the Kings Creek, crops out near the studied wells as a broad nickpoint. The Morrill is overlain by the Stearns Shale Member and underlain by the Florena Member, a gray calcareous argillaceous deep-water shale ~3 m thick (Zeller, 1968).

Quaternary deposits overlie the Permian units and include products of bedrock weathering, described generally as alluvium-colluvium. Downstream floodplains are filled with

Holocene fine-grained, light brown, reworked loess. This valley fill contains a discontinuous, chert-gravel lag at the base (Smith, 1991).

## 2.4. Soils

Type of parent rocks (loess, limestone, or shale) and landscape position (hilltops, slopes, footslopes, terraces, and floodplains) determine the characteristics of soil in Konza Prairie (Wehmueller et al., 1993). With the average thickness of 1-2 m, soils are the thickest at the bases of slopes and in valleys (Macpherson et al., 2008) and are almost absent near the stream, where limestone is exposed. Konza Prairie soils are mostly carbonate-poor, with moderately-low cation exchange capacities (mostly less than 40 meq/100 g) (Macpherson et al., 2008). Soils are silty clay loam and silty clay, well drained, 0 to 35% carbonate. At the sampling location soil were diagnosed as Ivan silt loam series (USDA-NRCS, 2007). These relatively deep, moderately well-drained, and moderately permeable soils are developed over colluvium-alluvium and found on foot slopes and valley bottoms. Ivan is classified as a fine-loamy, mixed, mesic Cumulic Hapludoll. The organic carbon content decreases with depth from 6% to less than 1% at 60 cm (Table A.1); the clay content varies from 26 to 39%, silt from 37 to 57 %, and sand and from 7 to 40% (Wehmueller et al., 2005).

## 2.5. Hydrogeology

The 1-to-2-m thick limestone layers and the colluvium-alluvial deposits act as aquifers in Konza Prairie, while thicker shale layers work as aquitards. In the northern part of N04d watershed, sandwich-type neo-karst limestone aquifers include the Morrill Limestone Member of the Beattie Limestone and the upper and lower portions of the Eiss Limestone Member of the Bader Limestone (Macpherson, 1996). Depth to water (thickness of the unsaturated zone) at the study location decreased from ~4 m to ~0 m in the stream. The limestone aquifers exhibit secondary porosity (solution-enlarged joints) (Macpherson et al., 2008). Hydraulic conductivities vary over five orders of magnitude, from about $10^{-8}$ to $10^{-3}$ m/s, as estimated from slug tests (Pomes, 1995). The Morrill Limestone aquifer, like others at the site, is hydraulically linked with South Brach Kings Creek. Unconfined reworked loess aquifers in the floodplain of Kings Creek have low values hydraulic conductivity (of the order of $3 \cdot 10^{-8}$ m/s) (Macpherson and

Sophocleous, 2004). In the N04d watershed, the few wells completed in alluvium have hydraulic conductivities of $10^{-7}$ to $10^{-3}$ m/s (Pomes, 1995).

The chemistry of shallow groundwater in the N04d watershed, regardless of the particular aquifer, is similar. Groundwater chemistry is dominated by $Ca^{2+}$ and $HCO_3^-$ with occasional peaks of $SO_4^{2-}$; in some units $Mg^{2+}$ is higher than in others (Macpherson, 1996). Karst processes, such as soil and bedrock carbonate weathering, are important controls on groundwater pH and alkalinity.

# 3. Methods

## 3.1. Field methods

The experiment took place in the northern part of the N04d watershed at the Konza Prairie LTER Site, where the soil is relatively thick but the water table is shallow. Because of this, the response of groundwater to recharge events was expected to be rapid and the soil signature in water composition was expected to be clear. For this reason, wells 2-4 Mor and 2-5 Mor, situated 20 m away from each other on the floodplain (terrace) and footslope respectively, were selected from a total of 36 observation wells installed between 1988 and 1997 to perform groundwater sampling and water-level monitoring. Most of the sampling site is located within lowland prairie occupied by the grass communities, except 2-4 Mor, located on a floodplain and surrounded by shrubs.

Observation wells are made of 5-cm-diameter PVC pipe. Well 2-5 Mor is 3.66 m deep, being completed in the Morrill Limestone aquifer (Fig. 2.3). Well 2-4 Mor, completed in the same aquifer, is 1.83 m deep. It is located just 5 meters from the stream on the edge of shrubby riparian area, near an outcrop of the Morrill Limestone. In addition to that, data from the well 3-5 Mor located about 200 m upstream from 2-5 Mor was used to compare annual behavior of alkalinity and the water level.

Depth to groundwater was measured in all the wells at least once a month with an electric sounder. In addition, one well at a time was monitored with Solinst® logger set consisting of two similar probes recording pressure, temperature, and the time of measurement. The Levellogger® submerged in the middle part of the water column recorded the hydrostatic pressure and groundwater temperature on 5-minute time interval, while the Barologger® recorded barometric pressure above the water for accurate barometric compensation.

The sampling was performed on a monthly basis. In addition to that, in the summer, the sampling was performed in conjunction with extreme recharge events, defined as heavy and relatively short-duration rains. Wells were bailed with a Teflon® bailer suspended on a Teflon®-coated wire to remove stagnant water prior to water sampling. Collected groundwater was poured into a sampling bottle using a Teflon® bottom emptying device. Samples were stored in a cold place (ice chest in the field; non-frost-free refrigerator in the lab) until water was analyzed.

An array of three soil-water samplers (model 1900, Soil Moisture Equipment Co.) constructed near 2-5 Mor (Fig. 2.3) to access soil water through the vertical profile. A sampler consists of 4.8 cm outside diameter PVC tube with a porous ceramic cup with 2 bar (200 kPa) air-entry value at the bottom and a Santoprene® stopper on the top (Fig. B.3). Neoprene® tubing that is attached to a 1/4-inch diameter access tube is used for connection with a pump. Clamping ring slips over the folded Neoprene® tubing to keep the vacuum. For simplicity, the soil was divided into 3 horizons: A (0-17. 8cm), B (17.8-152.4 cm), and C (>152.4 cm) (Table B.1), so that one soil-water sampler terminated in each layer. To collect samples, water samplers were left under a vacuum of 70–80 centibars until the following sampling event, typically for 1 month. It was presumed that the water had been being collected steadily during the entire period, so that the sample represented the averaged composition of soil water for that interval of time. Even if water was not drawn into the sampler steadily, at least a collected sample represented a composite of times when the soil contained enough moisture to be drawn into the sampler. The collected water was extracted and evacuated with 1/8" OD, 1/32" wall PFA tubing.

Soil gas wells were established at depths of 16, 84, and 152 cm so that the bottom hole of the gas well is at the same level as midpoint of the water sampler's ceramic cup. Each well consists of 5/32" aluminum tube protected with fine mesh at the bottom end to prevent clogging with fine soil particles (Fig. B.4). The top end is equipped with tube for connecting with the pump and sealed with rubber cap to prevent free gas exchange with atmosphere. Prior to sampling, 50-100 mL of gas were withdrawn using a vacuum pump with Tygon® tubing in order to completely evacuate stagnant air from the gas well and from the pump tubing. A 12 ml Exetainer® glass vial was then submerged in a bucket of boiled distilled deionized water and purged with 200 ml of soil gas to displace the water and flush the vial. The vial was then capped under water, sealed with Parafilm®, and stored in a cool place.

### 3.2. Lab methods

Groundwater samples were filtered (0.45 μm) on the day of collection with 25 mm Millex®-HA syringe driven filters (surface area - 3.9 $cm^2$) or peristaltic pump driven Gelman® high-capacity cartridge filter (surface area - 600 $cm^2$).

Alkalinity of water samples was determined by titration with ~0.02 N $H_2SO_4$ at the University of Kansas Aqueous Geochemistry Laboratory (KU AGL). Filtered aliquots (15 - 50 ml) were titrated within two days of sample collection. Concentrations of $Cl^-$, $SO_4^{2-}$, $NO_3$–$N^-$ and $F^-$ were determined at KU AGL by suppressed ion chromatography (IC) with a Dionex 4000i (AG4A-SC and AS4A-SC columns and anion self-regenerating suppressor) on filtered, non-acidified aliquots of 0.6 ml; samples were analyzed within a week of collection. Cations ($Na^+$, $K^+$, $Mg^{2+}$, $Ca^{2+}$, $Sr^{2+}$) and dissolved Si were determined on filtered and weighed aliquots preserved by acidification with $HNO_3$ to a level of 2% v/v within 3 days after collection. Analysis was accomplished using inductively-coupled plasma-optical emission spectroscopy (JY 138 Ultrace ICP-OES) at the University of Kansas Plasma Analytical Laboratory (KU PAL). Charge balances on the analyses, by the method of Fritz (1994), were normally between 1 and 3% and always less than 5%. Concentration of $CO_2$ in the samples of soil gas was measured with an Agilent Technologies 6890N Gas Chromatograph (GC) at the KU Geomicrobiology Lab.

High precision analysis of $^{18}O/^{16}O$ in water samples was performed at the KU PaleoEnvironmental Stable Isotope Lab (KPESIL) using a set of Gas Bench II coupled to MAT 253 mass spectrometer integrated with ThermoFinnigan Temperature Conversion Elemental Analyzers (TC/EA), designed for sample pyrolysis and continuous flow analysis. Oxygen isotope rations of water are reported relative to Vienna Standard Mean Ocean Water (VSMOW) standard (with a precision of better than 0.1‰):

$$\delta^{18}O = \left( \frac{(^{18}O/^{16}O)_{sample}}{(^{18}O/^{16}O)_{SMOW}} - 1 \right) \cdot 1000 \ (‰). \qquad (3.1)$$

# 4. Results

## 4.1. Recharge events and water level

The study period was relatively dry: meteoric precipitation in 2010 was 598 mm, which is approximately 72% of the 30-year mean precipitation rate of 835 mm (Hayden, 1998). 71% of annual precipitation (425 mm) fell in the growing season, from mid-May to mid-October 2010, with June and July being the wettest months (>100 mm/month). In the first three months of 2011 precipitation was 66 mm in the form of snow, rain, or fog. Nine significant rainfall events (> 25.4 mm) occurred over the study period (Table C.1) with relatively uniform distribution over the growing season.

At the Konza Prairie, precipitation is the main source of groundwater recharge. In some wells, water-level rise associated with a separate pulse of recharge can be up to 75 cm (5/6/07, Macpherson, unpublished data), while during extended dry periods water level fluctuates on a daily basis with ~1-cm amplitude (Macpherson et al., 2008).

During 14 years of monthly monitoring, water-table fluctuations in the well 2-5 Mor were mostly less than 10 cm (Fig. C.1), and showed less variability than in other wells completed in the same aquifer. Continuous pressure transducer logging in the summer of 2010 also showed small variability (Fig. 2.4) with very slow recovery (about 1 cm/hr). Water level reached the highest point in July, while in the late winter the well was almost dry.

Water level in 2-4 Mor demonstrated greater variability because of the shallow depth of the well, absence of thick soil, and proximity to the stream. Surprisingly, elevation of the water level in that well, located topographically lower and closer to the stream, was higher than the water levels in 2-5 Mor and 3-5 Mor during the entire study period. In 2-4 Mor, the highest water level was recorded in June and November of 2010, and the lowest level in August of 2010. Higher water level in February 2011 than in January 2011 can be attributed to recharge from snowmelt. Although increasing water-table elevation due to recharge can be attributed to a particular rainfall event, such an increase should not be confused with the slow recovery of water level after bailing or sampling of groundwater (dashed lines on Fig. 2.4).

The degree of the water-level response to precipitation was not uniform over the year (Fig. 2.5). During late April, a rainfall event resulted in a rise in water level in 3-5 Mor (~70 cm in 6 hours) accompanied by the drop in groundwater temperature (Fig. 2.5a). That well also demonstrated almost immediate recovery after bailing, suggesting higher hydraulic conductivity

zone within the aquifer and/or favorable construction of the well screen. Two types of recharge are distinguished within a 3-day period in September (Fig 2.5c): long-term light rain (9/23/10) with slow response of water level (~14 hrs.) and short-term violent rain (9/25/10, intensity up to 61 mm/hr) with rapid response of water level (8 cm in 1.5 hrs.). On the other hand, there was the elevation of the water level following the August storm of the similar intensity because during the mid-growing season infiltration was mainly consumed by the evapotranspiration (Fig. 2.5b).

Soil moisture content was dependent on recent rainfall or snowmelt events, with the highest values in spring to early summer following a general decline (Fig. 2.6) caused by evapotranspiration, with occasional peaks related to separate storm events.

## 4.2. Aqueous chemistry

Groundwater from the Morrill Limestone aquifer had relatively stable major ion chemical composition (Table D.2). Water is calcium-bicarbonate: bicarbonate accounted for more than 90% of anions, while cations were represented primarily by calcium with lesser magnesium (Fig. D.1). The Ca/Mg ratio was between 2 and 5 by mass. Groundwater TDS was 300-400 mg/l with some negative offset related to the dilution by rainwater.

Soil water had much higher TDS due to extremely high $SO_4^{2-}$ and $Mg^{2+}$ content (Table D.3). Samples from the B horizon were characterized by higher concentrations of all major ions compared to the A horizon. Rainwater had very low TDS, less than 100 ppm (2 and 84 ppm), and almost no alkalinity.

The detailed characterization of groundwater chemistry at the site was given in Macpherson (1996) and Gray et al. (1998).

## 4.3. Annual trends

### 4.3.1. Soil $CO_2$

Soil log $pCO_2$ was between –2.8 and –1.1, one to two orders of magnitude higher than atmospheric $pCO_2$. $CO_2$ concentration in soil air increased with depth except July and early August, when the concentration in the B horizon was similar or slightly higher than that in the C horizon (Fig. E.1). Observed temporal trends during the study period suggest annual cyclical patterns in $CO_2$ concentrations for all three horizons (Fig. 2.6). More importantly, there is a lag time in maximum and minimum concentrations between different depths. In the shallowest (A)

horizon, $CO_2$ reached its maximum of 3.5% of soil gas in early July, followed by the approximately two times higher peaks in the B and C horizons in late July and early August, respectively. After the annual maximum, $CO_2$ content decreased smoothly to less than 1% in the winter months in all three soil horizons, so that $CO_2$ distribution thorough the profile was more uniform.

### 4.3.2. Carbonate saturation

The annual alkalinity cycle in groundwater was in agreement with previous long-term observations of the Morrill Limestone aquifer at this site (Macpherson et al., 2008). In 2-5 Mor alkalinity was as low as 4.24 mmol/L in March, increased through the growing season and reached a maximum of 7.74 mmol/L in early fall. In mid-summer, alkalinity briefly decreased by 1.7 mmol/L because of the biggest storm event in early July, and then recovered slowly to the expected values as predicted by the annual trend by the end of August (Fig. 2.7). Groundwater alkalinity in the samples from 2-4 Mor obtained in the fall of 2010 and the spring of 2011 had similar alkalinity to that in 2-5 Mor. At the same time, alkalinity of groundwater from 3-5 Mor was, at the average, 1 mmol/L lower than that from 2-5 Mor and it reached its annual peak 1-2 months earlier. Streamwater alkalinity followed the same pattern through time and also showed light rain-dilution effect. The values were closer to those for 3-5 Mor.

Equilibrium with $CO_2$ from the soil horizon C, situated less than 2 m above the water table, or with calcite that is usually near saturation (Macpherson et al., 2008), was assumed to estimate pH for each 2-5 Mor sample because low well yield precluded measuring downhole pH or pumping through a flow-through cell. Estimated pH decreased during the growing season from slightly alkaline to neutral and slightly acidic values (Fig. 2.8). After reaching a minimum in October, pH started to increase until March. Because the pH was circumneutral, $HCO_3^-$ accounted for 80-90% of the DIC in groundwater all year long. Measured soil water pH was slightly acidic and increased with depth, demonstrating evolution of recharge water from acidic rainwater to neutral groundwater as it saturates with soil $CO_2$ and dissolves soil carbonate.

Saturation indexes (SI) of calcite and dolomite in groundwater, defined as:

$$SI=\log(IAP/K_{sp}), \qquad (4.1)$$

where IAP is ion activity product, increased during the growing season but exceeded saturation only in the winter (Fig. 2.8d). These results are consistent with log $SI_{calcite}$, log $SI_{dolomite}$, and pH annual cycles, inverse to dissolved solids and $pCO_2$, modeled for 3-5 Mor and 4-6 Mor by

Macpherson et al. (2008). There was a short-term drop in carbonate-mineral SI's in July following the storm events, because recharge water was even more undersaturated with respect to carbonates. The trend in calcite saturation index over the year is reflected in the seasonal trend in $Ca^{2+}$ concentration, the main source of which is calcite dissolution. During the growing season, $Ca^{2+}$ concentration in 2-5 Mor changed from 1.9 mmol/L to 2.6 mmol/L, while $Mg^{2+}$ content remained relatively stable (Table D.6). Calculated $pCO_2$ for groundwater (assuming equilibrium with calcite) remained less than that of soil gas until the fall; maximum $pCO_2$ occurred 2-3 months later, in October (Fig. 2.6c).

Oxygen isotopes in groundwater and soil water had values between −6 and −7‰ VSMOW (Fig. 2.7b), which is similar to what was measured in other wells and the stream over the last 5 years (Nippert and Knapp, 2007b, Macpherson, unpublished data) and within the greater range of $\delta^{18}O$ variations in precipitation (Coplen and Kendall, 2000). There was a 1–2‰ depletion in $^{18}O$ with increasing belowground depth that might be explained by near-surface enrichment of soil water due to evapotranspiration (Hsieh et al., 1998).

# 5. Discussion

## 5.1. Soil $CO_2$

$CO_2$ concentration in soil air has been traditionally attributed to the co-occurrence of three processes: soil respiration, diffusive loss to the atmosphere, and uptake by the aqueous phase (Reardon et al., 1979). Soil respiration includes microbial oxidation of stable soil organic matter by heterotrophs and rhizosphere respiration that represents the sum of root respiration and microbial respiration of labile carbon derived from live roots (Lin et al., 1999; Badalucco and Nannipieri, 2007). Rainfall determines the soil water content available for biological respiration and the air-filled pore spaces available for $CO_2$ flux (Ouyang and Zheng, 2000). In contrast, solar radiation governs water evaporation. The respiration rate in dry soil usually accelerates to a very high level after rainfall due to metabolic activity increases (Luo and Zhou, 2006), and thus soil $CO_2$ production and efflux increase in response to water addition (Liu, 2002; Wan et al., 2007). High production rate of $CO_2$ in soil can cause additional input of $CO_2$ to groundwater. On the other hand, when soils are 50–80% saturated, moisture has little effect since biological activity is at or near its maximum potential. When soils are water saturated, oxygen deficiencies inhibit aerobic respiration (Raich and Potter, 1995).

At the Konza Prairie, the seasonal cycle of $CO_2$ in the soil air was similar to that of soil and atmospheric temperature (Fig. 2.6c) and also dependent on moisture content (Fig. 2.6a, b) and photosynthetic production. In this ecosystem it has been demonstrated that moisture is a limiting factor for soil respiration in summer, while temperature became limiting in winter (Luo and Zhou, 2006). In the present study, soil air $CO_2$ concentrations started increasing early in the growing season, reached the maximum in mid-summer when net primary productivity was the highest, and started decreasing in mid-July to early August because of the drying of the soil and later in the fall and winter - due to the temperature decline. The concentration depth gradient is the result of the slow upward movement of $CO_2$ from sources of production towards the surface via diffusion and mass flow (Luo and Zhou, 2006). This gradient was negative, since the $CO_2$ content in atmosphere is about 0.03% whereas in soil air it was 1–2 orders of magnitude higher and usually increased with depth. In winter months the concentration gradient was smoother because soil air $CO_2$ content dropped due to lower respiration rates. This pattern of increase with depth was altered on 7/15/10 and 7/29/10 samples, when $CO_2$ concentration in the B horizon was higher than that in the C horizon, suggesting downward movement of gaseous $CO_2$ towards the water table via diffusion (Reardon et al., 1979). This downward $CO_2$ gradient might be the consequence of infiltration after intense storms in the early July or because groundwater $pCO_2$ was smaller than that in the soil horizon C.

As noted above, during the sampling period, $CO_2$ concentration reached the maximum in the A horizon first and the C horizon last. The same trend was observed for $CO_2$-concentration minima. These temporal patterns can be explained by moisture-limited respiration. The ground wets and dries from the surface downward, and so respiration rate at shallow depths should respond to water perturbations first. In addition, a decrease in $CO_2$ production might be initiated when moisture went below a threshold value, at the field site observed to be about 340 $kg/m^3$. Similar time lag in soil horizon $CO_2$ peaks was previously observed in unsaturated zones in Saskatchewan and Washington (Wood et al., 1993; Hendry et al., 1999; Keller and Bacon, 1998). The temperature effect on soil respiration at the field site was less significant in the summer because the limit imposed by seasonal cooling occurred later than the limit imposed by low moisture. It has been shown that elevated air temperature under low moisture conditions is not controlling or even tends to decrease soil respiration over the growing season at several sites (Carlyle and Ba Than, 1988; Wan et al., 2007), including Konza Prairie (Harper et al. 2005). At

the field site, an increase in soil moisture in the fall and winter did not affect respiration and $CO_2$ concentration in soil air, because the seasonal decline of atmospheric and soil temperature became the more important factor.

## 5.2. The role of recharge events in $CO_2$ transport to groundwater

Meteoric precipitation could 1) saturate soil, reducing soil gas efflux (Brady and Weil, 2008), forcing soil gas downward, and slowly recharging groundwater; 2) bypass the soil matrix by following macropores directly to the water table (Beven and Germann, 1982, Macpherson and Sophocleous, 2004) resulting in no involvement of soil gas with groundwater recharge and rapid aquifer water-level response; or 3) become surface runoff to streams where stream stage could temporarily be higher than head in a connected aquifer, resulting in stream recharge to groundwater. All three types of recharge occur at this site.

Rapid communication between water on the surface and groundwater at the study site is supported by observations of water level and water temperature changes within a few hours after precipitation events, and explained by fractures in limestone and cracks in soil that permit rapid infiltration of precipitation (Macpherson et al., 2008). We observed similar fast response in water level and water temperature changes, especially during the non-growing season or very early or very late in the growing season (Fig. 2.6a, b), supporting macropore or fast-path recharge. Despite the fact that most precipitation falls from April to November, groundwater recharge during this time is the lowest (Fig. 2.4b), most likely because, during this time period, temperatures were high and plant growth was active, so that evapotranspiration consumed most of the precipitation, reducing groundwater recharge. Non-growing season precipitation can result in slow groundwater-level response as well (Fig. 2.6c).

Water-level elevations suggested that apparent hydraulic gradient was decreasing with distance from the stream during the period from May to December 2010 (Fig. 2.4b). Moreover, in March-July of 2010 there was a good agreement between Kings Creek discharge and the water level (Fig. 2.4b, c). In that period the watershed was wet and storm events caused flooding because of the low infiltration capacity of wet soils and steep slopes (Gray et al., 1998). Surface runoff from the entire watershed easily reached South Branch of Kings Creek, the stream flow increased rapidly and recharged the aquifer. In winter, when water table dropped below the

stream bed, precipitation events did not contribute to the stream discharge, saturating groundwater first (Fig. 2.7c).

The Morrill Limestone aquifer is in contact with the soil and should be sensitive to $CO_2$ variations in the unsaturated zone. Being the shallowest aquifer, it was expected to have a rapid response to large recharge events reflected in water-table elevation and water composition. However large storms that happened on July of 2010 did not increase groundwater DIC, as a result of soil zone flush. Conversely, dilution resulted in the drop of TDS and alkalinity (Fig. 2.7c, d). This suggests rapid recharge through fissures and cracks in soil, such that recharge water did not equilibrate with soil air $CO_2$ and did not entrap it.

## 5.3. Carbon flux to groundwater

DIC can be produced in the aquifer via dissolution of carbonate rocks and oxidation of organic matter. A transport of carbon from the outside requires a flow of fluid (gas or water). Typical pathways are downward $CO_2$ transport from soil in the dissolved (Kessler and Harvey, 2001) or gaseous form (Appelo and Postma, 2005), upward flux of deep $CO_2$ of various origins through gas vents (Chiodini et al., 1999) or leakage from adjacent aquifers with higher DIC concentration.

So far, there is no evidence of a "deep" source of $CO_2$ such as leakage from underlying aquifers, volcanic activity, or hydrocarbon deposits. Shallow gas deposits (<1 km deep) of the Forest City basin and Nemaha Uplift of northeastern Kansas contain $CO_2$ concentrations up to 0.035% (Jenden et al., 1988). $CO_2$ from the oxidation of organic matter would not be a significant source of DIC to the aquifer if it is not continuously generated (McMahon and Chapelle, 1991), and dissolved organic carbon content in the Morrill aquifer is generally less than 1 mg/L (Pomes, 1995). DIC in precipitation is also very low. Thus, the two main sources of DIC are soil $CO_2$, discussed above, and dissolution of carbonate minerals in the aquifer and in the soil, that is enhanced by the presence of $CO_2$.

Similar trends in $pCO_2$ were noted in soil and groundwater at the field site (Fig. 2.6c), suggesting that seasonal trends must be considered when explaining $CO_2$ transport from soil to the aquifer. Highest soil respiration rates were measured in July-August while maximum $pCO_2$ in groundwater was measured in September-October.

The pulse scenario requires a storm event that induces a flush of a large amount of $CO_2$ accumulated in the soil during the summer season. However there were no big storms between $CO_2$ maximas in soil air and groundwater. A downward flux of gaseous $CO_2$ was favorable during the growing season when the amount of $CO_2$ in equilibrium with groundwater above the water table was lower than in the soil C horizon. Beginning in September, the gradient changed to upward, and after that the most realistic scenario was the movement of $CO_2$ in the dissolved form via diffuse flow that was formed during extensive rainfalls in June-July. In this case, an increase of alkalinity with depth (soil horizon A, B, and groundwater) might be better explained by greater residence time and increase in $CO_2$ concentrations reacting with water. Therefore, for slow uniform migration of the gas front, it takes about 2 months for soil $CO_2$ to be delivered to the aquifer, assuming that the high $pCO_2$ in groundwater is caused by high respiration rates of the same year. This assumption can be verified looking at the interannual variability. Some similarities were found between wet years with high groundwater alkalinity (1998) and between burn years that cause a peak in NPP and high alkalinity (1994). A comparable lag-time (0.5 to 2 months) was also noted between the peaks of groundwater level and dissolved oxygen pulse from reworked loess to the groundwater at a different location at the same research site (Macpherson and Sophocleous, 2004).

Since gas efflux is the dominant process for $CO_2$ removal from the soil, only a small portion of soil-generated $CO_2$ can be delivered to the saturated zone. Transport in the dissolved form was also limited by the low soil moisture during the dry season. So far, most estimates for DIC transport in soil water show that only 2 to 4% of the $CO_2$ produced in the vadose zone is carried to groundwater (Hendry et al., 1993; Solomon and Cerling, 1987). In this study, calculated flux of carbon dissolved in soil water from unsaturated zone to Morrill Limestone aquifer was 0.26±0.03 M/$m^2$/yr of C, based on the modeled recharge rate of 69-83 mm/yr for Tully/Ivan soil series (Steward et al., 2011) and average alkalinity of 6.7 mmol/l, assuming that only half of it originated from soil. This flux is only 0.25±0.03% of the flux from soil to atmosphere of 4.92 kg $CO_2$□/□$m^2$/d (Bremer and Ham, 2002).

Measured values and the annual behavior of surface water alkalinity were comparable to that of groundwater. Storm events contributed to the surface flow that delivered the most significant pulses of recharge in the spring and summer of 2010. However, a carbon flux during such events was reduced because storm recharge was very diluted. Some DIC might be produced

through the reaction of carbonate with atmospheric $CO_2$ or organic/sulfuric acids (Aucour et al., 1999; Kanduk et al., 2007). Conditions for groundwater discharge were favorable in the fall and winter, mostly upstream from the sampling location: the perennial pool was filled with water even in the driest period. Streamwater $pCO_2$ was the highest at that location and it decreased downstream together with pH rise due to outgassing, although remaining much higher than atmospheric (Ohmes et al., 2009), as is typical for streams (Butman and Raymond, 2011). Most likely, the source of DIC was groundwater discharge, which has been identified for other streams (Doctor et al., 2008). According to the gradients identified from the groundwater potentiometric surface, partially degassed water could then re-enter the aquifer downstream, resulting in apparent carbon loss in the groundwater.

Whether $CO_2$ is transported to the saturated zone at the study site in a gaseous form or dissolved in soil or stream water, the rates of root respiration and degradation of organic matter should affect carbonate saturation not on a yearly basis alone, but also on a larger time scale. It has been shown that $pCO_2$ was constantly increasing in the Morrill aquifer over a 15-year study period (Macpherson et al., 2008). Considering the proposed sources of groundwater DIC, an increased flux of soil $CO_2$ to the aquifer should be an initial driving factor for such long-term changes in water chemistry. Higher rates of soil respiration due to increase in temperature have been identified on a global scale (Bond-Lamberty and Thomson, 2010). Furthermore, Free-Air $CO_2$ Enrichment (FACE) experiments modeled elevated $CO_2$ on the respiration dynamics in soil and concluded that it could result in higher rates of chemical weathering that will increase a carbon flux to groundwater and acidify it (Andrews and Schlesinger, 2001; Cheng et al., 2010). Also at a FACE site, belowground $CO_2$ was shown to have increased in response to the imposed higher atmospheric $CO_2$ in the experiment (Jackson et al., 2009). On the other hand, warming of the climate may affect temperatures of groundwater and reduce the solubility of calcite. A coupled long-term monitoring of soil-respiration and groundwater $CO_2$ may help clarify the interactions between the two.

## 6. Conclusions

Seasonal trends of soil air $CO_2$ and DIC in a shallow limestone aquifer and their response to storm events were studied at the N04d watershed in the Konza Prairie LTER Site from spring 2010 to spring 2011.

Soil temperature and moisture content control distribution of $CO_2$ in soil both with depth and during the season. Soil air $CO_2$ concentrations reached the maximum in July to early August, when moisture was not limiting soil respiration, and gradually decreased until March because moisture deficiency sequentially affected $CO_2$ production in the A, B, and C horizons in the summer, and temperature inhibited microbial activity in the winter.

A flux of carbon during the year was variable depending of respiration and precipitation regimes and had two main pathways. Transport of soil $CO_2$ in the dissolved form with diffuse flow of recharge water was the most effective during the growing season. Downward movement of gaseous $CO_2$, followed by equilibration with groundwater at the water table was favorable in July to August. The main restriction of such mechanism is recharge water availability in the warmest period, when evapotranspiration consumed most of the precipitation, reducing groundwater recharge. Soil $CO_2$ delivered to the saturated zone intensified calcite dissolution, an additional source of DIC, and thus the annual carbonate saturation cycle was similar to the soil respiration cycle. A lag-time of 2-3 months between peaks in soil and groundwater may correspond to the time for $CO_2$-saturated recharge water to reach the shallowest aquifer with a wetting front.

Two other mechanisms that were considered have significant limitations. Recharge from the stream was possible in May-December, however there is a net carbon loss from baseflow that result in a decrease in groundwater $CO_2$. Storm rainfall events rapidly recharged the aquifer through preferential flow and stream-groundwater interaction. However the main effect of such events was dilution of groundwater rather than soil zone flush with $CO_2$ entrapping.

Calculated flux of carbon from unsaturated zone to the unconfined aquifer was 0.26±0.03 $M/m^2/yr$ of C, which is less than 1% of the $CO_2$ that is released by soil to the atmosphere via efflux. Previous investigations showed groundwater $pCO_2$ has been rising in Konza Prairie over the last 15 years (Macpherson et al., 2008). A coupled long-term monitoring of soil and groundwater $CO_2$ may show that increased respiration rates due to warming of the atmosphere could result in higher carbon flux to the saturated zone intensifying weathering and groundwater acidification.

## References


Andrews, J.A., Schlesinger, W.H., 2001. Soil $CO_2$ dynamics, acidification, and chemical weathering in a temperate forest with experimental $CO_2$ enrichment. Global Biogeochem. Cycles 15, 149-162.

Appelo, C.A.J.P., D., 2005. Geochemistry, Groundwater, and Pollution, 2nd ed. Balkema, Rotterdam.

Aucour, A.-M., Sheppard, S.M.F., Guyomar, O., Wattelet, J., 1999. Use of $^{13}C$ to trace origin and cycling of inorganic carbon in the Rhône river system. Chemical Geology 159, 87-105.

Badalucco, L., Nannipieri, P., 2007. Nutrient Transformations in the Rhizosphere, in: Pinton, R., Varanini, Z., Nannipieri, P. (Eds.), The Rhizosphere, 2 ed. CRC Press, pp. 111-133.

Beven, K., Germann, P., 1982. Macropores and water flow in soils. Water Resour. Res. 18, 1311-1325.

Bond-Lamberty, B., Thomson, A., 2010. Temperature-associated increases in the global soil respiration record. Nature 464, 579-582.

Brady, N.C., Weil, R.R., 2008. The Nature and Properties of Soils, 14 ed. Pearson-Prentice Hall, Upper Saddle River, NJ.

Bremer, D.J., Ham, J.M., 2002. Measurement and modeling of soil $CO_2$ flux in a temperate grassland under mowed and burned regimes. Ecological Applications 12, 1318-1328.

Butman, D., Raymond, P.A., 2011. Significant efflux of carbon dioxide from streams and rivers in the United States. Nature Geosciense advance online publication.

Carlyle, J.C., Than, U.B., 1988. Abiotic Controls of Soil Respiration Beneath an Eighteen-Year-Old Pinus Radiata Stand in South-Eastern Australia. Journal of Ecology 76, 654-662.

Cheng, L., Zhu, J., Chen, G., Zheng, X., Oh, N.H., Rufty, T.W., Richter, D.d., Hu, S., 2010. Atmospheric $CO_2$ enrichment facilitates cation release from soil. Ecology Letters 13, 284-291.

Chiodini, G., Frondini, F., Kerrick, D.M., Rogie, J., Parello, F., Peruzzi, L., Zanzari, A.R., 1999. Quantification of deep $CO_2$ fluxes from Central Italy. Examples of carbon balance for regional aquifers and of soil diffuse degassing. Chemical Geology 159, 205-222.

Cole, J.J., Prairie, Y.T., Caraco, N.F., McDowell, W.H., Tranvik, L.J., Striegl, R.G., Duarte, C.M., Kortelainen, P., Downing, J.A., Middelburg, J.J., Melack, J., 2007. Plumbing the global carbon cycle: Integrating inland waters into the terrestrial carbon budget. Ecosystems 10, 172-185.

Coplen, T.B., Kendall, C., 2000. Stable hydrogen and oxygen isotope ratios for selected sites of the U.S. Geological Survey's NASQAN and Benchmark surface-water networks. US Geological Survey Open-File Report 00-160, p. 424.

Doctor, D.H., Kendall, C., Sebestyen, S.D., Shanley, J.B., Ohte, N., Boyer, E.W., 2008. Carbon isotope fractionation of dissolved inorganic carbon (DIC) due to outgassing of carbon dioxide from a headwater stream. Hydrological Processes 22, 2410-2423.

Fay, P.A., Kaufman, D.M., Nippert, J.B., Carlisle, J.D., Harper, C.W., 2008. Changes in grassland ecosystem function due to extreme rainfall events: implications for responses to climate change. Global Change Biology 14, 1600-1608.

Freeman, C.C., 1998. The flora of Konza Prairie: a historical review and contemporary patterns, in: Knapp, A.K., Briggs, J.M., Hartnett, D.C., Collins, S.L. (Eds.), Grassland Dynamics – Long-Term Ecological Research in Tallgrass Prairie. Oxford University Press, New York, pp. 69-80.

Fritz, S.J., 1994. A Survey of Charge-Balance Errors on Published Analyses of Potable Ground and Surface Waters. Ground Water 32, 539-546.

Fung, I.Y., Doney, S.C., Lindsay, K., John, J., 2005. Evolution of carbon sinks in a changing climate. Proceedings of the National Academy of Sciences of the United States of America 102, 11201-11206.

Gray L. J., M.G.L., Koelliker J. K. and Dodds W. K., 1998. Hydrology and aquatic chemistry, in: Knapp, A.K., Briggs, J.M., Hartnett, D.C., Collins, S.L. (Eds.), Grassland Dynamics – Long-Term Ecological Research in Tallgrass Prairie. Oxford University Press, New York, pp. 159-176.

Harper, C.W., Blair, J.M., Fay, P.A., Knapp, A.K., Carlisle, J.D., 2005. Increased rainfall variability and reduced rainfall amount decreases soil $CO_2$ flux in a grassland ecosystem. Global Change Biology 11, 322-334.

Hayden, B., 1998. Regional climate and the distribution of tallgrass prairie, in: Knapp, A.K., Briggs, J.M., Hartnett, D.C., Collins, S.L. (Eds.), Grassland Dynamics – Long-Term Ecological Research in Tallgrass Prairie Oxford University Press, New York, pp. 19–34.

Hendry, M.J., Lawrence, J.R., Zanyk, B.N., Kirkland, R., 1993. Microbial production of $CO_2$ in unsaturated geologic media in a mesoscale model. Water Resour. Res. 29, 973-984.

Hendry, M.J., Mendoza, C.A., Kirkland, R.A., Lawrence, J.R., 1999. Quantification of transient $CO_2$ production in a sandy unsaturated zone. Water Resour. Res. 35, 2189-2198.

Houghton, R.A., 2007. Balancing the Global Carbon Budget. Annual Review of Earth and Planetary Sciences 35, 313-347.

Hsieh, J.C.C., Chadwick, O.A., Kelly, E.F., Savin, S.M., 1998. Oxygen isotopic composition of soil water: Quantifying evaporation and transpiration. Geoderma 82, 269-293.

Jackson, R.B., Cook, C.W., Pippen, J.S., Palmer, S.M., 2009. Increased belowground biomass and soil $CO_2$ fluxes after a decade of carbon dioxide enrichment in a warm-temperate forest. Ecology 90, 3352-3366.

Jenden, P.D., Newell, K.D., Kaplan, I.R., Watney, W.L., 1988. Composition and stable-isotope geochemistry of natural gases from Kansas, Midcontinent, U.S.A. Chemical Geology 71, 117-147.

Kanduč, T., Szramek, K., Ogrinc, N., Walter, L.M., 2007. Origin and Cycling of Riverine Inorganic Carbon in the Sava River Watershed (Slovenia) Inferred from Major Solutes and Stable Carbon Isotopes. Biogeochemistry 86, 137-154.

Keller, C.K., Bacon, D.H., 1998. Soil respiration and georespiration distinguished by transport analyses of vadose $CO_2$, $^{13}CO_2$, and $^{14}CO_2$. Global Biogeochem. Cycles 12, 361-372.

Kessler, T.J., Harvey, C.F., 2001. The global flux of carbon dioxide into groundwater. Geophys. Res. Lett. 28, 279-282.

Knapp, A.K., Beier, C., Briske, D.D., Classen, A.T., Luo, Y., Reichstein, M., Smith, M.D., Smith, S.D., Bell, J.E., Fay, P.A., Heisler, J.L., Leavitt, S.W., Sherry, R., Smith, B., Weng, E., 2008. Consequences of More Extreme Precipitation Regimes for Terrestrial Ecosystems. BioScience 58, 811-821.

Lauenroth, W.K., Milchunas, D.G., Dodd, J.L., Hart, R.H., Heitschmidt, R.K. & Rittenhouse, L.R., 1994. Effects of grazing on ecosystems of the Great Plains, in: Vavra, M., Laycock, W.A., Pieper, R.D. (Eds.), Ecological implications of livestock herbivory in the West. Society for Range Management, Denver, CO, pp. 69-100.

Lin, G., Ehleringer, J.R., Rygiewicz, P.T., Johnson, Mark G., Tingey, David T., 1999. Elevated $CO_2$ and temperature impacts on different components of soil $CO_2$ efflux in Douglas-fir terracosms. Global Change Biology 5, 157-168.

Liu, X., Wan, S., Su, B., Hui, D., Luo, Y., 2002. Response of soil $CO_2$ efflux to water manipulation in a tallgrass prairie ecosystem. Plant and Soil 240, 213-223.

Liu, Z., Dreybrodt, W., Wang, H., 2008. A possible important $CO_2$ sink by the global water cycle. Chinese Science Bulletin 53, 402-407.

Liu, Z., Zhao, J., 2000. Contribution of carbonate rock weathering to the atmospheric $CO_2$ sink. Environmental Geology 39, 1053-1058.

Luo, Y., Zhou, X., 2006. Soil Respiration and the Environment. Academic Press, Burlington.

Macpherson, G.L., 1996. Hydrogeology of thin limestones: the Konza Prairie Long-Term Ecological Research Site, Northeastern Kansas. Journal of Hydrology 186, 191-228.

Macpherson, G.L., Roberts, J.A., Blair, J.M., Townsend, M.A., Fowle, D.A., Beisner, K.R., 2008. Increasing shallow groundwater $CO_2$ and limestone weathering, Konza Prairie, USA. Geochimica et Cosmochimica Acta 72, 5581-5599.

Macpherson, G.L., Sophocleous, M., 2004. Fast ground-water mixing and basal recharge in an unconfined, alluvial aquifer, Konza LTER Site, Northeastern Kansas. Journal of Hydrology 286, 271-299.

McCarthy J, C.O., Leary N, Dokken D, White K, 2001. Climate Change 2001: Impacts, Adaptation, and Vulnerability. Contribution of Working Group II to the Third Assessment Report of the Intergovernmental Panel on Climate Change., Cambridge.

McMahon, P.B., Chapelle, F.H., 1991. Geochemistry of dissolved inorganic carbon in a Coastal Plain aquifer. 2. Modeling carbon sources, sinks, and $\delta^{13}C$ evolution. Journal of Hydrology 127, 109-135.

Nippert, J.B., Knapp, A.K., 2007. Soil water partitioning contributes to species coexistence in tallgrass prairie. Oikos 116, 1017-1029.

Ohmes, K.S., Macpherson, G.L., and Huff, Breanna L., 2009. Low stream-flow measurement and stream $CO_2$ emission calculation, Konza Prairie LTER site, Northeastern Kansas, USA, Geological Society of America Abstracts with Programs, p. 664.

Ouyang, Y., Zheng, C., 2000. Surficial processes and $CO_2$ flux in soil ecosystem. Journal of Hydrology 234, 54-70.

Peterson, D.L., Whistler, J.L., Egbert, S.L., Martinko, E.A., 2010. 2005 Kansas Land Cover Patterns Phase II: Final Report. KBS Report #167. Kansas Biological Survey, University of Kansas, p. 49.

Pomes, M.L., 1995. A study of the aquatic humic substances and hydrogeology in a prairie watershed, use of humic material as a tracer of recharge through soils. Ph.D. thesis, University of Kansas, p. 296.

Raich, J.W., Potter, C.S., 1995. Global patterns of carbon dioxide emissions from soils. Global Biogeochem. Cycles 9, 23-36.

Reardon, E.J., Allison, G.B., Fritz, P., 1979. Seasonal chemical and isotopic variations of soil $CO_2$ at Trout Creek, Ontario. Journal of Hydrology 43, 355-371.

Smith, G.N., 1991. Geomorphology and geomorphic history of Konza Prairie Research Natural Area, Riley and Geary counties, Kansas. Unpublished MS thesis, Kansas State University, Manhattan, KS, p. 122.

Solomon, D.K., Cerling, T.E., 1987. The annual carbon dioxide cycle in a montane soil: Observations, modeling, and implications for weathering. Water Resour. Res. 23, 2257-2265.

Steward, D.R., Yang, X., Lauwo, S.Y., Staggenborg, S.A., Macpherson, G.L., Welch, S.M., 2011. From precipitation to groundwater baseflow in a native prairie ecosystem: a regional study of the Konza LTER in the Flint Hills of Kansas, USA. Hydrol. Earth Syst. Sci. Discuss. 8, 4195-4228.

Sundquist, E.T., 1993. The Global Carbon Dioxide Budget. Science 259, 934-941.

Towne, E.G., 2002. Vascular plants of Konza Prairie Biological Station: an annotated checklist of species in a Kansas tallgrass prairie. Sida 20, 269-294.

Twiss, P.C., 1988. Beattie Limestone (Lower Permian) of eastern Kansas, in: Hayward, O.T. (Ed.), G.S.A. Centennial Field Guide Volume 4, South-Central Section of the Geological Society of America. Geol. Soc. Am., pp. 35-41.

Wan, S., Norby, R.J., Ledford, J., Weltzin, J.F., 2007. Responses of soil respiration to elevated $CO_2$, air warming, and changing soil water availability in a model old-field grassland. Global Change Biology 13, 2411-2424.

Wehmueller, W.A., Campbell, H.V., Hamilton, V.L., Graber, S.P., 2005. Soil survey of Geary County, Kansas: U.S. Dept. of Agriculture, Natural Resources Conservation Service, p. 230.

Wehmueller, W.A., Ransom, M.D., Nettleton, W.D., 1993. Micromorphology of polygenetic soils in a small watershed, north central Kansas, U.S.A, in: Ringrose-Voase, A.J., Humphreys, G.S. (Eds.), Developments in Soil Science. Elsevier, pp. 247-255.

White, A., Cannell, M.G.R., Friend, A.D., 2000. $CO_2$ stabilization, climate change and the terrestrial carbon sink. Global Change Biology 6, 817-833.

Wood, B.D., Keller, C.K., Johnstone, D.L., 1993. In situ measurement of microbial activity and controls on microbial $CO_2$ production in the unsaturated zone. Water Resour. Res. 29, 647-659.

U.S. Department of Agriculture, National Resources Conservation Service (USDA-NRCS), 2007. http://websoilsurvey.nrcs.usda.gov/app/WebSoilSurvey.aspx.

Zeller, D.E., ed., 1968. The stratigraphic succession in Kansas: Kansas Geol. Survey Bull. 189, p. 81.

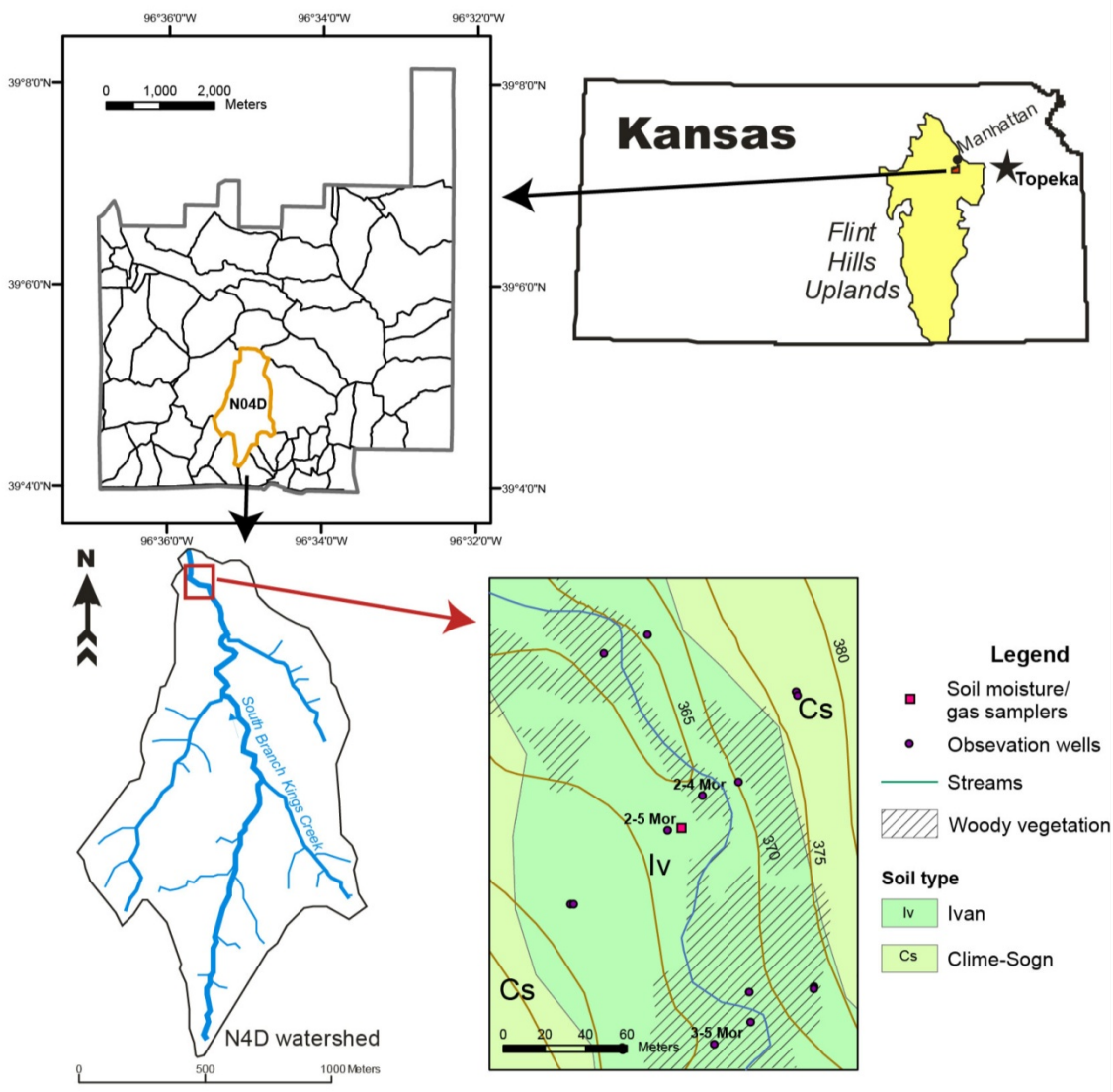


Figure 2.1. Location of the study area.

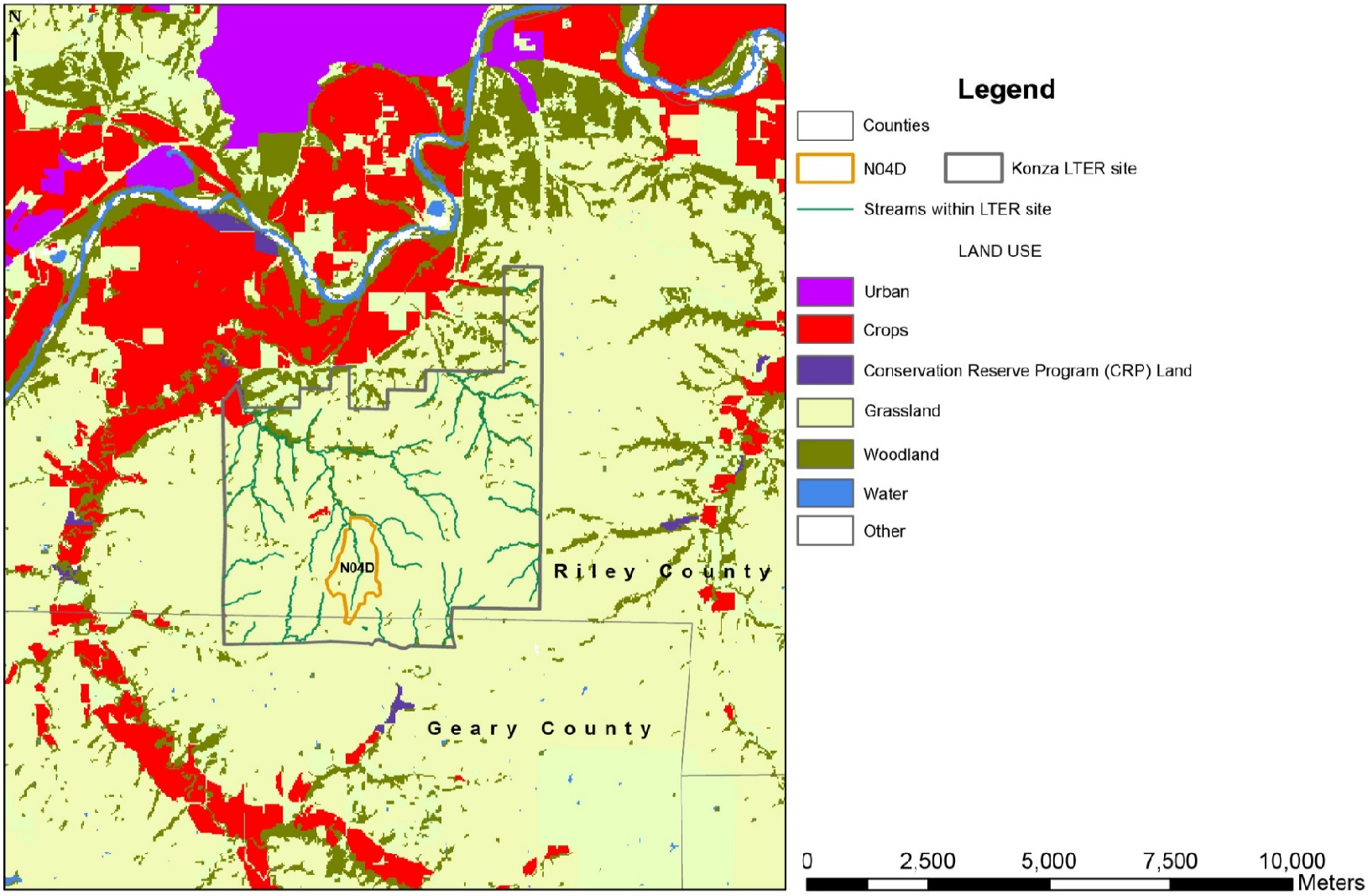


Figure 2.2. Land use map of the area showing the isolation of the studied watershed N04d from the cropland. Modified from 2005 Kansas Land Cover Patterns (Peterson et al., 2010). Area identified as cropped just northeast of the N04d watershed is a former hayfield that has been fallow for at least 25 years, and probably more.

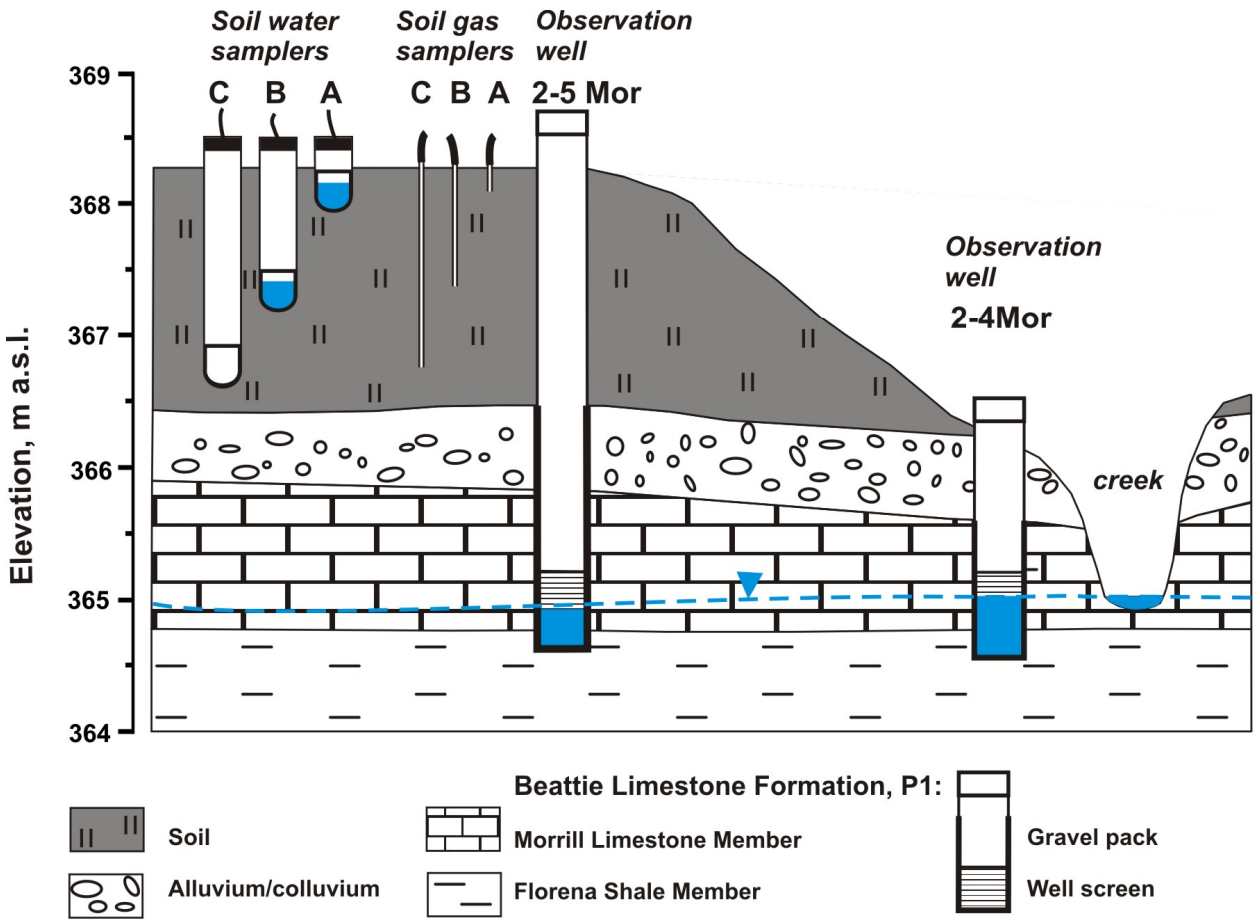


Figure 2.3. Schematic design of the sampling site. Thickness of soil is 180 cm and it decreases towards the stream. Limestone-chert colluvium-alluvium is thickest on the floodplain. The Morrill Limestone aquifer, 90-30 cm thick, is exposed and on the bottom and the sides of the stream. Water level is within the limestone layer, with the average depth of 320 cm (well 2-5 Mor) and 150 cm (well 2-4 Mor).

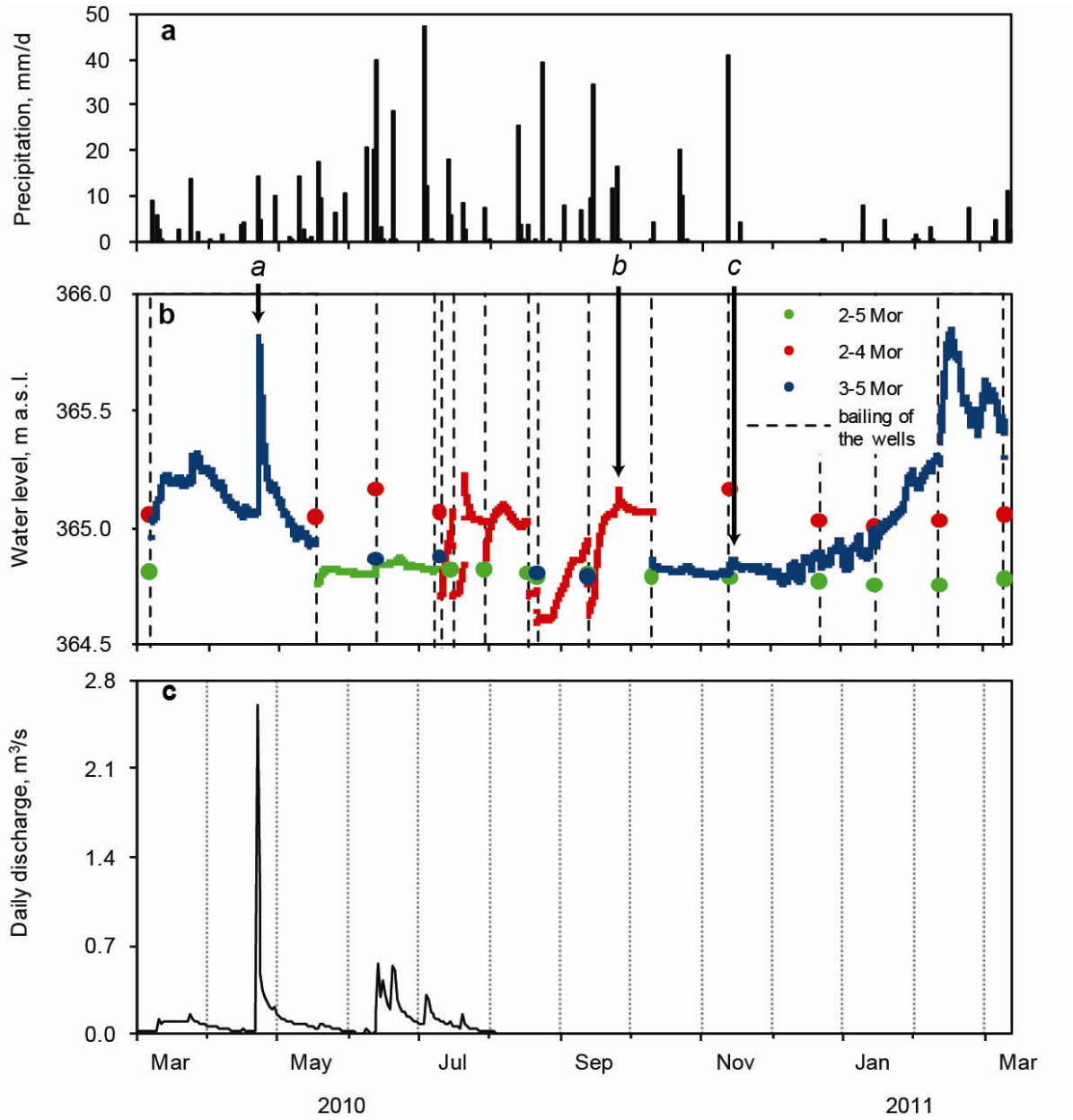


Figure 2.4. The effect of precipitation (a) on water level in three observation wells measured with the pressure transducer (lines) and e-line (circles) (b) and discharge of Kings Creek (USGS gauging station 0679650) (c). Arrows with letters identify separate recharge events detailed in Fig. 2.5.

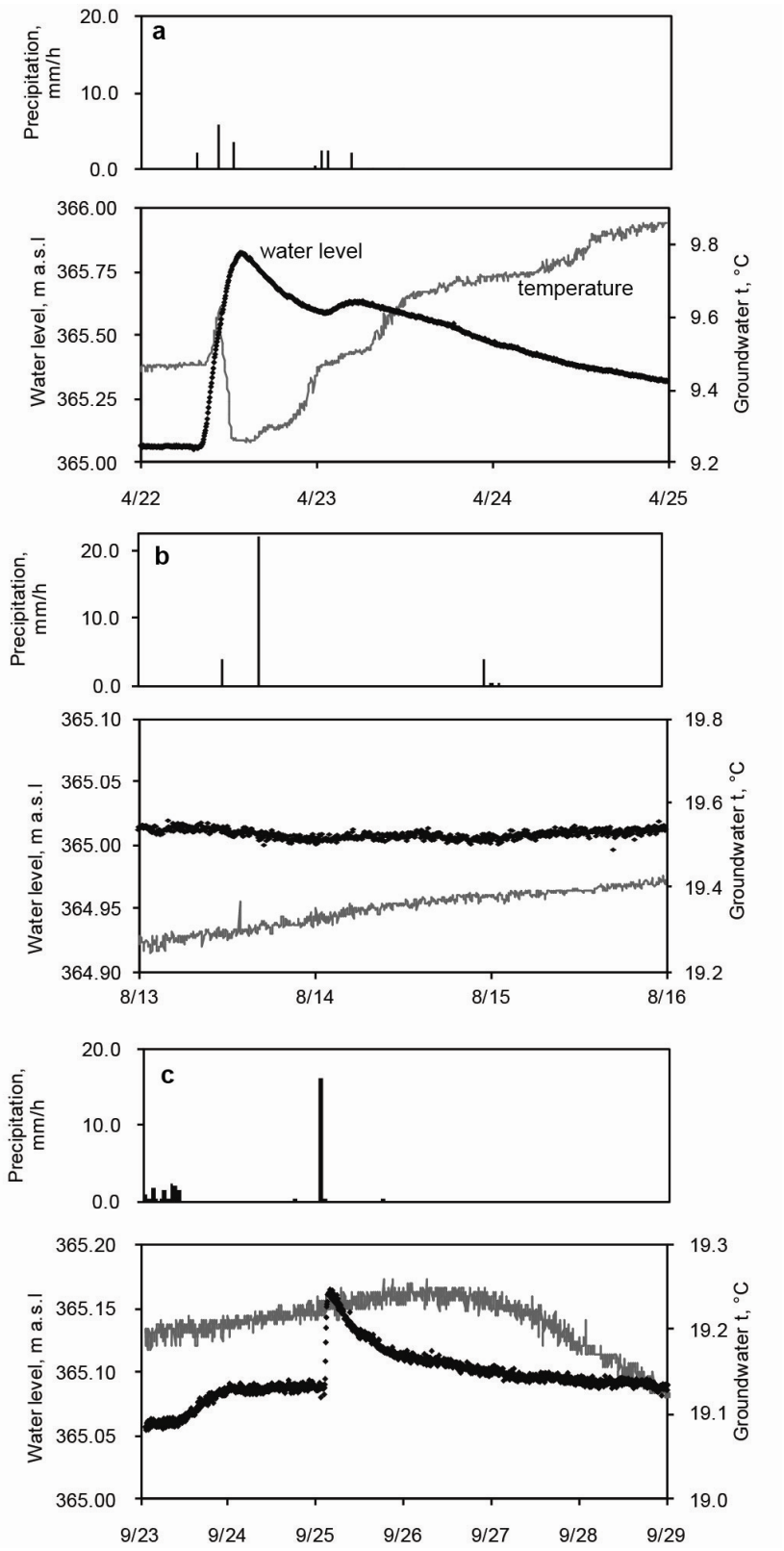


Figure 2.5. Response of water level to precipitation events in (a) early growing season (3-5 Mor), (b) mid-growing season (2-4 Mor) and (c) late growing season (2-4 Mor) of 2010.

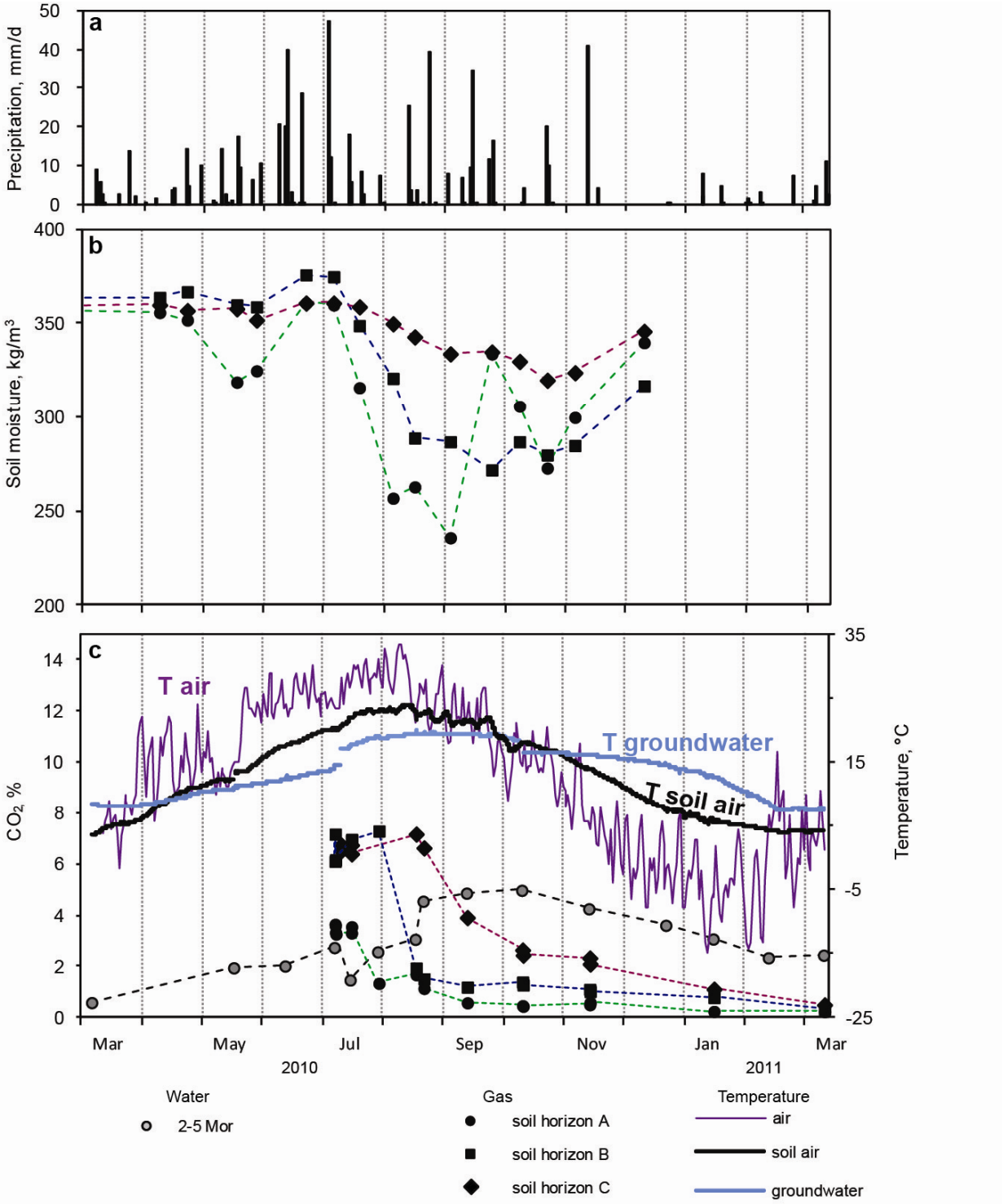


Figure 2.6. Effect of (a) precipitation events, (b) soil moisture and (c) temperature on soil air $CO_2$ concentration.

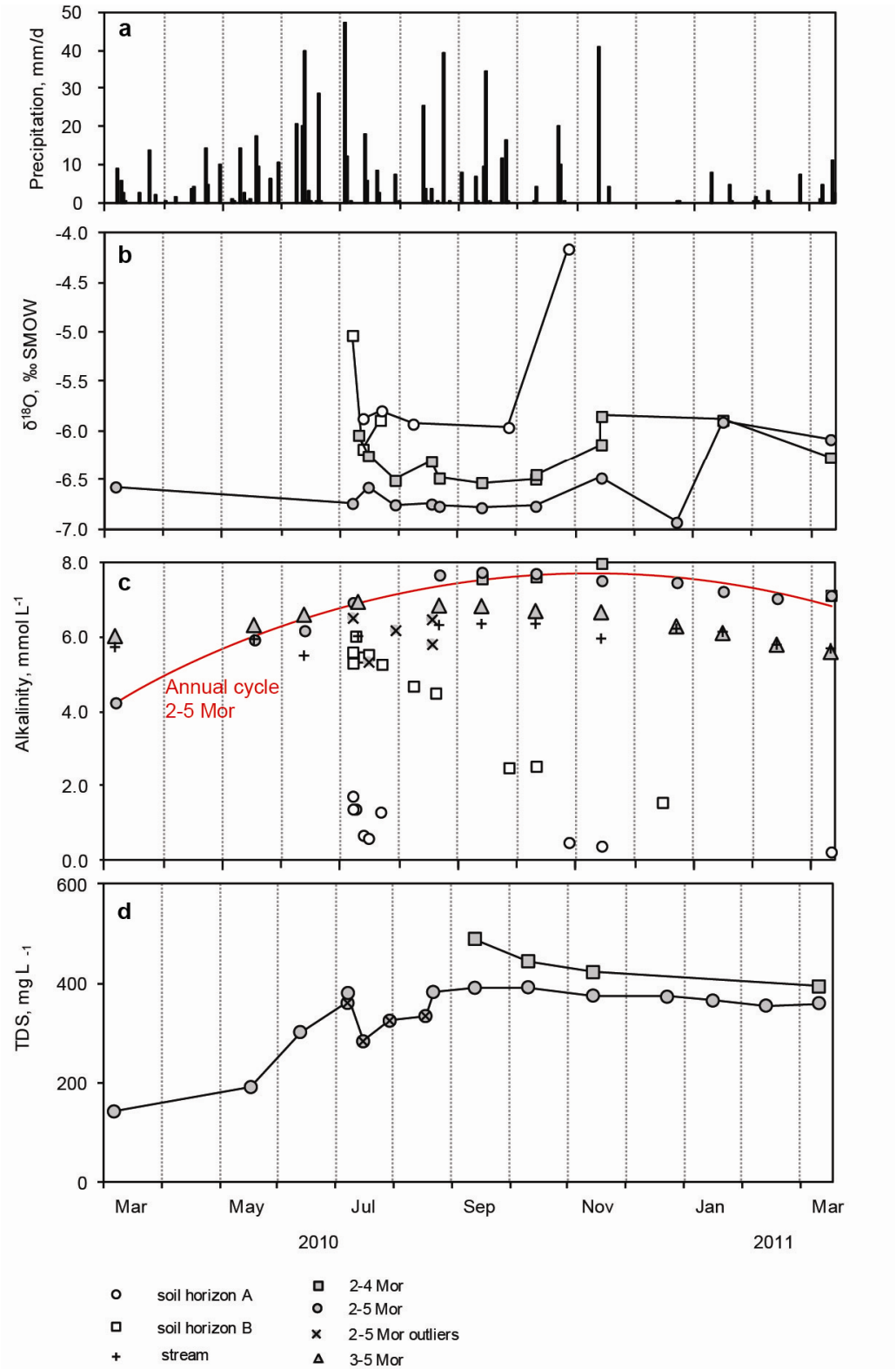


Figure 2.7. Precipitation and measured chemical characteristics of soil water and groundwater. There is an annual trend of alkalinity in groundwater. Outliers for 2-5 Mor were caused by dilution due to recharge.

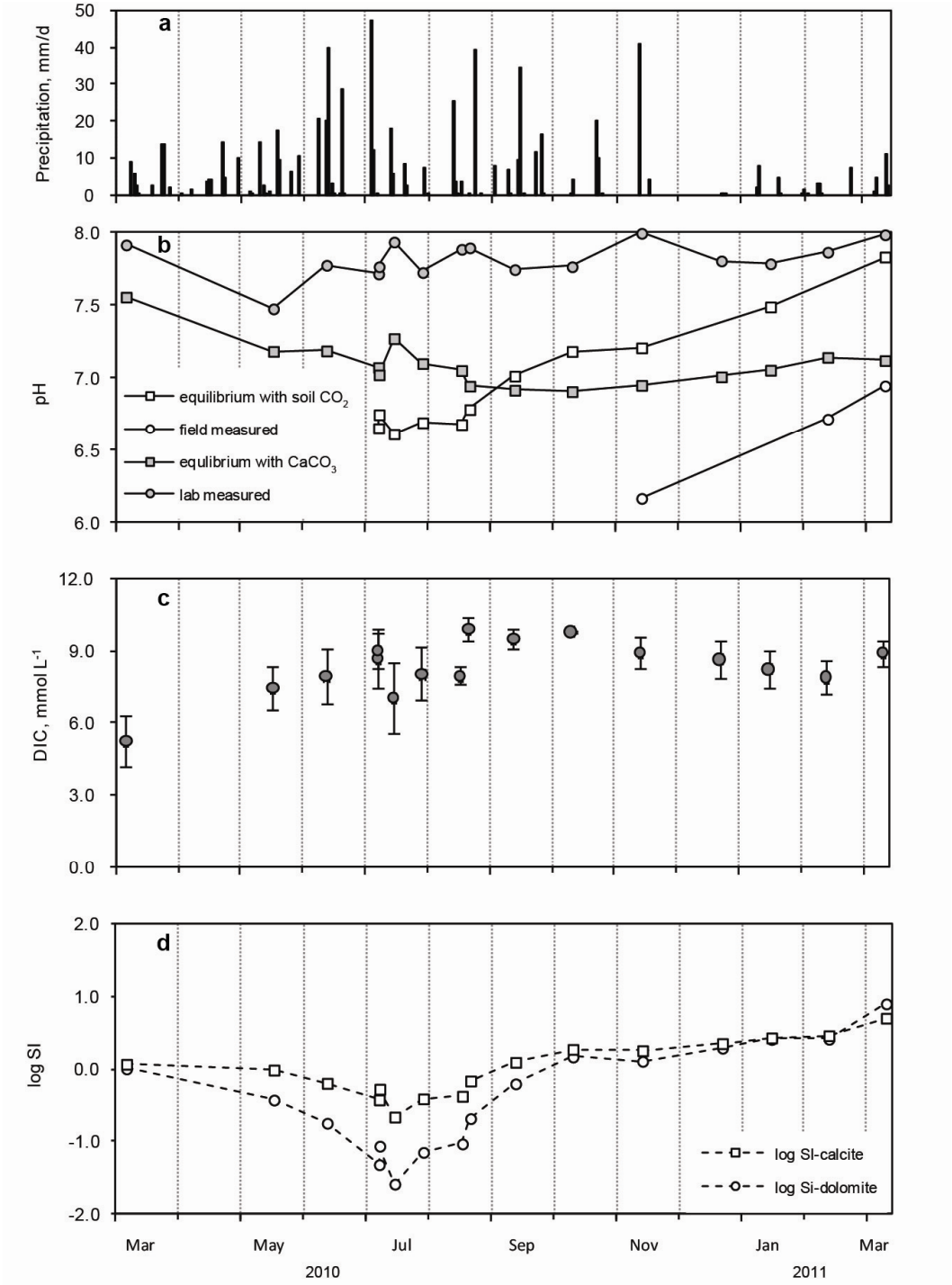


Figure 2.8. Meteoric precipitation (a), pH (b), DIC (c) and carbonate-mineral saturation in groundwater from 2-5 Mor. pH was determined using 4 different methods (see text for details). DIC was calculated using the average pH estimated from calcite equilibrium and soil $CO_2$ equilibrium methods. The saturation indexes for calcite and dolomite were calculated using estimated pH and measured alkalinity.

# CHAPTER 3. SOURCES OF DISSOLVED INORGANIC CARBON IN SOIL AND SHALLOW GROUNDWATER, KONZA PRAIRIE LTER SITE, NE KANSAS, USA

## Chapter summary

Sources and seasonal trends of dissolved inorganic carbon (DIC) in the shallow limestone aquifer were studied for 1 year at the Konza Prairie LTER (Long-Term Ecological Research) Site, from spring 2010 to spring 2011. Annual cycles of soil air $CO_2$, groundwater DIC, and isotope characteristics showed a strong dependency on weather conditions and soil respiration. Soil $CO_2$ reached its annual maximum in the middle of the growing season, when moisture was not limiting to soil respiration. Following the maximum, the $CO_2$ decreased because of moisture deficiency in the late summer and temperature decline in the fall and winter. The decrease began first in the shallowest part of the soil and last in the deepest part. Groundwater $CO_2$ reached its annual maximum in October; this lag-time between the soil and groundwater $CO_2$ maxima of 2-3 months may correspond to the travel time of soil-generated $CO_2$ to the water table.

Soil $CO_2$ and dissolution of carbonate minerals are the two main sources of DIC in the shallow limestone aquifer. The time-variable $CO_2$ caused an annual carbonate-mineral saturation cycle, intensifying limestone dissolution when $CO_2$ content was high and thus creating an additional source of DIC.

The stable carbon isotope composition of soil air $CO_2$ and DIC exhibited $C_4$ plant signature and were similar to that of soil organic matter, suggesting that both root and bacterial respiration are sources of $CO_2$. Soil air $CO_2$ became isotopically heavier during extended dry periods and lighter following large precipitation events. DIC was enriched in 7-10‰ relative to the $CO_2$ source due to isotope fractionation in a system open to soil $CO_2$. An annual cycle of $\delta^{13}C_{DIC}$ with the lightest composition corresponding to the highest DIC in groundwater was primarily controlled by $pCO_2$ that caused the isotopic enrichment factor to be the smallest when pH was the lowest.

Considering the processes of DIC production studied at this site, the prediction of increased respiration rates, temperature, and frequency of extreme rainfall events also predicts increased carbon flux to groundwater accompanied by more intense weathering.

# 1. Introduction

Grasslands occupy 11% of the earth's terrestrial surface (Sala, 2001). Tallgrass prairie, the wettest of the grassland provinces, is an important ecosystem for studying carbon storage and soil carbon dioxide fluxes (DeLuca and Zabinski. 2011). Long-term events such as erosion, karst processes, expansion of woody vegetation and short-period perturbations such as extreme storm events or drought are factors that would significantly affect carbon sources and belowground redistribution in the tallgrass prairie ecosystems.

The Konza Prairie Long Term-Ecological Research (LTER) Site, situated in the northern Flint Hills of Kansas, is characterized by shallow water-level depth and relatively thick soil, suggesting an important influence of soil gas, moisture, and matrix on groundwater carbonate chemistry, while remoteness from croplands limits the impact of agricultural contaminants. Moreover, 30 years of intensive studies at the Konza Prairie LTER Site has addressed the affects of multiple global change phenomena on the sustainability and dynamics of grassland ecosystems, and created a complex picture of interaction within ecosystems (Knapp and Seastedt, 1998). Among other findings, water-chemistry monitoring of a shallow limestone aquifer at Konza Prairie over a 15-year study period (1991-2005) showed that groundwater $pCO_2$ cycles annually with maxima during the fall even though soil respiration rates are at a maximum during the growing season (Harper et al., 2005; Macpherson et al., 2008). This suggests that there is an indirect link and a lag time between the extrema of soil air $CO_2$ concentrations and $CO_2$ in groundwater that is depth dependent (Macpherson et al., 2008). At the same time, it was found that $pCO_2$ increases in groundwater from two wells, 6 and 12 m deep, are higher (18-36%) than the increase of atmospheric $CO_2$, which was around 7% over that time period (Macpherson et al., 2008). A similar below-ground $CO_2$ increase in response to atmospheric $CO_2$ increase has been documented at a Free-Air $CO_2$ Experiment (FACE) sites (Andrews and Schlesinger, 2001; Jackson et al., 2009).

Several hypotheses may explain increasing belowground $CO_2$ (Table G.1), including reforestation of prairie areas (Liu et al., 2008), increasing groundwater residence time, increased atmospheric nitrogen loading (Macpherson et al., 2008), or higher rates of soil organic matter (SOM) decomposition (Bond-Lamberty and Thomson, 2010). Most of them consider the importance of increased soil respiration rates. Although most of $CO_2$ that is produced in soil

escapes to the atmosphere as gas efflux, some $CO_2$ will dissolve in soil water and potentially recharge the underlying aquifer contributing to the groundwater DIC. Assuming this mechanism of $CO_2$ transport into the shallow aquifer, increased $pCO_2$ in soil due to seasonal elevation of soil respiration rates could result in similar temporal trends in groundwater.

The goal of this research was to characterize variations in sources of shallow groundwater DIC over the year and explain a relationship between groundwater DIC and soil air $CO_2$. This goal required:

1. Characterization of soil gas and water $CO_2$, and DIC carbon isotopic composition variations in time and with belowground depth.

2. Estimation of the contribution of such sources as carbonates, plants, and SOM to the belowground $CO_2$ based on isotopic composition of each end member and prior data.

Stable carbon isotopes are used to test the proposed hypothesis because sources of belowground $CO_2$ have different carbon isotopic compositions and transformations in the carbonate system can be inferred using equilibrium and kinetic fractionation and isotope mixing models. Investigations into the DIC behavior in the groundwater systems began in late 1960s and 1970s, when the carbon isotopes techniques were applied in environmental studies. The theoretical and experimental works determined fractionation factors between $CO_2$, $CaCO_3$ and dissolved carbonate species (Bottinga, 1968; Mook et al., 1974). Field measurements were then taken to obtain typical values for soil $CO_2$ and groundwater (Galimov 1966; Deines et al., 1974). The data revealed relationships between soil $CO_2$ and inorganic carbon in groundwater (Rightmire and Hanshaw, 1973; Fritz et al., 1978; Reardon et al., 1979). Subsequent works considered additional sources of carbon that can potentially alter $\delta^{13}C$ values of DIC, such as pedogenic carbonates (Cerling, 1984) and dissolved organic matter (Schiff et al., 1990). Some useful analogues for understanding soil and groundwater carbon-isotope-differentiated processes can be found in studies on the origin and cycling of DIC in surface aquatic systems in contact with atmospheric $CO_2$: lakes (Quay et al., 1986; Wachniew and Rozanski, 1997), rivers (Atekwana and Krishnamurthy, 1998; Kanduč et al., 2007; Doctor et al., 2008; Aucour et al., 1999), and oceans (Tans et al., 1993).

The research presented in this paper shows inorganic carbon transformations in a prairie environment with carbonate bedrock based on year-round sampling of stream, soil, and ground water, and soil gas. It focuses on relatively small-scale systems, such as a watershed and aquifer.

The concentration and isotopic composition DIC reflect near-surface conditions such as $pCO_2$, temperature, and moisture regime, under which they were formed.

## 2. Research site

The Konza Prairie LTER Site occupies more than 34 $km^2$ in the northern part of Flint Hills, in parts of Riley and Geary Counties of Kansas (Fig. 3.1). It is located on the western edge of the Midwest tallgrass prairie and characterized by temperate, mid-continental climate with high variability in temperature and precipitation (Hayden, 1998). The average annual air temperature is 13°C with mean January and July ranging between –9 to 3°C and 20 to 33°C, respectively (Nippert and Knapp, 2007a). Average annual total precipitation is 835 mm with 75% falling during the growing season (Hayden, 1998). Kings Creek, the main stream draining the Konza Prairie LTER Site, empties into McDowell Creek north of the Konza Prairie; McDowell Creek is a tributary to the Kansas River.

The vegetation at the Konza Prairie LTER Site is a mesic, native tallgrass prairie dominated by $C_4$ perennial grasses with woody riparian zones (Towne, 2002). The most common perennial warm-season grasses are big bluestem (*Andropogon gerardii*), little bluestem (*A. scoparius*), Indian grass, and switchgrass (*Panicum virgatum*). Buckbrush and smooth sumac are the dominant woody species (Freeman, 1998). Konza Prairie soils are silty clay loam and silty clay, well drained, mostly carbonate-poor, with an average thickness of 1 to 2 m. At the sampling study location, soil is developed over colluvium-alluvium and was identified as Ivan / Tully silt loam series (USDA-NRCS, 2007).

Geologic strata are composed of Lower Permian couplets of limestone and shale from the Council Grove Group of the Wolfcampian Series (Fig. A.1), overlain by Quaternary colluvium / alluvium. Thin, sandwich-type aquifers are created in the limestone layers, one of which, the Morrill Limestone Member (the Morrill) of the Beattie Limestone was utilized for the present study. The Morrill is a brownish-gray, shallow-marine limestone, about 1.2-m thick, underlain by the Florena Member, gray calcareous argillaceous deep-water shale. The aquifer exhibits secondary porosity (solution-enlarged joints and other dissolution features) and has hydraulic conductivities from about $10^{-8}$ to $10^{-3}$ m/s as estimated from slug tests (Pomes, 1995). Groundwater chemistry is dominated by $Ca^{2+}$ and $HCO_3^-$ with TDS usually lower than 500 mg/L

(Macpherson, 1996). Contamination of groundwater by agricultural chemicals is highly unlikely because the closest agricultural area, located 5 km away, is separated by a local watershed divide (Fig. 2.2).

Details on physiography, climate conditions, geological setting, and hydrogeology of Konza Prairie are given in Macpherson et al. (2008).

Previous studies on carbon stable isotope composition from different pools at Konza Prairie suggest a range of $\delta^{13}C$ values that might be expected for DIC (Fig. 3.2) and highlight belowground processes to consider. In the nearby Rannells Flint Hills Prairie Preserve, $\delta^{13}C$ values of net $CO_2$ fluxes ranged between −14 and −9‰ between June and August, reflecting the dominance of $C_4$ photosynthesis in the region, whose contribution to net ecosystem exchange ranged from 68% to nearly 100%, in response to an impulse of intense precipitation (Lai et al., 2003). Johnson et al. (2007) showed that historical changes in plant communities are reflected in the $\delta^{13}C$ profile of paleosol soil organic carbon (SOC) and that $\delta^{13}C$ values of aboveground plant tissue is about 2‰ heavier than soil-surface SOC. Composition of modern soil carbonates differ by 14−16‰ from SOM, reflecting isotopic equilibrium between $CO_2$ derived from SOM oxidation, and dissolved and solid carbonate species (Cerling et al. 1989). $\delta^{13}C$ ratios for groundwater humic material denotes a mixed $C_3$ / $C_4$ vegetation source, while groundwater fulvic acid is spatially distinct from either woody or grass sources (Pomes, 1995).

## 3. Methods

Detailed monitoring of groundwater chemistry and water-table elevation started in 1990 at a 1.2–$km^2$ (N04d) watershed in the southern part of the Konza Prairie LTER Site, along the Kings Creek watershed divide. This study focuses on two observation wells located on the second transect of N04d watershed, on the west bank of the South Fork of Kings Creek (Fig. 3.3). Wells 2-5 Mor and 2-4 Mor fully penetrate the unconfined aquifer in the Morrill Limestone Member of the Beattie Limestone. Well 2-5 Mor is located on the footslope occupied by the grass communities. Well 2-4 Mor, located 5 m away from the stream, is surrounded by woody vegetation. Well 3-5 Mor, situated in the riparian zone about 100 m upstream, was used for general comparisons, because it has the most detailed history of observations.

Depth to groundwater was measured at least once a month with an electric sounder and continuously monitored with Solinst® pressure transducer. Sampling was performed on a

monthly basis plus in conjunction with large recharge events. Prior to sampling, wells were bailed with a Teflon® bailer suspended on a Teflon®-coated wire to remove stagnant water. Collected groundwater was delivered to a HDPE bottle using a Teflon® bottom emptying device.

An array of three soil-water samplers allowed access soil moisture from the A, B, and C soil horizons. To collect soil moisture, samplers were left under a vacuum of 70-80 centibars until the following sampling event, typically 1 month later. It was presumed that the water had been collecting steadily during the entire period, so that the sample represented a composite of soil water for that interval of time. The collected water was extracted and evacuated with PFA tubing using a hand pump.

Three 5/32" aluminum tubes positioned to same depth as the soil-water samplers were used to sample soil gas. Prior to sampling, 50–100 mL of gas were withdrawn using a hand-vacuum pump with Tygon® tubing in order to completely evacuate stagnant air from the gas well and from the pump tubing. A 12 ml Exetainer® glass vial was then submerged in a bucket of boiled distilled deionized water, purged with 200 ml of soil gas to displace the water and flush the vial, and then capped under water.

Samples were stored in a cold place (ice chest in the field; non-frost-free refrigerator in the lab) until water or gas were analyzed. Groundwater samples were filtered (0.45 μm) on the day of collection. Alkalinity of water samples was determined by titration with ~0.02 N $H_2SO_4$ at the University of Kansas Aqueous Geochemistry Laboratory (KU AGL) within two days of sample collection. Concentrations of $Cl^-$, $SO_4^{2-}$, $NO_3$–$N^-$ and $F^-$ were determined at KU AGL by suppressed ion chromatography (IC) with a Dionex 4000i within a week of collection. Cations ($Na^+$, $K^+$, $Mg^{2+}$, $Ca^{2+}$, $Sr^{2+}$) and dissolved Si were determined on filtered and weighed aliquots preserved by acidification with $HNO_3$ to 2% v/v within 3 days after collection. Analysis was accomplished using inductively-coupled plasma-optical emission spectroscopy (JY 138 Ultrace ICP-OES) at the University of Kansas Plasma Analytical Laboratory (KU PAL). Concentration of $CO_2$ in the samples of soil gas was measured with an Agilent Technologies 6890N Gas Chromatograph (GC) at the KU Geomicrobiology Lab.

Stable carbon isotope compositions of groundwater and soil water DIC as well as soil air $CO_2$ were determined by stable-isotope-ratio-mass-spectrometry (SIRMS) on a ThermoFinnigan MAT 253 mass spectrometer at The University of Kansas W.M. Keck Paleoenvironmental and

Environmental Stable Isotope Laboratory (K-PESIL). For DIC analysis, sealed glass Exetainers® were flushed with He for 5 minutes using input and output needles, then 7 drops of concentrated $H_3PO_4$ were added with a syringe. Groundwater (0.6 ml) or soil water (5 ml) were then injected and left for 24 hours for equilibration and $CO_2$ release from acidified water into headspace. The evolved-gas samples were loaded in ThermoFinnigan GasBench II, on-line gas preparation and introduction system. During the analysis, the $CO_2$ is introduced into the mass spectrometer in continuous flow mode, using He as the carrier gas. Carbon isotope ratios of the DIC and $CO_2$ are reported in the delta notation in per mil (‰) relative to Vienna Pee Dee Belemnite (VPDB) carbon standard (with a precision of better than 0.1‰):

$$\delta^{13}C = \left( \frac{(^{13}C/^{12}C)_{sample}}{(^{13}C/^{12}C)_{VPDB}} - 1 \right) \cdot 1000 \ (‰). \qquad (3.1)$$

# 4. Results

## 4.1 Groundwater recharge

Meteoric precipitation in 2010 was 598 mm, which is approximately 72% of the 30-year mean precipitation rate of 835 mm (Hayden, 1998). 71% of annual precipitation (425 mm) fell in the growing season, from mid-May to mid-October 2010, with June and July being the wettest months (>100 mm/month). In the first three months of 2011 precipitation was 66 mm in form of snow, rain, or fog.

Precipitation is the main source of groundwater recharge at the Konza Prairie. During extended dry periods water level fluctuates on a daily basis with ~1-cm amplitude (Macpherson et al., 2008), while a single pulse of recharge can cause a water-level rise of up to 75 cm (5/6/07, Macpherson, unpublished data). During 14 years of monthly monitoring of 2-5 Mor, water-table fluctuations were mostly within 10 cm (Fig. C.1), smoother than in other wells completed in the same aquifer. Continuous pressure transducer logging in the summer of 2010 also showed small variability (Fig. 3.4). The recovery after groundwater sampling was extremely slow (about 1 cm/hr). Water level reached the highest point in July, while in the late winter the well was almost dry. Water level in 2-4 Mor demonstrated greater variability because of the shallow depth of the well, absence of thick soil, and proximity to the stream. Well 3-5 Mor demonstrated almost immediate recovery after bailing, suggesting higher hydraulic conductivity within the aquifer and/or favorable construction of the well screen. Water-level gradient (Fig.

3.4b) and stream discharge data (Fig. 3.4d) suggest that groundwater recharge from the stream was possible at least from May to July of 2010.

Soil moisture content reflected recent rainfall or snowmelt events, with the highest values in spring to early summer following a general decline (Fig. 3.4c) caused by evapotranspiration, with occasional peaks in the soil horizon A related to individual storm events.

## 4.2 Aqueous chemistry

Groundwater from the Morrill aquifer had relatively stable major ion chemical composition (Table D.2). Water is calcium-bicarbonate: bicarbonate accounted for more than 90% of anions, while cations were represented primarily by calcium with lesser magnesium. The Ca/Mg weight ratio was between 2 and 5 by mass. Groundwater TDS was 300–400 mg/l with some negative offset related to dilution by rainwater. Detailed characterization of groundwater chemistry at the Konza Prairie LTER Site was given in Macpherson (1994) and Gray et al. (1998).

Soil water had much higher TDS due to elevated $SO_4^{2-}$ and $Mg^{2+}$ content. Samples from the B horizon were characterized by higher concentrations of all major ions relative to the A horizon. Rainwater had very low TDS, less than 100 ppm (2 and 84 ppm), and almost no alkalinity.

## 4.3 Annual trends

### 4.3.1. Soil $CO_2$

Soil air $pCO_2$ was 1-2 orders of magnitude higher than in the atmosphere. $CO_2$ concentration in soil gas increased with depth except July and early August, when the concentration in the B horizon was similar or higher than in the C horizon (Fig. E.1). Observed temporal trends during the study period suggest cyclical patterns in $CO_2$ concentrations for all three horizons (Fig. 3.6b). In the A horizon, $CO_2$ reached its maximum of 3.5% of soil gas in early July. Following this, the maximum $CO_2$ in the B and C horizons, approximately twice as high as the A horizon, occurred in late July and early August, respectively. After the annual maximum, $CO_2$ content decreased smoothly to less than 1% in the winter months in all three soil horizons, so that soil air $CO_2$ distribution thorough the profile was more uniform.

$\delta^{13}C$ of soil air $CO_2$ varied from −12.3 to −19.7‰ with the mean value of −14.8±1.7‰ (Fig. 3.5d), which is typical for the respired $CO_2$ by plants following $C_4$ photosynthetic cycle (O'Leary, 1988). Gas samples were collected in the grassy area near 2-5 Mor, where $C_4$ warm-season grasses are dominant. There was a slight enrichment in the heavy carbon isotope with depth: samples from the soil horizon A were usually 1–2‰ heavier than in the rest of the soil (Fig. E.1). Annual trends in $\delta^{13}C_{CO2}$ were not as distinct as for $pCO_2$. There was an enrichment in the A horizon in late July, corresponding to a drop in $CO_2$ content. Increased $\delta^{13}C_{CO2}$ values can be correlated with periods of relatively low soil moisture: at the end of July, in October, and during the winter (Fig. 3.5a).

### 4.3.2 Groundwater and soil water

In 2-5 Mor, alkalinity was the lowest in the spring, increased through the growing season and reached a maximum of 7.74 mmol/L in early fall. In mid-summer, alkalinity decreased briefly by 1.7 mmol/L because of the biggest storm event in early July, and then recovered slowly to the expected values by the end of August (Fig. 3.5c). Groundwater alkalinity in the samples from 2-4 Mor obtained in the fall of 2010 and the spring of 2011 had similar alkalinity to that in 2-5 Mor. Alkalinity of the streamwater and from 3-5 Mor was slightly lower, between 5.5 and 7.0 mmol/L, but nevertheless followed the same pattern through time and also showed a slight rain-dilution effect.

Equilibrium either with $CO_2$ from the soil horizon C or with calcite was assumed to estimate pH for each 2-5 Mor sample, because low well yield precluded measuring downhole pH or pumping through a flow-through cell. Estimated pH decreased during the growing season from slightly alkaline (7.5–7.8) to neutral and slightly acidic values (6.2–6.8) (Fig. 3.6b). After reaching a minimum in October, pH started to increase through March. Because the pH was circumneutral, $HCO_3^-$ accounted for 80–90% of the DIC in groundwater all year long. Measured soil water pH was slightly acidic and increased with depth, demonstrating evolution of recharge water from acidic rainwater to neutral groundwater as it saturates with soil $CO_2$ and dissolves soil carbonate.

Saturation indexes (SI) of calcite and dolomite in groundwater increased during the growing season but exceeded saturation only in the winter (Fig. 3.6d). These results are consistent with log $SI_{calcite}$, log $SI_{dolomite}$, and pH annual cycles, inverse to dissolved solids and

$pCO_2$, modeled for 3-5 Mor and another nearby well (4-6 Mor, not used in this study; Macpherson et al., 2008). The trend in calcite saturation index over the year is reflected in the seasonal trend in $Ca^{2+}$ concentration, the main source of which is calcite dissolution. During the growing season, $Ca^{2+}$ concentration in 2-5 Mor increased from 1.9 mmol/L to 2.6 mmol/L, while $Mg^{2+}$ content only increased from 0.8 mmol/L to 1 mmol/L (Table D.2). Calculated $pCO_2$ for groundwater (assuming equilibrium with calcite) remained less than that of soil gas until the fall and reached its maximum 2-3 months later, in October (Fig. 3.5b).

Carbon isotopic composition of DIC in soil water was 6–10‰ heavier than that of soil air $CO_2$ (Fig. 3.5d). In addition, the values of $\delta^{13}C_{DIC}$ were 1.5–2‰ lighter in the soil horizon A than in the soil horizon B. In both horizons there was a 1.5‰ decrease during the period from July to November. The values of $\delta^{13}C_{DIC}$ in groundwater showed less annual variation than $\delta^{13}C_{CO2}$ in the soil. In 2-5 Mor, groundwater $\delta^{13}C_{DIC}$ ranged from −7.0 to −4.7‰. The values appear to follow an annual cycle with the lightest composition in September-October when groundwater alkalinity, $pCO_2$, and modeled DIC reached the maximum. Such "out-of-phase" relationship is in agreement with existing data on stable isotope ratio variations in groundwater from 3-5 Mor (Fig. G.3) and streamwater collected in 2008-2009 (Macpherson, unpublished data). DIC from 2-4 Mor exhibited greater variability with samples being up to 3‰ lighter than those from 2-5 Mor.

# 5. Discussion

## 5.1 Soil $CO_2$

$CO_2$ content in soil air is the result of the co-occurrence of three processes: soil respiration, diffusive loss to the atmosphere, and uptake by the aqueous phase (Reardon et al., 1979). Soil respiration includes microbial oxidation of stable SOM by heterotrophs and rhizosphere respiration that represents the sum of root respiration and microbial respiration of labile carbon derived from live roots (Lin et al., 1999; Badalucco and Nannipieri, 2007).

At the Konza Prairie, $CO_2$ in the soil air started increasing early in the growing season and reached the maximum in mid-summer when photosynthate production and soil moisture were high. Soil $CO_2$ began decreasing in mid-July to early August because of moisture deficiency (Fig. 3.4c), and, later in the fall and winter, because of temperature decline (Fig. 3.5b; Luo and Zhou, 2006). The mostly negative concentration-depth gradient is the result of the slow

upward diffusion of $CO_2$ from sources of production towards the surface. Downward movement of gaseous $CO_2$ towards the water table via diffusion (Reardon et al., 1979) was possible in July when $CO_2$ concentration in the B soil horizon was higher than that in the C horizon.

Since the main sources of soil $CO_2$ are root respiration and microbial oxidation, the $\delta^{13}C$ values of soil air $CO_2$ are dependent on the type of vegetation and the composition of organic matter. Average $\delta^{13}C$ value of Tully series SOM is −14.9±1.1‰ (Cerling et al., 1989). The warm-season grasses of Konza Prairie sampled in the toe slope position show a very strong $C_4$ signal (−11.9‰), while average values on the upland are slightly lighter (−13.6‰; Johnson et al., 2007). Field site data showed that soil air $CO_2$ is characterised by a mean $\delta^{13}C_{CO2}$ of −14.8‰, similar to that of prarie plants and SOM. Suggested +4.4‰ enrichment of soil $CO_2$ relative to the source flux accounted for diffusion-related fractionation of carbon isotopes (Cerling et al., 1991) was not observed.

Mixing with isotopically heavier atmospheric $CO_2$ (−8‰, Lai et al., 2006) should have had the greatest effect during the winter, when the soil $CO_2$-depth concentration gradient was smaller. A detailed profile sampling on 11/13/10 showed 2‰ enrichment in the upper 15 cm of soil (Fig. E.1). A positive gradient deeper in the soil contradicts the negative gradient of SOC isotope signature (Cerling et al., 1989; Johnson et al., 2007). However degradation of the shallower SOM was more significant source of $CO_2$ because $C_{org}$ below 50 cm of subsurface depth was <1% while in the less mineralized A horizon it was 3-6% (Fig. E.1).

Temporal variation of $\delta^{13}C_{CO2}$ signal in soil air did not exhibit a smooth annual trend similar to the trend observed for $pCO_2$. Soil A horizon varied by 7‰ from July 2010 until March 2011. Soil horizon B demonstrated a similar pattern but with a smaller scatter. Such changes are likely related to composition of the source: during a year, $\delta^{13}C$ of ecosystem respiration varies by 3-8‰ in Oklahoma-Kansas prairie region (Lai et al., 2006; Torn et al., 2011). Variability can also be related to weather-associated changes in the $\delta^{13}C$ signature of root respiration and organic matter decomposition, variations in the relative contribution of those two sources to the total soil respiration, or photosynthetic discrimination (Bowling et al., 2002; Ekblad et al., 2005). We found an enrichment in $\delta^{13}C_{CO2}$ that was caused by relatively dry periods and depletion associated with the higher moisture on a monthly time scale. An analogous correlation was shown previously between respiration isotope signature and vapor pressure deficit and available soil moisture (Fessenden and Ehleringer, 2003). Thus, the variability of the $\delta^{13}C$ at the study site

is within prior measured ranges for seasonal variability. Diurnal changes in prairie soil respiration can reach 1‰ (Lai et al., 2003; Bahn et al., 2009), but the sampling frequency in this study precluded identifying the specific reasons for the smaller isotope variability on the shorter time scales.

## 5.2. Sources of DIC

Natural sources of inorganic carbon in an aquifer include downward $CO_2$ transport from soil in the dissolved form with recharge (Kessler and Harvey, 2001) or as a gas via diffusion (Appelo and Postma, 2005), leakage from underlying aquifers, or upward flux of deep $CO_2$ of various origins through gas vents (Chiodini et al., 1999). DIC is also produced in the aquifer via dissolution of carbonate rocks and oxidation of dissolved organic carbon (DOC) or organic matter present in sediments (Keller and Bacon, 1998).

Natural gas deposits (~1 km deep) are present in northeastern Kansas (Newell et al., 1987), but there is no evidence of upward leakage and the carbon isotope signature of $CO_2$ produced during methane oxidation should be should be distinctive (Schoell, 1988). Precipitation is not a significant source of carbon because of the very low TDS. Oxidation of buried or dissolved organic matter would not be an important source of DIC to the aquifer since DOC content in the Morrill aquifer is generally less than 1 mg/L (Pomes, 1995) and the aquifer would not be a significant source of organic matter available for oxidation because it is a shallow-marine, fossiliferous limestone. Similar annual trends in $pCO_2$ in soil gas and groundwater at the field site (Fig. 3.6c) suggest that soil $CO_2$ contributes to DIC and also drives limestone dissolution that is not uniform over time. The latter two sources are discussed in detail below.

The belowground evolution of DIC in water, including change in concentration, isotopic composition, and speciation, begins as soon as meteoric water infiltrates. Depending on the partial pressure of soil air $CO_2$, temperature, and availability and chemical composition of recharge water, the amount of dissolved $CO_2$ will be different. The peak for $CO_2$ concentration in soil air was in July-August while maximum $pCO_2$ in groundwater was measured in September-October. Therefore, assuming uniform migration of soil gas, it takes about 2–3 months for soil $CO_2$ to be delivered to the aquifer, assuming that the high $pCO_2$ in groundwater is caused by high respiration rates of the same year.

Carbon isotope enrichment of groundwater DIC relative to soil air $CO_2$ is explained by isotopic fractionation between gaseous $CO_2$ and dissolved carbonate species in water. Temperature-dependent fractionation factors were calculated using theoretical and experimentally derived relationships, summarized in Clark and Fritz (1997):

$$10^3 \ln\alpha^{13}C_{CO2(a)\text{-}CO2(g)} = -0.373(10^3T^{-1}) + 0.19 \quad (5.1)$$

$$10^3 \ln\alpha^{13}C_{HCO3\text{-}CO2(g)} = 9.552(10^3T^{-1}) - 24.10 \quad (5.2)$$

$$10^3 \ln\alpha^{13}C_{CO3\text{-}CO2(g)} = 0.87(10^6T^{-2}) - 3.4, \quad (5.3)$$

where α is the isotope fractionation factor and T is the temperature in degrees Kelvin. The fractionation factor then used together with measured $\delta^{13}C_{CO2}$ values to predict isotopic composition of each of the aqueous species ($_X$):

$$\delta^{13}C_X = \alpha_{X-CO_2}\,\delta^{13}C_{CO_2} + \left(\alpha_{X-CO_2} - 1\right)10^3 . \quad (5.4)$$

Increase in dissolved carbon associated with higher $pCO_2$ allows more mineral carbonate to dissolve, which at this site was described by (Macpherson et al., 2008). Two types of carbonates were present at the sampling location. Tully soil series pedogenic carbonates with average $\delta^{13}C$ values of –0.4±0.3‰ (Cerling et al., 1989) and calcite and dolomite of the Morrill Limestone Member that comprise the aquifer and also are present as clasts in colluvium-alluvium. A sample of the limestone with no visual dissolution features from a core had a $\delta^{13}C$ value of 1.3‰; a sample of the limestone with secondary porosity had a value of –0.4‰. Because the $Mg^{2+}$ concentration in groundwater was three to four times smaller than the $Ca^{2+}$ concentration, calcite is expected to be the primary source of DIC. The amount of mineral dissolved depends on the degree to which the system is open to the source of $CO_2$, pH, and temperature of water (Denies et al., 1974; Aucour et al., 1999). These controls are discussed next.

In the Morrill Limestone, a shallow unconfined aquifer partially in the unsaturated zone, groundwater is in contact with soil air, suggesting an open-system conditions that permit quick continuous $CO_2$ gas/water isotopic exchange. According to the net dissolution reaction:

$$CO_{2(g)} + H_2O + CaCO_{3(s)} \Leftrightarrow Ca^{2+} + 2HCO_3^- \quad (5.5)$$

in the two moles of bicarbonate, one originates from isotopically lighter soil air $CO_2$ and one from the heavier limestone calcite. However in an open system the isotopic composition of the mineral will not affect the isotope ratio of the groundwater because all bicarbonate produced in the reaction will quickly equilibrate with soil air $CO_2$ (Deines et al., 1974; Appelo and Postma,

2005). The combined isotopic composition of all inorganic carbon species in equilibrium with $CO_2$ is calculated assuming the molar fraction of each species of DIC:

$$\delta^{13}C_{DIC} = \left(mH_2CO_3 \times \delta^{13}C_{H_2CO_3} + mHCO_3^- \times \delta^{13}C_{HCO_3^-} + mCO_3^{2-} \times \delta^{13}C_{CO_3^{2-}}\right)/DIC. \quad (5.6)$$

Observed values of groundwater $\delta^{13}C_{DIC}$ from 2-5 Mor were between –7.0‰ and –4.7‰, which was, on average, 7–10‰ heavier than the soil gas. Groundwater $\delta^{13}C_{DIC}$ from 2-4 Mor and 3-5 Mor, situated in the woody riparian zone, were 1–3‰ lighter than that in 2-5 Mor, suggesting that $C_3$ shrubs that have average $\delta^{13}C$ values about 10–16‰ lower than $C_4$ grasses (McCarron and Knapp, 2001) contributed to root respiration.

Measured groundwater alkalinity (used for comparison with DIC isotopic compostion, because $HCO_3^-$ accounts for as much as 80–90% of DIC at the field site) is negatively correlated with groundwater $\delta^{13}C_{DIC}$. The inverse trend between DIC and $\delta^{13}C_{DIC}$ is usually explained as conservative mixing of water from two sources in equilibrium with $CO_2$ of different origin and partial pressure, such as streamwater and groundwater (Doctor et al., 2008) or highland and lowland water (Aucour et al., 1999). However, at the N04d watershed the chemical and isotopic composition of shallow groundwater, streamwater, and soil water suggest a similar origin (Fig. 3.5). Seasonal effects explain this trend better than mixing of waters from two sources. $\delta^{13}C_{DIC}$ was the lightest in fall, i.e. out-of-phase with groundwater alkalinity (Fig. 3.5c, d). Possible factors contributing to the seasonal variations in groundwater $\delta^{13}C_{DIC}$ are:

**1. Soil air $CO_2$ isotopic composition.** Respiration isotope signature did not exhibit a smooth annual trend and corresponded to the plant and SOM composition (*5.1*). Groundwater $\delta^{13}C_{DIC}$ values demonstrated less variability than $\delta^{13}C_{CO2}$, probably because gas-phase $CO_2$ was affected by short-term, moisture-related variations of $\delta^{13}C$ from soil respiration. Mixing with isotopically light atmospheric $CO_2$ that was expected to be measureable in the winter, when $pCO_2$ in soil is low, was limited to the upper 15 cm of the soil, and so is not an important factor.

**2. $pCO_2$ and pH.** The enrichment factor between the gaseous $CO_2$ and DIC depends on the molar fractions of aqueous carbonate species, thus $\delta^{13}C_{DIC}$ is pH-dependent. During the growing season, when $pCO_2$ was the highest, pH became lower, and thus the enrichment factor was the smallest due to increased molar fraction of $H_2CO_3$, which has the lightest carbon isotope composition in equilibrium with the gaseous $CO_2$ (Fig. F.2). In order to evaluate the effect of $pCO_2$, an open-system dissolution of calcite was modeled for the highest and the lowest values

measured during the year. Figure 3.7 shows $Ca^{2+}$ and alkalinity concentrations in samples from 2-5 Mor plotted along the line produced by calcite equilibrium over the measured range of soil air $CO_2$. Dissolved calcium concentrations calculated for the condition of equilibrium with calcite over the measured range of soil air $CO_2$ are very similar to the measured $Ca^{2+}$ concentrations. Alkalinities calculated for equilibrium with calcite are lower than measured values (Fig 3.7b). Additional bicarbonate might be formed during oxidation of organic matter or dissolution of dolomite or feldspar. Figure 3.7 suggests that seasonal variations in $pCO_2$ explain the observed $\delta^{13}C_{DIC}$ decrease with increasing Ca and alkalinity, as well as its overall 2–3‰ range.

**3. Temperature.** The carbon-isotope fractionation factor is directly proportional to temperature (Eq 5.1-5.3). The seasonal range of soil temperatures can cause up to 1.5‰ variations in $\delta^{13}C_{DIC}$, assuming constant $pCO_2$. On the other hand, temperature also controls dissociation constants in the system $CO_2$-$H_2O$-$CaCO_3$. The combination of these effects is that lower temperatures should result in heavier DIC and higher calcite solubility.

$\delta^{13}C_{DIC}$ was simulated for each sampling date, taking into the account the combined effect of factors 1, 2, and 3. Figure 3.8 shows the calculated and measured values. Calculated values, no matter which method was used to estimate pH, showed a difference from the measured values within 0.5‰, except during the middle of the growing season and early spring when measured $\delta^{13}C_{DIC}$ were up to 3.5‰ higher than predicted. This could be due to flooding of the soil during large storm events and/or lowest rates of soil respiration, either of which might reduce the openness of the system. If this was the case, then DIC was unable to equilibrate isotopically with soil air $CO_2$, and the heavier isotope values results from the contribution from limestone dissolution. Ideally, for the closed system:

$$\delta^{13}C_{DIC} = \left(mH_2CO_3 \times \delta^{13}C_{H_2CO_3} + mHCO_3^- \times \delta^{13}C_{HCO_3^-} + mCO_3^{2-} \times \delta^{13}C_{CO_3^{2-}}\right) + (mCa^{2+} \times \delta^{13}C_{limestone})/DIC \,. \quad (5.7)$$

Two parameters that exhibited a clear annual cycle, temperature and $pCO_2$, affect limestone dissolution and isotope fractionation in the opposite manner. However $pCO_2$ has the greater effect on calcite solubility (Fig. F.1) and isotope enrichment, causing $\delta^{13}C_{DIC}$ to be the lightest in the late growing season. The primary importance of temperature is in controlling respiration rate that in turn controls soil $CO_2$ concentration.

## 6. Conclusions

Sources and seasonal trends of dissolved inorganic carbon (DIC) in the shallow limestone aquifer were studied at the N04d watershed in the Konza Prairie LTER Site from spring 2010 to spring 2011. Annual cycles of soil air $CO_2$, groundwater DIC, and isotope characteristics of those two showed a strong dependency on weather and photosynthate production, particularly on respiration rate, temperature, and moisture content.

Soil air $CO_2$ reached its annual maximum in July to early August, when moisture was not limiting to soil respiration. Following the maximum was a depth-dependent decrease in $CO_2$ because of moisture deficiency in the late summer and temperature decline in the fall and winter: $CO_2$ decreased earliest in the shallowest part of the soil and latest at the deepest depth monitored. The isotopic composition of $CO_2$ under warm-season grasses exhibited $C_4$ plant signature becoming heavier during the extended dry periods and lighter during following intensive precipitation periods, events.

Soil $CO_2$ and dissolution of carbonate minerals are the two main sources of DIC in the shallow limestone aquifer (Fig. 3.9). DIC can be produced in soil, where recharge water reacts with soil $CO_2$ and dissolves soil carbonates. In the aquifer DIC is produced during reaction with $CO_2$ in the soil atmosphere at the water table and dissolution of the Morrill limestone. An annual cycle of groundwater $CO_2$ and DIC with the maximum during the late growing season was influenced by seasonal variations in $CO_2$ respiration rate with a 2–3 months lag time between maximas, probably related to the transport time of soil $CO_2$ to the saturated zone.

$\delta^{13}C$ values of DIC were enriched in 7–10‰ relative to $CO_2$ source due to isotope fractionation between gas and water in an open system that allowed fast equilibration of all DIC produced with the large reservoir of soil $CO_2$. Difference in isotopic $\delta^{13}C_{DIC}$ between the wells could reflect the proportion of root respiration of $C_4$ and $C_3$ plants near each well site.

High $pCO_2$ in soil leads to limestone dissolution and increased groundwater DIC during the growing season. High $pCO_2$ also lowers pH, thereby increasing the molar fraction of carbonic acid in DIC and shifting $\delta^{13}C_{DIC}$ towards lighter values. Higher temperature has the opposite effect on DIC, because of retrograde calcite solubility, and the similar effect on the isotopic composition, because the enrichment factor between gaseous $CO_2$ and aqueous carbonate species is inversely proportional to the temperature. Therefore, seasonal variation of $pCO_2$ was the more important control on $\delta^{13}C_{DIC}$, and resulted in $\delta^{13}C_{DIC}$ being out-of-phase with groundwater

alkalinity, $pCO_2$, and temperature: $\delta^{13}C_{DIC}$ was the most negative (lightest) in the late growing season. Very high moisture content due to storm events may limit the openness of the system, so that the isotopically heavy carbon from limestone dissolution may also affect $\delta^{13}C_{DIC}$.

Previous investigations at Konza Prairie showed groundwater $pCO_2$ has been increasing at the Konza Prairie over the last 15 years (Macpherson et al., 2008). The results presented here show that the dominant control on groundwater $\delta^{13}C_{DIC}$ is the seasonal variation in soil $pCO_2$, with perturbation of trends caused by storm events and soil moisture deficit. The combination of increasing soil respiration rates (Bond-Lamberty and Thompson, 2010) and predicted climate change in this region toward increasing temperature and frequency of extreme rainfall events (McCarthy et al., 2001) suggests that the future may be characterized by higher carbon flux to the saturated zone intensifying weathering and groundwater acidification (Macpherson et al, 2011).

## References


Andrews, J.A., Schlesinger, W.H., 2001. Soil $CO_2$ dynamics, acidification, and chemical weathering in a temperate forest with experimental $CO_2$ enrichment. Global Biogeochem. Cycles 15, 149-162.

Appelo, C.A.J.P., D., 2005. Geochemistry, Groundwater, and Pollution, 2 ed. Balkema, Rotterdam.

Atekwana, E.A., Krishnamurthy, R.V., 1998. Seasonal variations of dissolved inorganic carbon and $\delta^{13}C$ of surface waters: application of a modified gas evolution technique. Journal of Hydrology 205, 265-278.

Aucour, A.-M., Sheppard, S.M.F., Guyomar, O., Wattelet, J., 1999. Use of $^{13}C$ to trace origin and cycling of inorganic carbon in the Rhône river system. Chemical Geology 159, 87-105.

Badalucco, L., Nannipieri, P., 2007. Nutrient Transformations in the Rhizosphere, in: Pinton, R., Varanini, Z., Nannipieri, P. (Eds.), The Rhizosphere, 2 ed. CRC Press, pp. 111-133.

Bahn, M., Schmitt, M., Siegwolf, R., Richter, A., Brüggemann, N., 2009. Does photosynthesis affect grassland soil-respired $CO_2$ and its carbon isotope composition on a diurnal timescale? New Phytologist 182, 451-460.

Bond-Lamberty, B., Thomson, A., 2010. Temperature-associated increases in the global soil respiration record. Nature 464, 579-582.

Bottinga, Y., 1968. Calculation of fractionation factors for carbon and oxygen isotopic exchange in the system calcite-carbon dioxide-water. The Journal of Physical Chemistry 72, 800-808.

Bowling, D., McDowell, N., Bond, B., Law, B., Ehleringer, J., 2002. $^{13}C$ content of ecosystem respiration is linked to precipitation and vapor pressure deficit. Oecologia 131, 113-124.

Cerling, T.E., 1984. The stable isotopic composition of modern soil carbonate and its relationship to climate. Earth and Planetary Science Letters 71, 229-240.

Cerling, T.E., Quade, J., Wang, Y., Bowman, J.R., 1989. Carbon isotopes in soils and palaeosols as ecology and palaeoecology indicators. Nature 341, 138-139.

Cerling, T.E., Solomon, D.K., Quade, J., Bowman, J.R., 1991. On the isotopic composition of carbon in soil carbon dioxide. Geochimica et Cosmochimica Acta 55, 3403-3405.

Chiodini, G., Frondini, F., Kerrick, D.M., Rogie, J., Parello, F., Peruzzi, L., Zanzari, A.R., 1999. Quantification of deep $CO_2$ fluxes from Central Italy. Examples of carbon balance for regional aquifers and of soil diffuse degassing. Chemical Geology 159, 205-222.

Clark, I., Fritz, P., 1997. Environmental Isotopes in Hydrogeology. Lewis Publishers, Boca Raton.

Deines, P., Langmuir, D., Harmon, R.S., 1974. Stable carbon isotope ratios and the existence of a gas phase in the evolution of carbonate ground waters, Geochimica et Cosmochimica Acta, pp. 1147-1164.

DeLuca, T.H., Zabinski, C.A., 2011. Prairie ecosystems and the carbon problem. Frontiers in Ecology and the Environment 9, 407-413.

Doctor, D.H., Kendall, C., Sebestyen, S.D., Shanley, J.B., Ohte, N., Boyer, E.W., 2008. Carbon isotope fractionation of dissolved inorganic carbon (DIC) due to outgassing of carbon dioxide from a headwater stream. Hydrological Processes 22, 2410-2423.

Ekblad, A., Boström, B., Holm, A., Comstedt, D., 2005. Forest soil respiration rate and $\delta^{13}C$ is regulated by recent above ground weather conditions. Oecologia 143, 136-142.

Fessenden, J.E., Ehleringer, J.R., 2003. Temporal variation in $\delta^{13}C$ of ecosystem respiration in the Pacific Northwest: links to moisture stress. Oecologia 136, 129-136.

Freeman, C.C., 1998. The flora of Konza Prairie: a historical review and contemporary patterns, in: Knapp, A.K., Briggs, J.M., Hartnett, D.C., Collins, S.L. (Eds.), Grassland Dynamics – Long-Term Ecological Research in Tallgrass Prairie. Oxford University Press, New York, pp. 69-80.

Fritz, P., Reardon, E.J., Barker, J., Brown, R.M., Cherry, J.A., Killey, R.W.D., McNaughton, D., 1978. The carbon isotope geochemistry of a small groundwater system in northeastern Ontario. Water Resour. Res. 14, 1059-1067.

Galimov, E.M., 1966. Carbon isotopes of soil $CO_2$. Geochemistry International 3, 889-897.

Gray L. J., M.G.L., Koelliker J. K. and Dodds W. K., 1998. Hydrology and aquatic chemistry, in: Knapp, A.K., Briggs, J.M., Hartnett, D.C., Collins, S.L. (Eds.), Grassland Dynamics – Long-Term Ecological Research in Tallgrass Prairie. Oxford University Press, New York, pp. 159-176.

Harper, C.W., Blair, J.M., Fay, P.A., Knapp, A.K., Carlisle, J.D., 2005. Increased rainfall variability and reduced rainfall amount decreases soil $CO_2$ flux in a grassland ecosystem. Global Change Biology 11, 322-334.

Hayden, B., 1998. Regional climate and the distribution of tallgrass prairie, in: Knapp, A.K., Briggs, J.M., Hartnett, D.C., Collins, S.L. (Eds.), Grassland Dynamics – Long-Term Ecological Research in Tallgrass Prairie Oxford University Press, New York, pp. 19–34.

Jackson, R.B., Cook, C.W., Pippen, J.S., Palmer, S.M., 2009. Increased belowground biomass and soil $CO_2$ fluxes after a decade of carbon dioxide enrichment in a warm-temperate forest. Ecology 90, 3352-3366.

Johnson, W.C., Willey, K.L., Macpherson, G.L., 2007. Carbon isotope variation in modern soils of the tallgrass prairie: Analogues for the interpretation of isotopic records derived from paleosols. Quaternary International 162-163, 3-20.

Kanduč, T., Szramek, K., Ogrinc, N., Walter, L.M., 2007. Origin and Cycling of Riverine Inorganic Carbon in the Sava River Watershed (Slovenia) Inferred from Major Solutes and Stable Carbon Isotopes. Biogeochemistry 86, 137-154.

Keller, C.K., Bacon, D.H., 1998. Soil respiration and georespiration distinguished by transport analyses of vadose $CO_2$, $^{13}CO_2$, and $^{14}CO_2$. Global Biogeochem. Cycles 12, 361-372.

Kessler, T.J., Harvey, C.F., 2001. The global flux of carbon dioxide into groundwater. Geophys. Res. Lett. 28, 279-282.

Knapp, A.K., Seastedt, T.R., 1998. Grasslands, Konza Prairie, and Long-Term Ecological Research, in: Knapp, A.K., Briggs, J.M., Hartnett, D.C., Collins, S.L. (Eds.), Grassland Dynamics—Long-Term Ecological Research in Tallgrass Prairie. Oxford University Press, New York, pp. 3-15.

Lai, C.-T., Riley, W., Owensby, C., Ham, J., Schauer, A., Ehleringer, J.R., 2006. Seasonal and interannual variations of carbon and oxygen isotopes of respired $CO_2$ in a tallgrass prairie: Measurements and modeling results from 3 years with contrasting water availability. J. Geophys. Res. 111, D08S06.

Lai, C.-T., Schauer, A.J., Owensby, C., Ham, J.M., Ehleringer, J.R., 2003. Isotopic air sampling in a tallgrass prairie to partition net ecosystem $CO_2$ exchange. J. Geophys. Res. 108, 4566.

Lin, G., Ehleringer, J.R., Rygiewicz, P.T., Johnson, Mark G., Tingey, David T., 1999. Elevated $CO_2$ and temperature impacts on different components of soil $CO_2$ efflux in Douglas-fir terracosms. Global Change Biology 5, 157-168.

Liu, Z., Dreybrodt, W., Wang, H., 2008. A possible important $CO_2$ sink by the global water cycle. Chinese Science Bulletin 53, 402-407.

Luo, Y., Zhou, X., 2006. Soil Respiration and the Environment. Academic Press, Burlington.

Macpherson, G.L., 1996. Hydrogeology of thin limestones: the Konza Prairie Long-Term Ecological Research Site, Northeastern Kansas. Journal of Hydrology 186, 191-228.

Macpherson, G.L., Roberts, J.A., Blair, J.M., Townsend, M.A., Fowle, D.A., Beisner, K.R., 2008. Increasing shallow groundwater $CO_2$ and limestone weathering, Konza Prairie, USA. Geochimica et Cosmochimica Acta 72, 5581-5599.

Macpherson, G.L., Tsypin, M.A., Roberts J.A., Ching, G.B., 2011. Natural groundwater acidification by increasing $CO_2$, Geological Society of America Abstracts with Programs, Vol. 43, No. 5, p. 110.

Mazzullo, S., Boardman, D., Grossman, E., Dimmick-Wells, K., 2007. Oxygen-carbon isotope stratigraphy of upper carboniferous to lower Permian marine deposits in Midcontinent U.S.A. (Kansas and ne Oklahoma): Implications for sea water chemistry and depositional cyclicity. Carbonates and Evaporites 22, 55-72.

McCarron, J.K., Knapp, A.K., 2001. $C_3$ woody plant expansion in a $C_4$ grassland: are grasses and shrubs functionally distinct? American Journal of Botany 88, 1818-1823.

McCarthy J, C.O., Leary N, Dokken D, White K, 2001. Climate Change 2001: Impacts, Adaptation, and Vulnerability. Contribution of Working Group II to the Third Assessment Report of the Intergovernmental Panel on Climate Change., Cambridge.

Mook, W.G., Bommerson, J.C., Staverman, W.H., 1974. Carbon isotope fractionation between dissolved bicarbonate and gaseous carbon dioxide. Earth and Planetary Science Letters 22, 169-176.

Newell, K.D., Watney, W. L., Cheng, S. W. L., and Brownrigg, R. L., 1987. Stratigraphic and spatial analysis of oil and gas production in Kansas, Kansas Geological Survey Subsurface Geology Series 9, p. 86.

Nippert, J., Knapp, A., 2007. Linking water uptake with rooting patterns in grassland species. Oecologia 153, 261-272.

O'Leary, M.H., 1988. Carbon Isotopes in Photosynthesis. BioScience 38, 328-336.

Pomes, M.L., 1995. A study of the aquatic humic substances and hydrogeology in a prairie watershed, use of humic material as a tracer of recharge through soils. Ph.D. thesis, University of Kansas, p. 296.

Quay, P.D., Emerson, S.R., Quay, B.M., Devol, A.H., 1986. The Carbon Cycle for Lake Washington-A Stable Isotope Study. Limnology and Oceanography 31, 596-611.

Reardon, E.J., Allison, G.B., Fritz, P., 1979. Seasonal chemical and isotopic variations of soil $CO_2$ at Trout Creek, Ontario. Journal of Hydrology 43, 355-371.

Rightmire, C.T., Hanshaw, B.B., 1973. Relationship between the carbon isotope composition of soil $CO_2$ and dissolved carbonate species in groundwater. Water Resour. Res. 9, 958-967.

Sala, O.E., 2001. Temperate grasslands, in: F.S. Chapin, O.E.S., E. Huber-Sannwald (Ed.), Global Biodiversity in a Changing Environment: Scenarios for the 21st Century. Springer-Verlag, New York, NY, USA, pp. 121–137.

Schiff, S.L., Aravena, R., Trumbore, S.E., Dillon, P.J., 1990. Dissolved Organic Carbon Cycling in Forested Watersheds: A Carbon Isotope Approach. Water Resour. Res. 26, 2949-2957.

Schoell, M., 1988. Multiple origins of methane in the Earth. Chemical Geology 71, 1-10.

Tans, P.P., Berry, J.A., Keeling, R.F., 1993. Oceanic $^{13}C/^{12}C$ observations: A new window on ocean $CO_2$ uptake. Global Biogeochem. Cycles 7, 353-368.

Torn, M.S., Biraud, S.C., Still, C.J., Riley, W.J., Berry, J.A., 2011. Seasonal and interannual variability in $^{13}C$ composition of ecosystem carbon fluxes in the U.S. Southern Great Plains. Tellus B 63, 181-195.

Towne, E.G., 2002. Vascular plants of Konza Prairie Biological Station: an annotated checklist of species in a Kansas tallgrass prairie. Sida 20, 269-294.

Wachniew, P., Różański, K., 1997. Carbon budget of a mid-latitude, groundwater-controlled lake: Isotopic evidence for the importance of dissolved inorganic carbon recycling. Geochimica et Cosmochimica Acta 61, 2453-2465.

USDA-NRCS, 2007. U.S. Department of Agriculture, National Resources Conservation Service. http://websoilsurvey.nrcs.usda.gov/app/WebSoilSurvey.aspx.

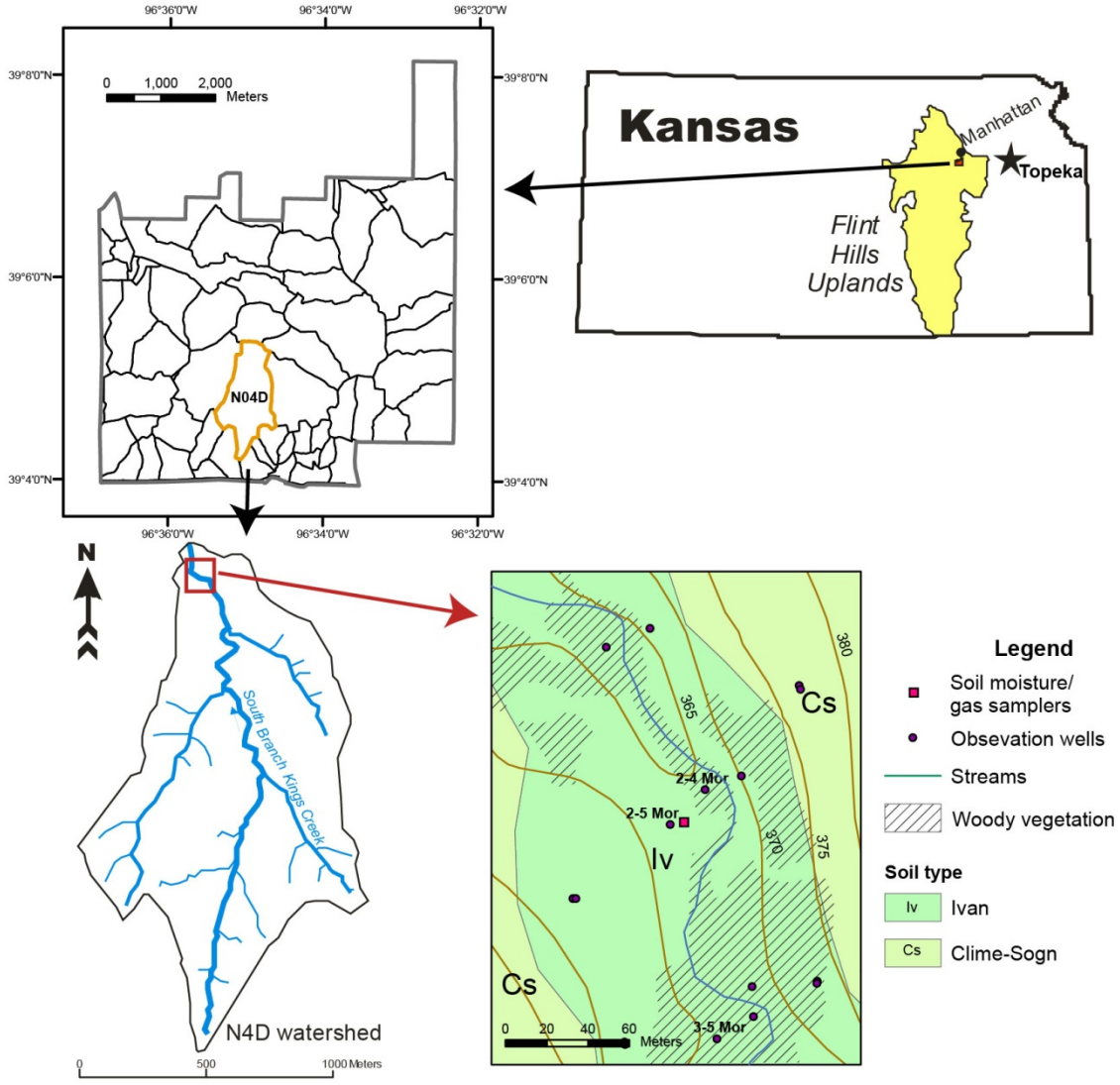


Figure 3.1. Location of the study area.

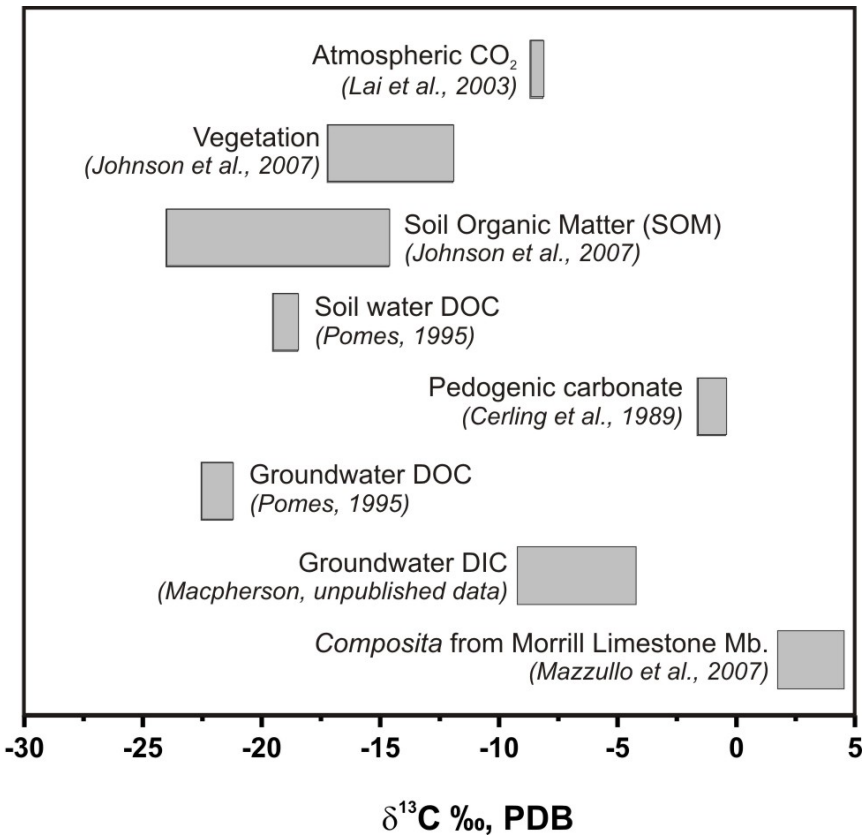


Figure 3.2. $\delta^{13}C$ values in some carbon reservoirs at Konza Prairie.

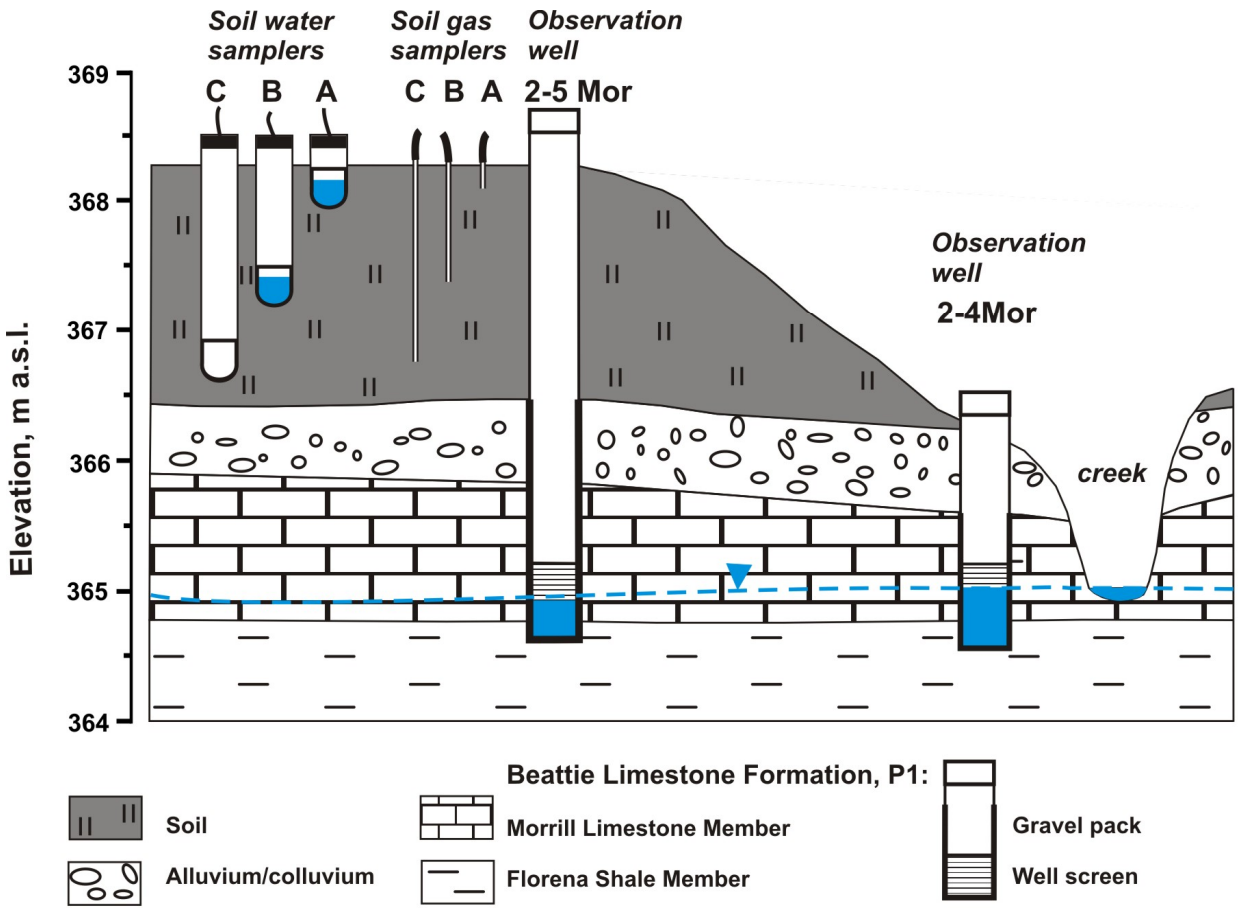


Figure 3.3. Schematic design of the sampling site. Thickness of soil is 180 cm at the soil-sampler location and it decreases towards the stream. Limestone-chert colluvium-alluvium is thickest on the floodplain. The Morrill Limestone aquifer, 90-30 cm thick, is exposed and on the bottom and the sides of the stream. Groundwater level is within the limestone layer, with an average depth below the ground surface of 320 cm (well 2-5 Mor) and 150 cm (well 2-4 Mor).

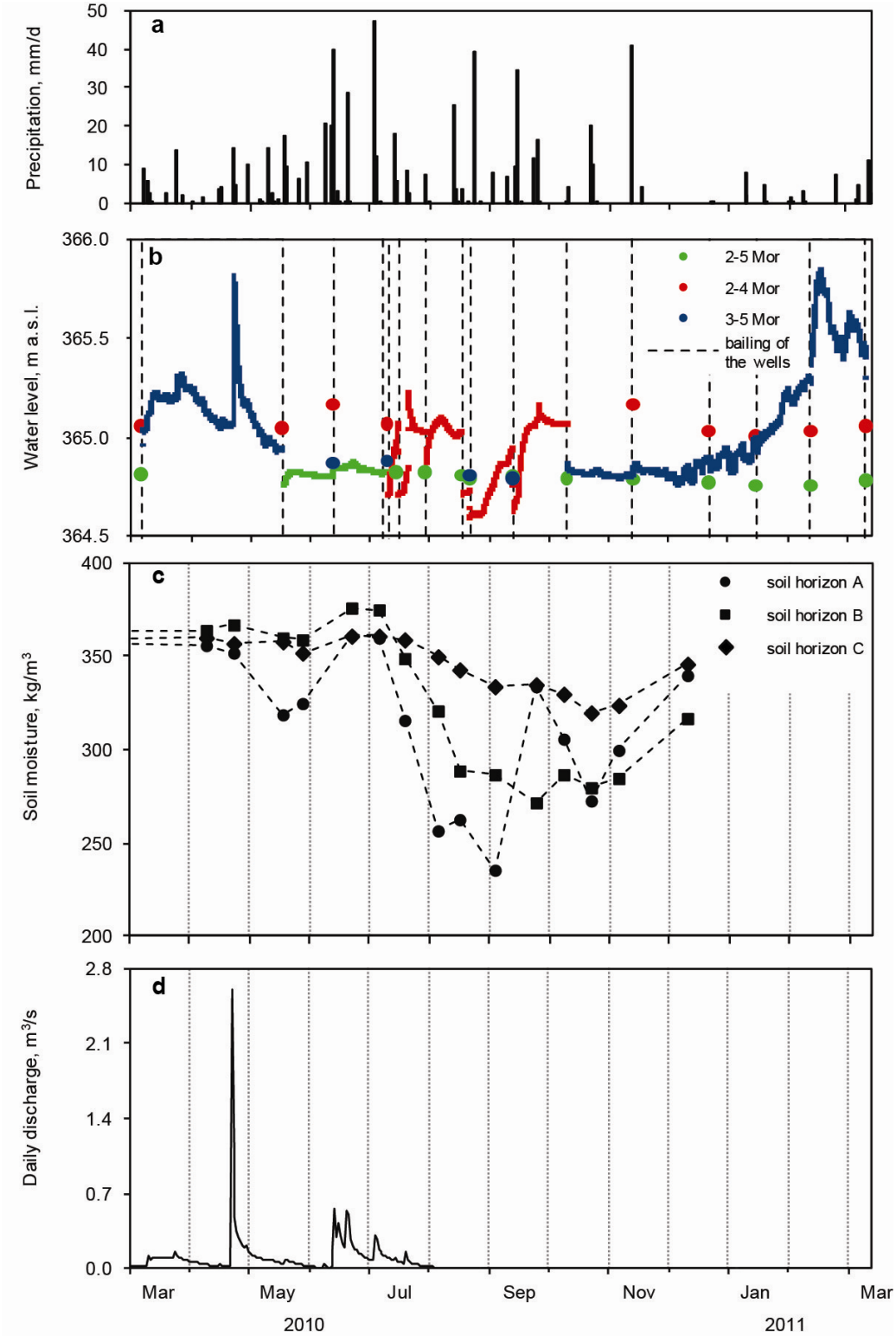


Figure 3.4. The effect of precipitation on (a) water level in three observation wells measured with the pressure transducer (lines) and e-line (circles) (b), soil moisture content (c), and discharge of Kings Creek (USGS gauging station 0679650) (d).

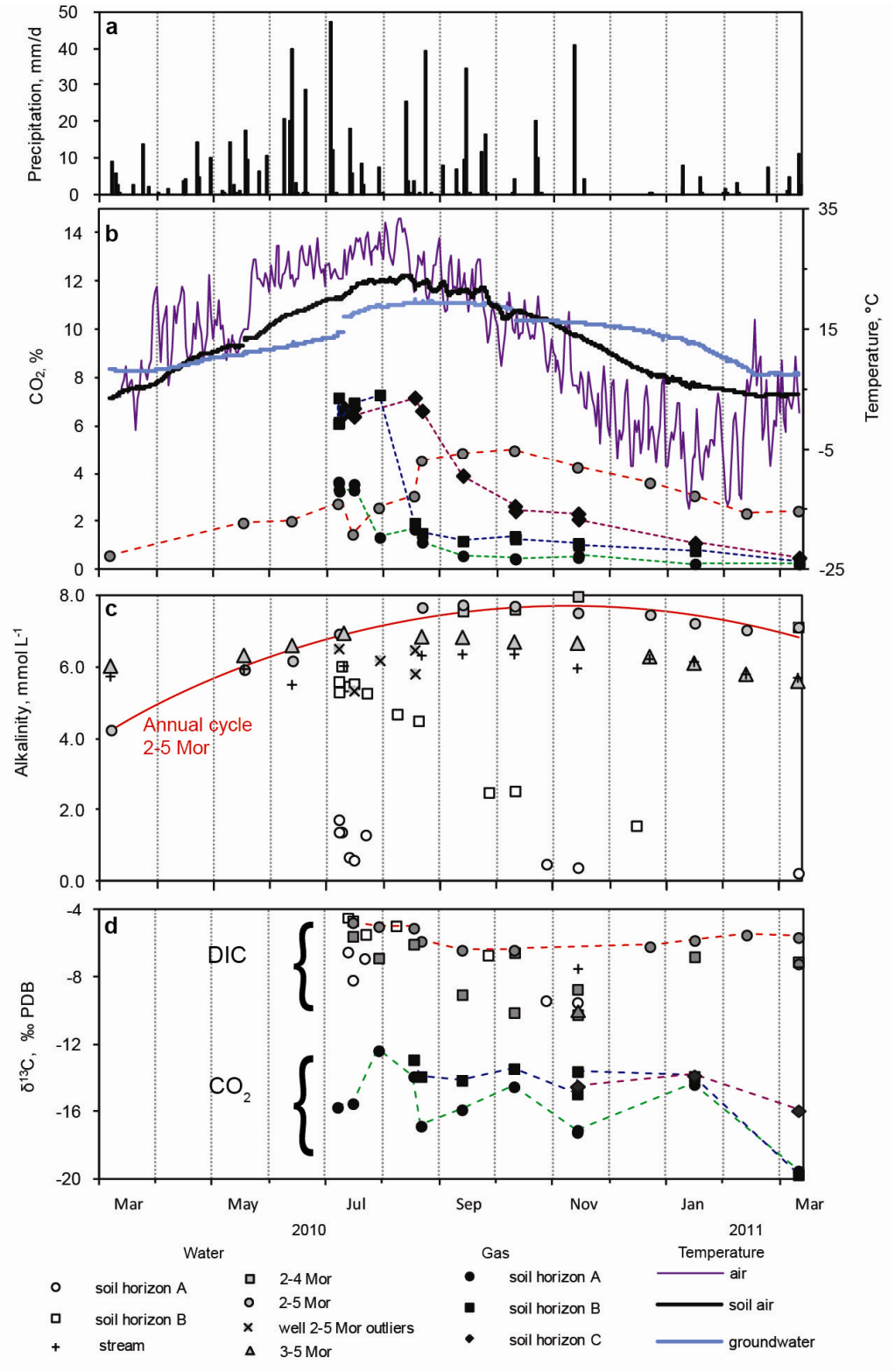


Figure 3.5. Precipitation and measured chemical and isotopic characteristics of carbon-containing species. There is an annual trend of alkalinity in groundwater. Outliers for 2-5 Mor were caused by dilution due to recharge and are excluded from the trend.

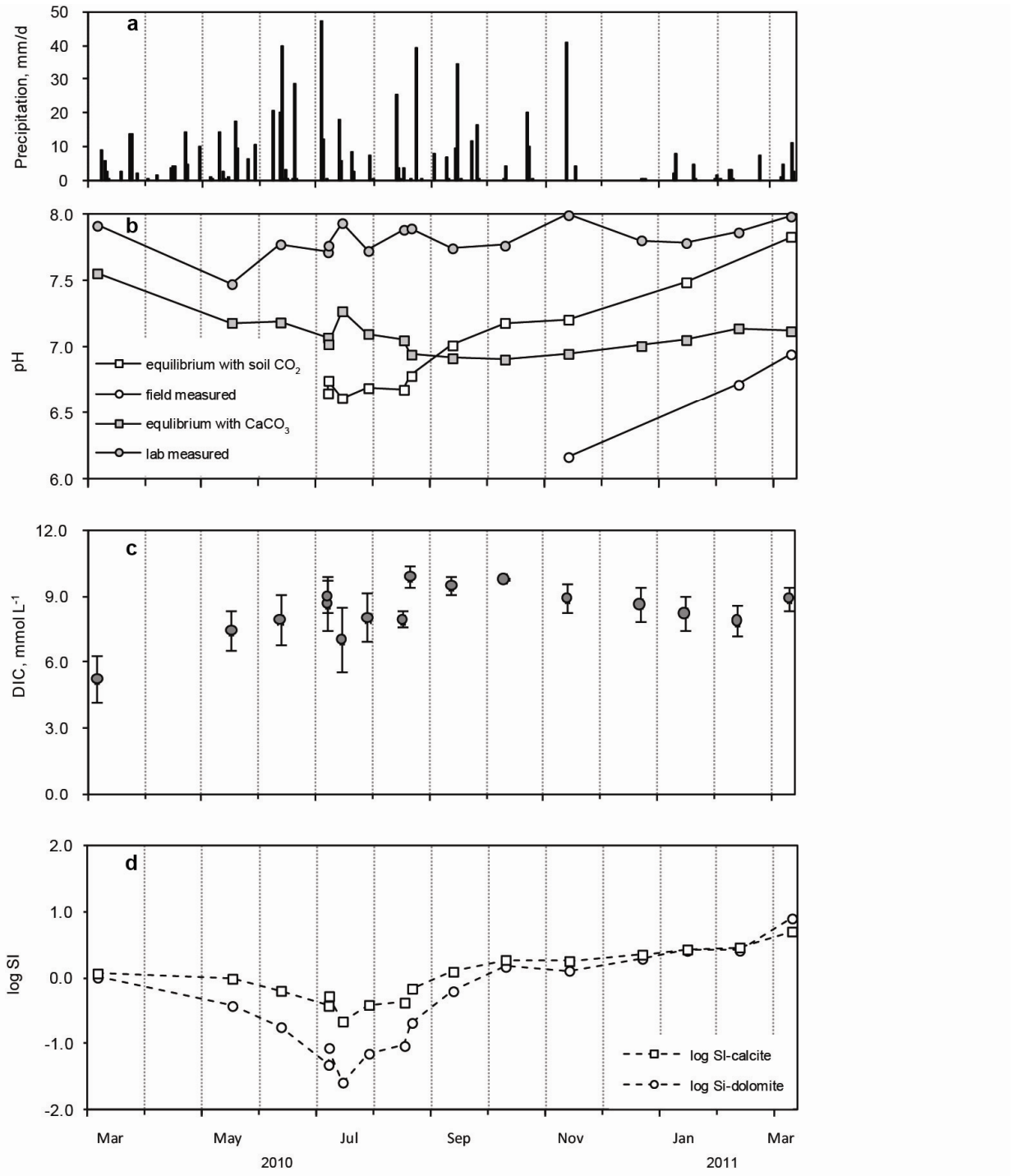


Figure 3.6. Meteoric precipitation (a), pH (b), DIC (c) and carbonate-mineral saturation in groundwater from 2-5 Mor (d). pH was determined using four different methods (see text for details). DIC was calculated using the average pH estimated from calcite equilibrium and soil $CO_2$ equilibrium methods. The saturation indexes for calcite and dolomite were calculated using estimated pH and measured alkalinity.

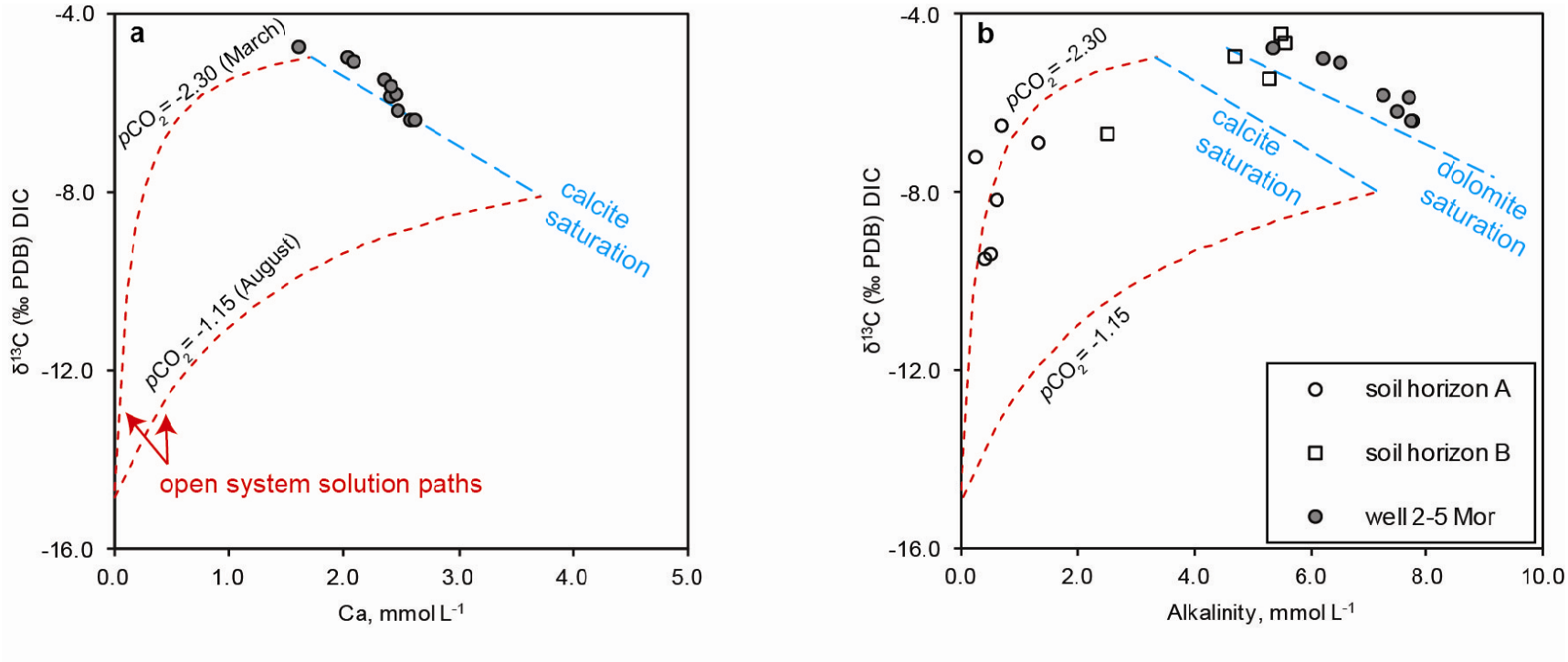


Figure 3.7. $\delta^{13}C_{DIC}$ plotted against (a) calcium concentration and (b) alkalinity. Open system solution path was modeled for the lowest and highest soil $pCO_2$ measured during the year. Soil water $\delta^{13}C_{DIC}$ exhibits a positive trend with alkalinity and $Ca^{2+}$ concentration (not shown), and fall near the ideal curve describing calcite dissolution in a system open to soil $CO_2$. The trend also shows that there is an increase of the degree of saturation, with respect to calcite, with depth in the soil. Groundwater data fall close to the carbonate-mineral saturation lines, and within the measured range of $pCO_2$. Excess alkalinity may be explained by dolomite dissolution.

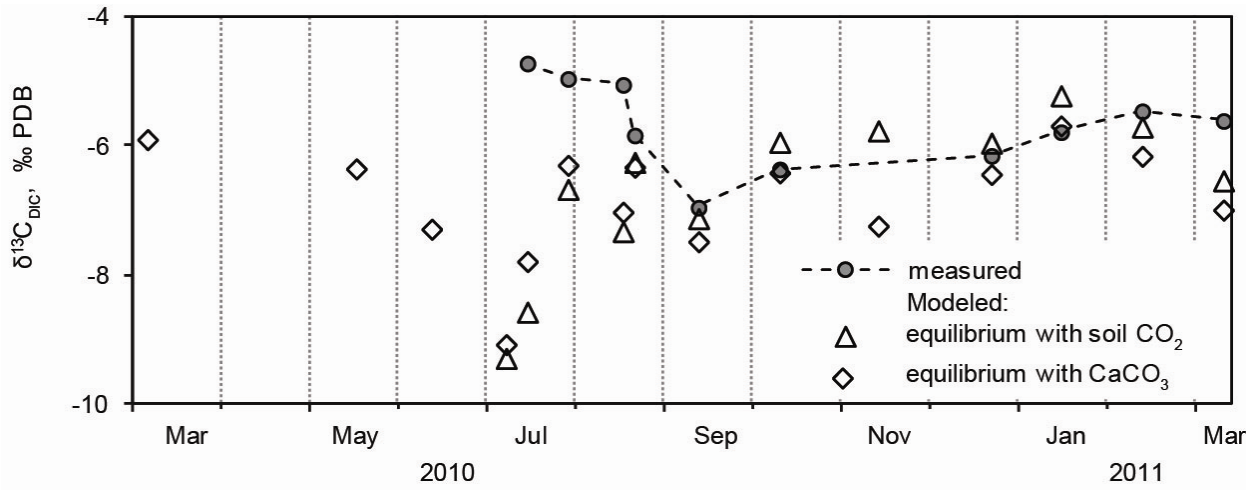


Figure 3.8. Measured and calculated $\delta^{13}C_{DIC}$ for each sampling event. Calculated values used field-measured $pCO_2$, $\delta^{13}C_{CO2}$, temperature, and molar fractions of carbonate aqueous species for pH that was estimated assuming equilibrium with soil $CO_2$ or with calcite (Fig. 3.6b).

.

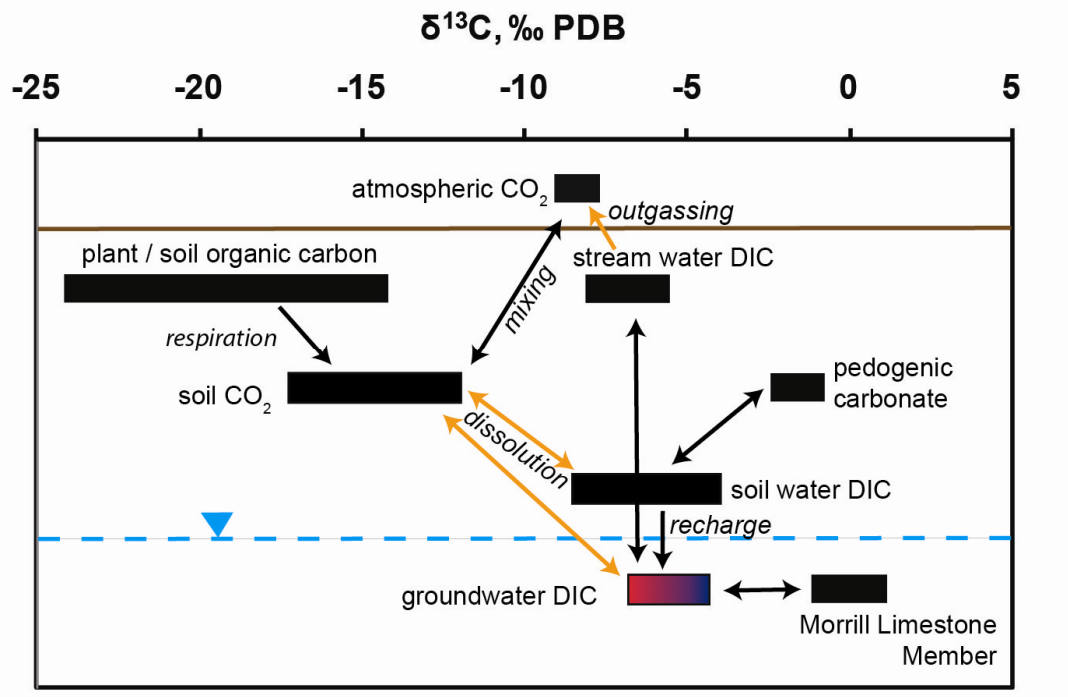


Figure 3.9. Sources of shallow groundwater DIC in Konza Prairie. Orange arrows denote reactions with isotope fractionation between the water and gas phase.

# APPENDICIES

## Appendix A. Research site

At the N04d watershed, bedrock exposed at the surface is composed of Lower Permian couplets of limestone and shale from the Council Grove Group of the Wolfcampian Series (Fig. A.1). The Morrill Limestone Member of the Beattie Limestone hosts the aquifer considered in this research project.

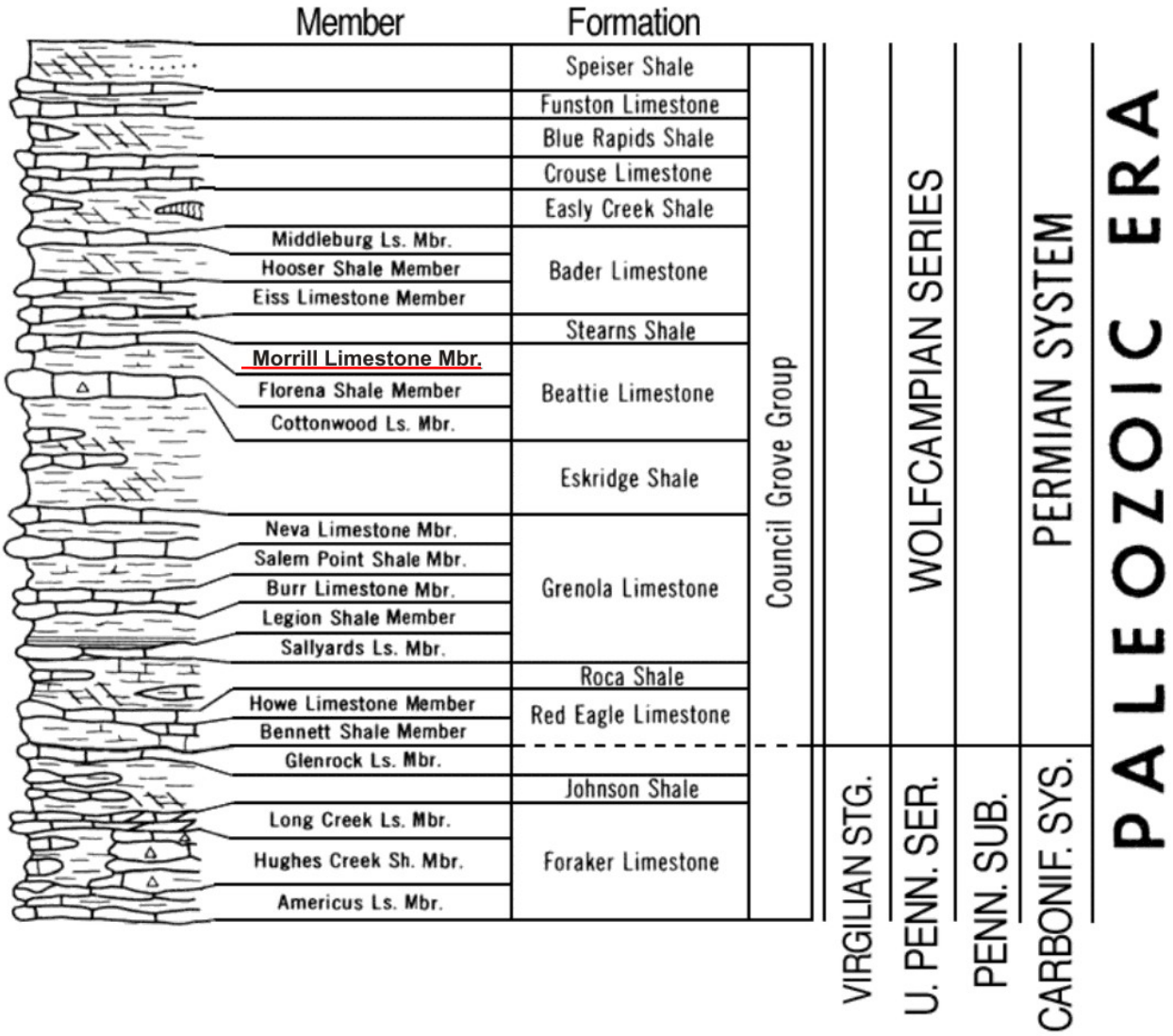


Figure A.1. The stratigraphic succession of Council Grove Group in Kansas (Zeller, 1968).

Table A.1. Characteristics of the Ivan soil series at the study location (Wehmueller et al., 2005). Soils at the sampling location were diagnosed as Ivan silt loam (USDA-NRCS, 2007) or Tully silty clay loam (Pomes, 1995). Ivan is typical for less than 0–3° slopes, while Tully is formed on 3–7° slopes (USDA-NRCS, 2007).

| **Horizon** | **Depth, cm** | **Corg, %** | **$CaCO_3$, <2 mm %** | **pH 1:1 $H_2O$** | **Water content @ 1500 kPa** |
|---|---|---|---|---|---|
| A1 | 0-12 | 5.94 | | 6.7 | 22.9 |
| A2 | 12-33 | 2.99 | | 7.1 | 20.3 |
| A3 | 33-43 | 2 | 3 | 7.6 | 18.7 |
| BW1 | 43-53 | 1.09 | 12 | 7.8 | 15.3 |
| BW2 | 53-68 | 0.69 | 19 | 7.9 | 13.7 |
| 2BWB | 68-86 | 0.63 | 19 | 8 | 14.6 |
| 2C | 86-121 | 0.45 | 27 | 8 | 13.1 |
| 3BWB1 | 121-140 | 0.71 | 5 | 8 | 18.2 |
| 3BWB2 | 140-155 | 0.63 | 4 | 8 | 18.7 |
| 4R | 155-156 | | | | 3.3 |

# Appendix B. Methods

In order to test the proposed hypothesis a set of hydrogeological methods was used that included field (site description, on-site measurements, sampling), laboratory work (stable isotope and chemical analysis), and geochemical computer modeling. Long-term detailed meteorological data, available through Konza Prairie LTER (http://www.konza.ksu.edu) and Weather Underground (http://www.wunderground.com) online databases, demonstrated that the best target window for assessing the effect of recharge events is late May through November with most intensive storms typically occurring between July and October.

The field part of the experiment (Fig. B.1) lasted from March 2010 until March 2011, which allowed data collection representing an annual cycle of chemical constituents. Soil water and soil gas samplers were installed in July 2010. Thus, the most extensive sampling was performed between July and November 2010, i.e. from the peak growing season to the late growing season. Ideally, soil water and groundwater should have been collected before the rain, in the beginning, at the highest point, before the end and after the end of the storm to observe the recovery behavior. But in fact, the maximum number of sampling event within one day was no more than two, because of the slow recovery of the water level in wells and slow soil moisture collection in samplers.

## Water-level monitoring

A total of 31 wells were installed in this watershed by the U.S. Geological Survey (Lawrence, KS) during 1988-1990 (Macpherson, 1996) with 4 additional wells installed in 1997 (Macpherson, personal communication, 2011). Three wells were used to monitor water level with Solinst® logger set at a 5-min increment. Data presented for May-July 2010 period is from the well 2-5 Mor, for July-October 2010 - from the well 2-4 Mor, for October 2010 - March 2011 from the well 3-5 Mor. In addition to that, depth to groundwater was measured in all the wells at least once a month with an electric sounder.

Each water-level logging set combines pressure transducer, data logger, battery, and temperature sensor with the ability to program the frequency of measurements. The Levellogger® submerged in the middle part of the water column recorded the hydrostatic pressure and groundwater temperature, while the Barologger® recorded barometric pressure

above the water for accurate barometric compensation. Once a month, the data files are downloaded to Leveloader® data transfer unit in the field and after that copied to the PC in the lab. To obtain absolute water level for any pressure transducer measurement, following calculations must be done:

$WL = (WC-WC_0)+LL+ h_{LL} - h_0 = (WC-WC_0)+(MP-h_{LL})+h_{LL}-h_0= (WC-WC_0) + (MP-h_0) = (WC-WC_0) -WL_0 = (LL-BL)-(LL-BL)_0-WL_{0,}$

where

WC - thickness of water column above Levellogger®; WC = LL−BL,

**LL** -water elevation above the Levellogger® (Levellogger® measurement),

**BL** - barometric pressure (Barologger® measurement),

WL - absolute elevation (relative to sea level) of water level. WL = MP−h,

LL - Levelloger® absolute elevation; $LL= MP-h_{LL,}$

MP - absolute elevation of the measuring point,

**h** - depth to water measured with e-line,

$h_{LL}$ - depth of Levellogger®,

$_0$ - initial time, when **h** is measured and loggers are reset.

## Groundwater sampling

The sampling was performed on a monthly basis. In addition to that, in the summer, the sampling was performed in conjunction with extreme recharge events, defined as heavy and relatively short-duration rains. Wells were bailed with a Teflon® bailer suspended on a Teflon®-coated wire to remove stagnant water prior to water sampling. The amount of water in the wells was small and recovery rate was slow. This precluded discarding a volume equivalent to at least twice the volume of water within the casing and gravel pack before sample collection. Collected groundwater was poured into sampling bottle using a Teflon® bottom emptying device. Samples were stored in a cold place (ice chest in the field; non-frost-free refrigerator in the lab) until water was analyzed.

The following containers were used for the water samples collection:

- 60 ml low-density polyethylene (LDPE) bottles - for alkalinity determination and anions analysis.

- 60 ml low-density polyethylene (LDPE) pre-weighed bottles - for cations analysis.
- 30 ml glass vials with septum cap - for $\delta^{13}C_{DIC}$ determination
- 25 ml polyethylene (HDPE) bottles - for $\delta^{18}O$ and $\delta D$ determination in water.

In order re-establish connection between the well and the aquifer, 3 L of water were injected in 2-5 Mor before the regular groundwater sampling had started. The well was then bailed intensively to remove all the water. Injected water contained KCl tracer of known concentration that permitted tracing of the water chemistry stabilization after the bailing (Fig. B.2).

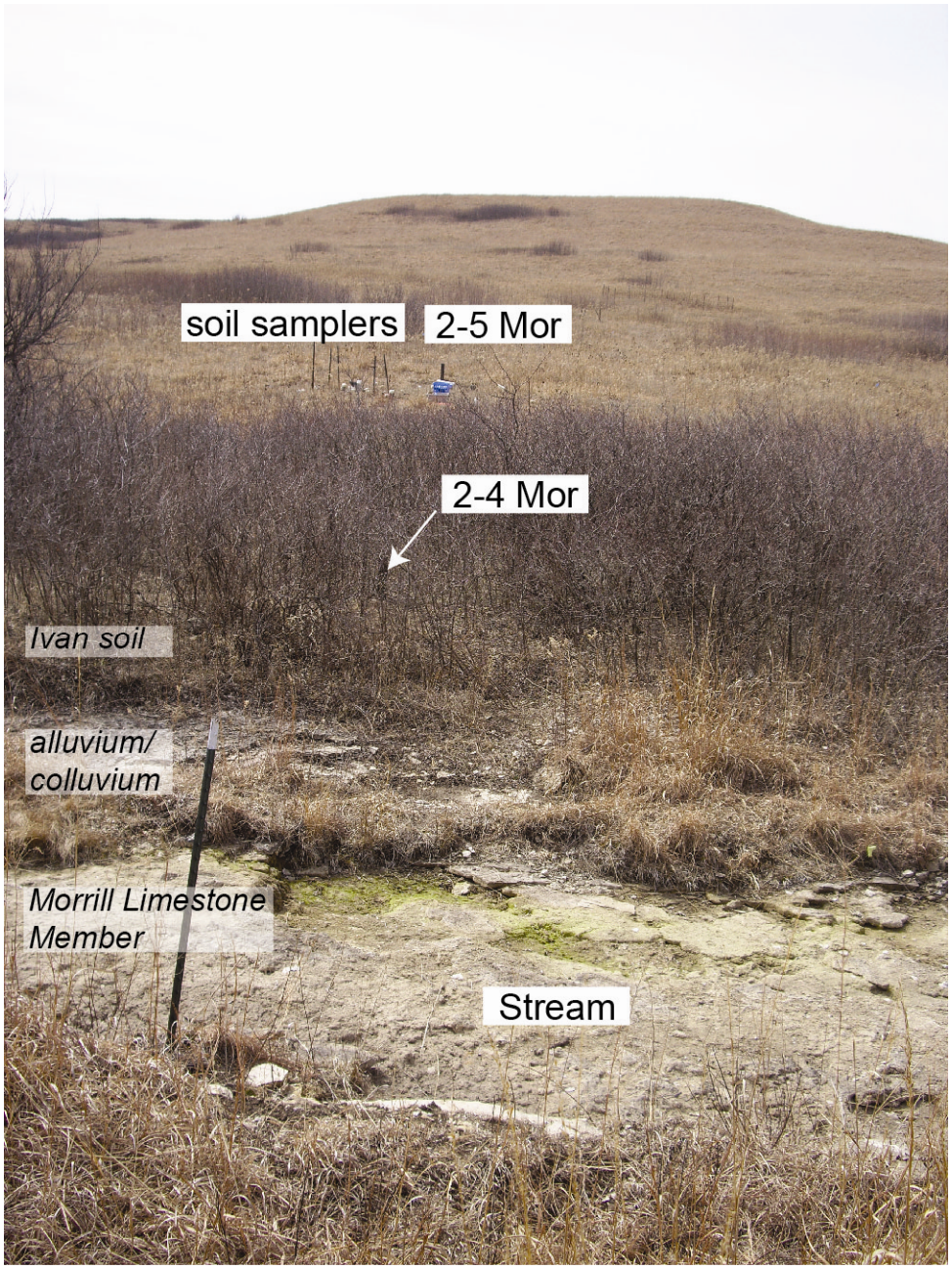


Figure B.1. North part of the N04d watershed, left bank of the South Branch Kings Greek on 03.12.10. Sampling site consists of the well 2-5 Mor and soil gas/water samplers located at the footslope, and the well 2-4 Mor situated in the riparian zone on the left bank of the stream.

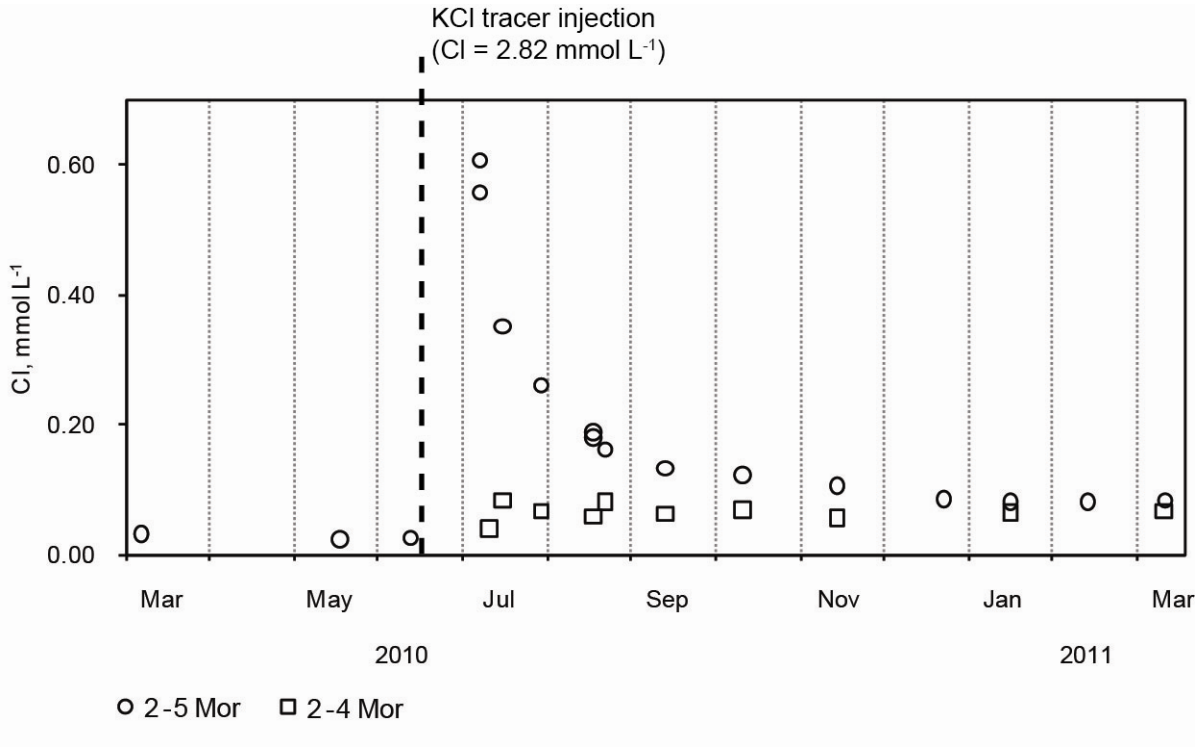


Figure B.2. Decrease in $Cl^-$ level in 2-5 Mor after the injection of KCl solution on 6/12/10. After the KCl solution with a $Cl^-$ concentration of 2.8 mmol/L was injected and bailed out of the well, the $Cl^-$ concentration dropped exponentially from 0.61 mmol/L after the bailing until the background values of 0.09 mmol/L 5 months later. Data for 2-4 Mor is shown as a background reference. Performed tracer test suggests very slow removal of salts from 2-5 Mor.

## Soil water sampling

The network of 70 soil water samplers was installed by the U.S. Geological Survey during 1988-1990 (Macpherson, 1996). Such samplers are commonly called suction lysimeters or simply lysimeters, however they should not be confused with an array of meteorological instruments such as evapotranspirometer and monolith lysimeter (Litaor, 1988). Our inspection discovered that 2 of 3 samplers near 2-5 Mor did not hold vacuum because they probably had a crack in the PVC pipe or ceramic cup. Broken samplers were replaced with new ones. Before installation, in the lab, air was evacuated from the samplers and they were placed in a bucket of water in order to saturate ceramic cups. At the field site, a hand auger was used to drill 5.7 cm wide boreholes slightly deeper that the length of the pipe (Table B.1). Two-three cm of wet bentonite clay was poured into the bottom of the hole in order to prevent upward migration of soil water from beneath the cup. Silica flour mixed with water was poured to the bottom before placing the sampler. Then the soil water sampler was inserted into the hole and more silica flour was added around it until the porous ceramic cup became completely covered. The mixture of silica with water produces slurry that helps to maintain hydraulic conductivity between the sides of the hole and the ceramic cup. After that, several layers of soil and bentonite were added to the surface to prevent downward leakage of water in the area between soil and the pipe. A Santoprene® stopper sealed the sampler, and additional caps covered each sampler for protection from the rain, extreme temperatures, fire, insects, and bison.

To collect samples, the soil water samplers were left under a vacuum of 70-80 centibars until the following sampling event, typically for 1 month (Fig. B.3a). While the soil solution suction was less than the applied vacuum, solution is drawn across the porous wall into the cup by the induced pressure gradient (Litaor, 1998). The amount of water entering the cup is somewhat proportional to the moisture content of the soil. On average, the minimum period of time to collect a sufficient amount of sample at the study location was 2 hours.

To extract and evacuate water sample, Santoprene® stopper was removed, 1/8" OD, 1/32" wall PFA tubing plastic tube was inserted into the pipe and pushed down until it reached the bottom of the sampler (Fig. B.3b). The other end of the tube was connected to the sample bottle. The vacuum hand pump was then connected to other hole in the bottle. Stroking the hand pump creates a vacuum within the bottle that in turn sucks the sample up from the sampler and into the sample bottle.

In general, it is recommended that the soil solution sampler system be installed a year before sampling begins to let the sampler surface equilibrate with the surrounding soil (Litaor, 1998). Unfortunately, in this study, only several weeks past between the installation and the beginning of the sampling, which might explain the observed enrichment in the concentration of some ions in the soil water. Some other factors that must be considered when accepting the composition of the obtained water samples as a representative of the soil water are:

- root response to massive soil and rhizosphere perturbation causes a change in concentrations of carbohydrates and several trace metals in the soil water (Litaor, 1998);

- inherent soil heterogeneity affects soil moisture retention and thus causes non-uniform and irregular solution flow from the soil to the sample (Cochran et al., 1970);

- solute concentrations from macropores might be different from that collected from micropores.

Table B.1. Depths of soil water and gas samplers installed for this project next to the well 2-5 Mor, N04d watershed, Konza Prairie LTER Site.

| Soil horizon | Interval, cm | Sampling depth, cm |
|---|---|---|
| A | 0 – 17.8 | 16 |
| B | 17.8 – 152.4 | 84 |
| C | >152.4 | 152 |

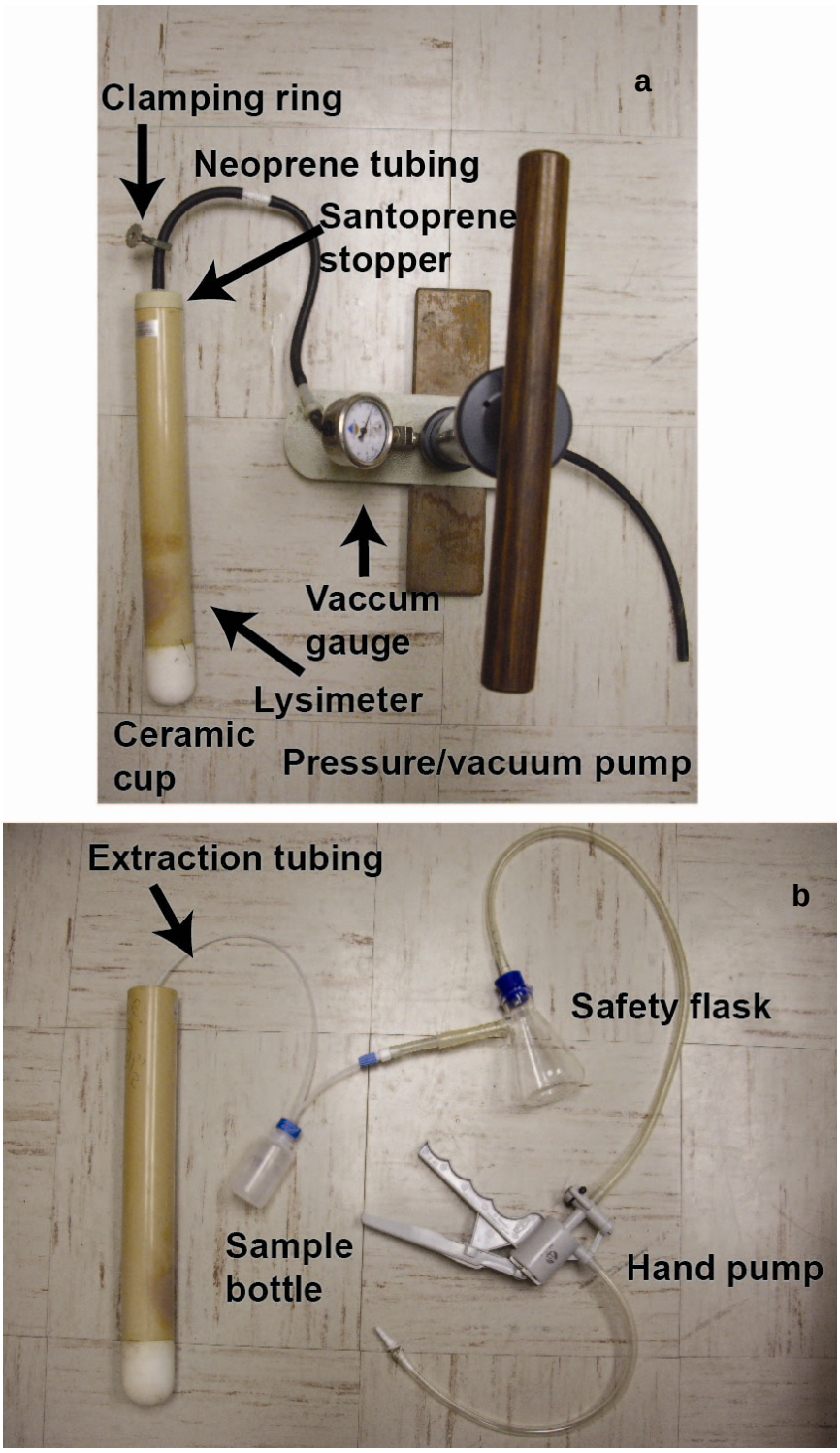


Figure B.3. Principle design of the soil water sampling: creating a vacuum in the sampler (a); evacuation of the collected soil moisture to the sample bottle (b).

## Soil gas sampling

Gas wells were established at depths of 16, 84, and 152 cm so that the bottom hole of the gas well is at the same level as midpoint of the water sampler's ceramic cup. To install soil gas samplers at the Konza Prairie, three holes with a diameter of 2 cm were drilled in the soil using shallow depth Backsaver® soil sampling handle designed with a foot pedal to drive the sampler using gravity and the weight of the body. The temporary outer copper pipe with the diameter of 1.5 cm served as a casing. The bottom of the hole was filled with sand to allow free gas flow. Then 5/32" aluminum tube protected with fine mesh at the bottom end to prevent clogging with fine soil particles were carefully inserted into the hole (Fig. B.4). Three cm of wet bentonite clay was added above the sand in order to isolate the particular interval for gas sampling. The hole was then backfilled with soil and covered with another layer of bentonite to the top. The top end is equipped with tube for connecting with the pump and sealed with rubber cap to prevent free gas exchange with atmosphere.

The sampling technique was developed at Geohydrologic Experimental and Monitoring Site (GEMS) (Fig. B.5). GEMS, a research site of Kansas Geological Survey and KU Field Station lies in the floodplain of the Kansas River just north of Lawrence, Kansas. At this site, soils are developed on 22 m Holocene alluvium deposits of Kansas River, consisting of 11.5 m of primarily clay and silt overlying 10.7 m of sand and gravel resting on bedrock that is Pennsylvanian sandstone (Schulmeister et al., 2003). The soil type at this site is Wabash silty clay loam, with similar thickness and lithology to the one found at the Konza Prairie (USDA-NRCS, 2007).

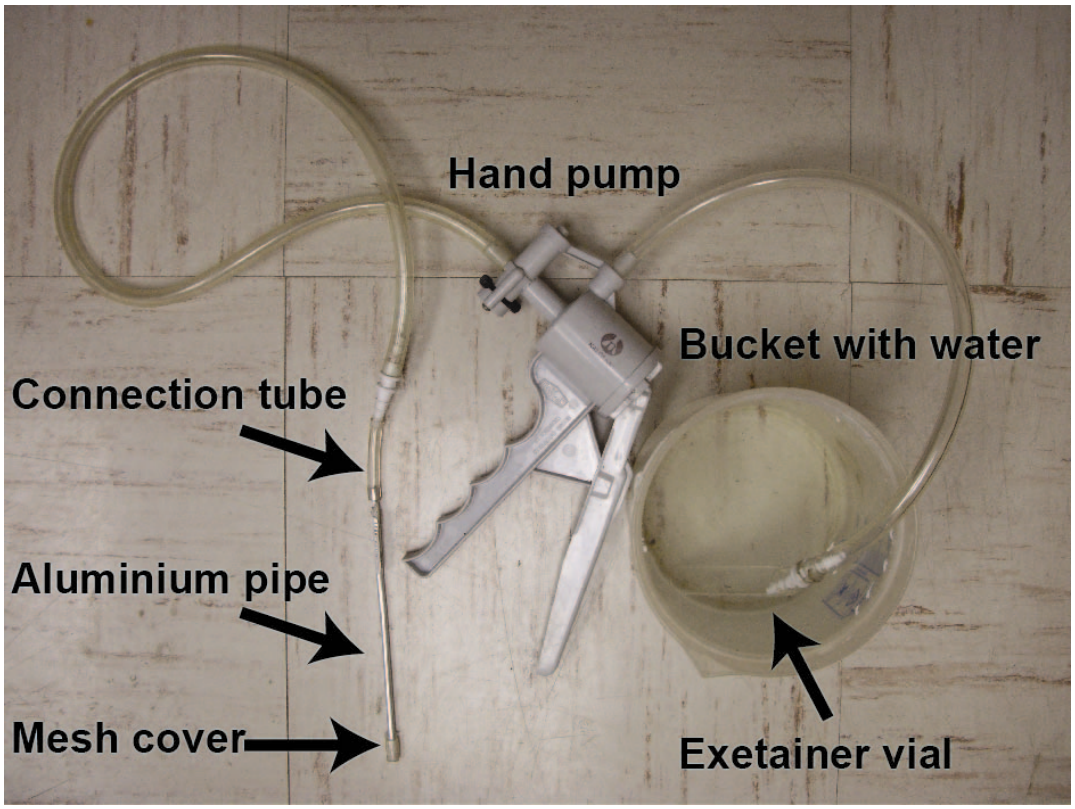


Figure B.4. Principle design of the soil gas sampling.

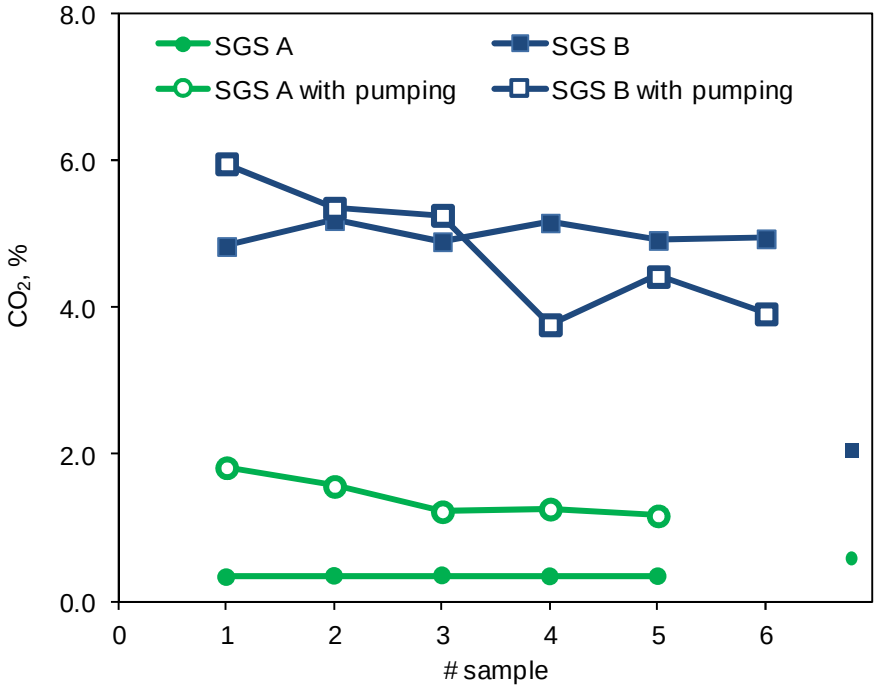


Figure B.5. A comparison of two methods of soil gas sampling from 2 soil gas samplers (SGS) installed in the A and B horizons at the GEMS site, 10 cm and 40 cm of soil depth respectively. Five minutes purging prior to the collection of the each subsequent sample (6/22/10; hollow symbols) caused a significant decline in $\%CO_2$, because continuous pumping initiated an inflow of air from the atmosphere with low $CO_2$ content. A short purging that (6/30/10; filled symbols) led to a higher reproducibility between replicas. In such purging only 50–100 mL of gas were withdrawn using vacuum pump with Tygon® tubing that was sufficient to completely evacuate stagnant air from the gas well and from the pump tubing. A 12 ml Exetainer® glass vial was then submerged in a bucket of boiled distilled deionized water and purged with 200 ml of soil gas to displace the water and flush the vial. The vial was then capped under water, sealed with Parafilm®, and stored in a cool place. During each sampling event, two samples were obtained each time from a single well: one for $CO_2$ isotopic analysis and one for $CO_2$ concentration determination by gas chromatography.
Smaller symbols represent control samples collected on 4/13/11.

## Laboratory analyses

Groundwater samples were filtered (0.45 μm) on the day of collection with 25 mm Millex®-HA syringe driven filters (surface area - 3.9 $cm^2$) or peristaltic pump driven Gelman® high-capacity cartridge filter (surface area - 600 $cm^2$).

### Titration

Alkalinity of water samples was determined by titration with ~0.02 N $H_2SO_4$ at the University of Kansas Aqueous Geochemistry Laboratory (KU AGL). Filtered aliquots (15–50 ml) were titrated within two days of sample collection.

### IC

Concentrations of $Cl^-$, $SO_4^{2-}$, $NO_3$–$N^-$ and $F^-$ were determined at KU AGL by suppressed ion chromatography (IC) with a Dionex 4000i (AG4A-SC and AS4A-SC columns and anion self-regenerating suppressor) on filtered, non-acidified aliquots of 0.6 ml; samples were analyzed within a week of collection. Because the signal of $SO_4^{2-}$ peak in soil water samples exceeded the high standard, the samples were diluted with distilled deionized water in 10–20 times by volume.

### ICP-OES

Cations ($Na^+$, $K^+$, $Mg^{2+}$, $Ca^{2+}$, $Sr^{2+}$) and dissolved Si were determined on filtered and weighed aliquots preserved by acidification with $HNO_3$ to a level of 2% v/v within 3 days after collection. Analysis was accomplished using inductively-coupled plasma-optical emission spectroscopy (JY 138 Ultrace ICP-OES) at the University of Kansas Plasma Analytical Laboratory (KU PAL). Soil water samples were diluted with distilled deionized water in 10–20 times by weight.

Charge balances on the analyses, by the method of Fritz (1994), were normally between 1 and 3% and always less than 5%.

### $CO_2$

Concentration of $CO_2$ in the samples of soil gas was measured with an Agilent Technologies 6890N Gas Chromatograph (GC) at the KU Geomicrobiology Lab. Three different volumes of the reference gas, 250 μl, 500 μl, and 1000 μl, with the $CO_2$ concentration of about 0.99%vol were analyzed and a calibration line is built based on the obtained values for $CO_2$ peaks area. 250 μl of soil gas was injected in the GC and $CO_2$ concentration is then calculated in volume percent.

**Stable carbon isotope analyses**

Stable carbon isotope compositions of groundwater and soil water DIC as well as soil $CO_2$ were determined by stable-isotope-ratio-mass-spectrometry (SIRMS) on a ThermoFinnigan MAT 253 mass spectrometer at The University of Kansas W.M. Keck Paleoenvironmental and Environmental Stable Isotope Laboratory (K-PESIL). For DIC analysis, sealed glass Exetainers® were flushed with He for 5 minutes using input and output needles, then 7 drops of concentrated $H_3PO_4$ were added with a syringe. Groundwater (0.6 ml) or soil water (5 ml) were then injected and left under +25°C for 24 hours for equilibration and $CO_2$ release from acidified water into headspace. The evolved-gas samples were loaded in ThermoFinnigan GasBench II, on-line gas preparation and introduction system. During the analysis, the $CO_2$ was introduced into the mass spectrometer in continuous flow mode, using helium as the carrier gas.

The set of standards for DIC included Calcite #1, Merck calcite, NBS-18, NBS-19, and NIST Dolomitic Limestone 88b. For $CO_2$ analysis, gas tanks with 4 different concentrations, ~288, ~500, ~980 and ~4900 ppm $CO_2$ in air and known $^{12}C/^{13}C$ were used as a reference. Some of the $CO_2$ peaks had failed due to the voltage offscale because of the high $CO_2$ content in soil gas (presumably >5%). Carbon isotope ratios of the DIC and $CO_2$ are reported in the delta notation in per mil (‰) relative to Vienna Pee Dee Belemnite (VPDB) carbon standard (with a precision of better than 0.1‰):

$$\delta^{13}C = \left( \frac{(^{13}C/^{12}C)_{sample}}{(^{13}C/^{12}C)_{VPDB}} - 1 \right) \cdot 1000 \ (‰) \qquad \text{(B.1)}$$

**Water isotope analyses**

High precision analysis of $^{18}O/^{16}O$ in water samples used the same set of Gas Bench II coupled to a MAT 253 mass spectrometer integrated with ThermoFinnigan Temperature Conversion Elemental Analyzers (TC/EA), designed for sample pyrolysis and continuous flow analysis. Exetainer® vials were flushed for 5 min with helium containing 0.3% $CO_2$ at a rate of 1000 mL/min. Then the samples (0.5 mL) were introduced into the vials and the water oxygen is allowed to come into isotopic equilibrium with the headspace $CO_2$ over a period of 24 hours. After this equilibration period, the headspace gas was entrained into a He stream, passed through two nafion dryers and passed through a GC column. The GC column separated $CO_2$ from

contaminant $N_2O$ gas of the same mass before introduction into the mass spectrometer for isotopic analysis.

In addition to that, D/H and $^{18}O/^{16}O$ ratios in water were also measured with Picarro® L1102-i Isotopic Water Liquid analyzer. A 1 ml of sample was injected into the 2 ml vials with a PTFE/silicone septa cap. Autosampler introduced 0.5 μl of liquid water to the vaporizer where the ensuing water vapor is passed into the optical cavity. Wavelength Scanned Cavity Ringdown Spectroscopy (WS CRDS) was used to scan the absorption lines unique to $H_2{}^{16}O$, $H_2{}^{18}O$, and $HD^{16}O$. Each sample was injected 6 times, but the first 3 were ignored to remove memory.

Raw data was corrected versus a series of internally calibrated secondary standards, which were analyzed after every 8–10 samples. These are Elemental Microanalysis Zero Natural Water - B2192, and Elemental Microanalysis Medium Natural Water - B2193, EVIAN, AICW (Alberta Ingenuity Centre for Water), LBDW, DI Water, Kansas snow, Kansas rain (2). Hydrogen and oxygen isotope rations of water are reported relative to Standard Mean Ocean Water (VSMOW) standard:

$$\delta D = \left( \frac{(D/H)_{sample}}{(D/H)_{VSMOW}} - 1 \right) \cdot 1000 \ (‰), \tag{B.2}$$

$$\delta^{18}O = \left( \frac{(^{18}O/^{16}O)_{sample}}{(^{18}O/^{16}O)_{VSMOW}} - 1 \right) \cdot 1000 \ (‰). \tag{B.3}$$

## Appendix C. Recharge events

The study period was relatively dry: meteoric precipitation in 2010 was 598 mm, which is about 72% of the 30-year mean precipitation rate. At the Konza Prairie, precipitation is the main source of groundwater recharge. During 14 years of monthly monitoring, water table in 2-5 Mor showed annual fluctuations limited in 10 cm with occasional higher rises related to precipitation events (Fig. C.1).

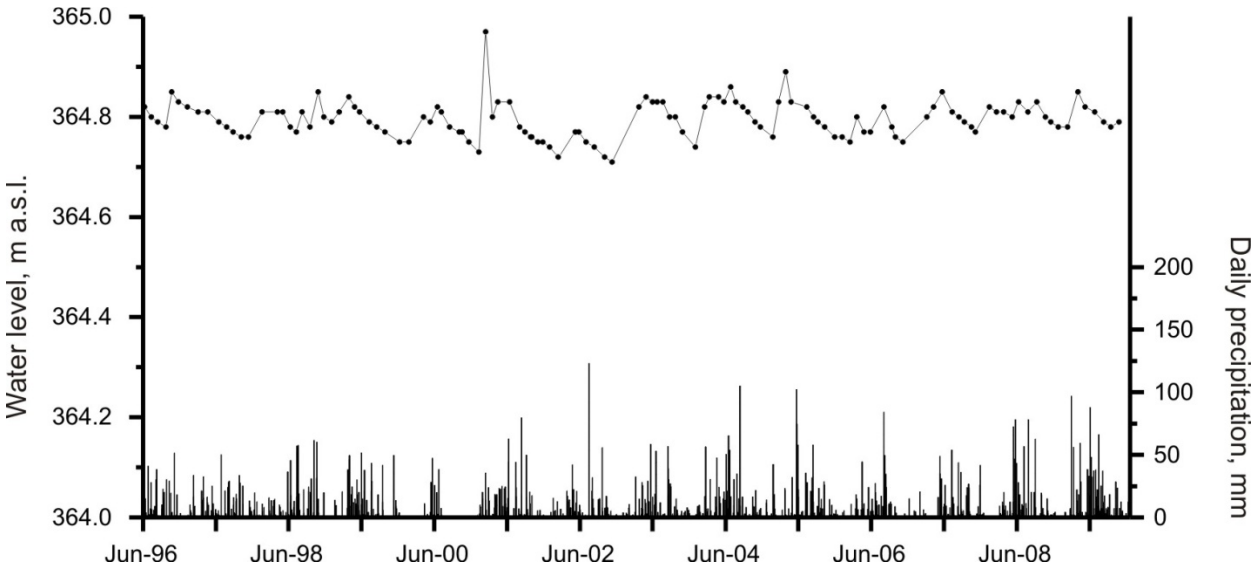


Figure C.1. Water level (points) in 2-5 Mor during the 15-year observation period.
M a.s.l. - meters above the sea level.
Bar height corresponds to the daily precipitation amount.

Table C.1. Summary of significant and high-intensity rainfall events in Konza Prairie during the study period. Intensity of rainfall showers is categorized as moderate (precipitation rate between 2.5 and 10 mm/hr), heavy (precipitation rate between 10 to 50 mm/hr), or violent (precipitation rate above 50 mm/hr) (Lamb, 1972). However, only one storm exceeded the intense-rainfall rate threshold of 56 mm/hr introduced by Hayden (1998) for the Konza Prairie.

| Event (date) | Total (mm) | Daily maximum (mm) | Max. precipitation rate (mm/hr) | Rainfall intensity |
|---|---|---|---|---|
| 19 - 20 May | 27 | 17 | 18.3 | heavy |
| 12 - 14 June | 60 | 40 | 78.5 | violent |
| 19 - 20 June | 29 | 28 | 32.3 | heavy |
| 4 - 5 July | 59 | 47 | 29.7 | heavy |
| 14 - 15 July | 24 | 18 | 55.9 | violent |
| 13 August | 26 | 26 | 54.9 | violent |
| 24 August | 39 | 39 | 28.2 | heavy |
| 15 September | 34 | 34 | 28.7 | heavy |
| 22 - 23 October | 30 | 20 | 45.7 | heavy |
| 12 November | 41 | 41 | 7.2 | moderate |

Table C.2. Response of the water level, temperature, chemical parameters, and visual wetness of soil to the storm events during the growing season of 2010. There is a well-pronounced seasonal effect of increasing groundwater alkalinity, Ca, $SI_{calcite}$ and TDS, and decreasing pH during the growing season. Precipitation events disturb such trends by diluting groundwater with the low TDS rain water. The most common response to a precipitation event was in increase in the water-level elevation, high moisture content in soil, lower alkalinity, and sometimes temperature increase. However, such an effect of storm recharge was not evident and uniform year round due to difference in water uptake by plants. Water level in 2-5 Mor was the least sensitive to the recharge events due to poor communication with the aquifer or low-conductivity zone.

| Date of the rainfall | Precip., mm. | Water level | Groundwater temperature | Sampling date | Alkalinity | $Ca^{2+}$ | Soil moisture |
|---|---|---|---|---|---|---|---|
| 19 - 20 May | 27 | n.r.* (2-5 Mor) | n.r. | none | n.d.** | n.d. | n.d. |
| 12 - 14 June | 60 | n.r. (2-5 Mor) | n.r. | 6/12/10 | n.r. | n.r. | n.d. |
| 19 - 20 June | 29 | n.r. (2-5 Mor) | n.r. | none | n.d. | n.d. | n.d. |
| 4 - 5 July | 59 | n.r. (2-5 Mor) | n.r. | 7/7/10, 7/10/10 | n.r. | n.r. | **very wet** |
| 14- 15 July | 24 | **higher rate of increase (2-4 Mor)** | n.r. | 7/15/10 | **drop by 1.7 mmol/l below expected value, similar to soil water (2-5 Mor); drop by 2.7 mmol/L (2-4 Mor)** | **drop by 0.7 mmol/l below expected value (2-5 Mor)** | **very wet** |
| 13 August | 26 | **1-2 cm slow increase in several stages (2-4 Mor)** | **slow increase in several stages** | 8/17/10 | **drop by 1.4 mmol/l below expected value (2-5 Mor); drop by 2.7 mmol/L (2-4 Mor)** | n.r. | **wet** |
| 24 August | 39 | n.r. (2-4 Mor) | n.r. (2-4 Mor) | none | n.r. | n.r. | n.d. |
| 15 September | 34 | **higher rate of increase with 3 hr. lag time (2-4 Mor)** | n.r. (2-4 Mor) | none | n.r. | n.r. | n.d. |
| 25 September | | **fast immediate increase in 7 cm (2-4 Mor)** | n.r. | 10/10/10 | n.r. | n.r. | n.d. |
| 22 - 23 October | 30 | n.r. (3-5 Mor) | n.r. | none | n.d. | n.d. | n.d. |
| 12 November | 41 | **slow increase in 2 stages (3-5 Mor)** | n.r. | 11/13/10 | **drop by 0.9 mmol/l below expected value (2-4 Mor)** | n.r. | **wet** |

* n.r. - no response; ** n.d. - no data

## Downhole logging

The Hydrolab H20G Multiprobe was tested once in order to reveal potential response of the groundwater chemistry on recharge events on an hourly time scale. The probe was suspended into the well 3-5-1 Mor, located near the 3-5 Mor, at two different depths to perform monitoring during the light rain for one hour at each level (Fig. C.2). The probe was recording pH, temperature and specific conductance on a 5-second time interval. The field notebook connected to the probe with RS-232 cable captured data using HyperTerminal and saved it into a text file.

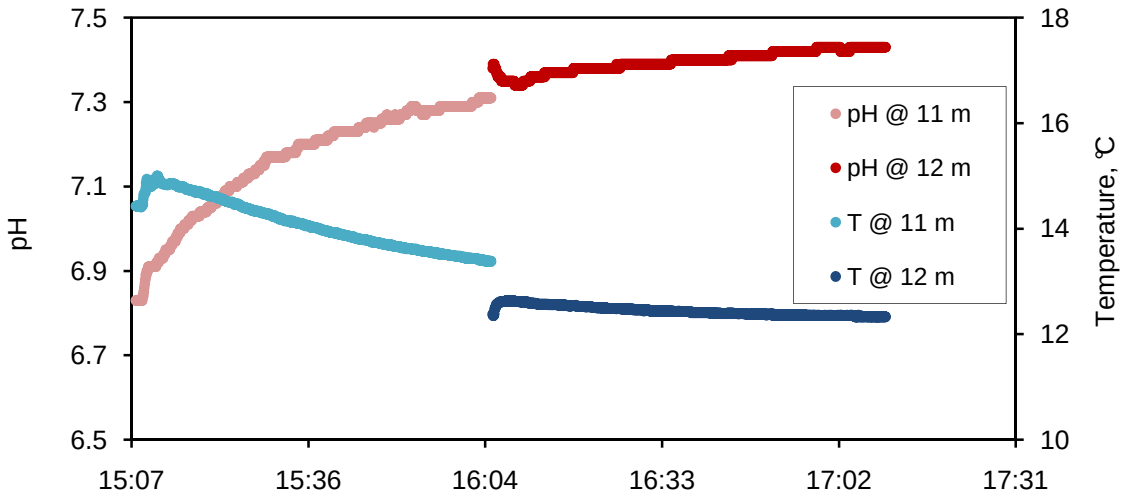


Figure C.2. Example of slow pH and temperature stabilization during the downhole logging with Hach© Hydrolab MS5 sonde in 3-5-1 Mor on 10/10/10. After the 2-hour monitoring at 2 different depths (11 m and 12 m), parameters were still stabilizing.

## Soil moisture

Two tensiometers (model 2725 jet fill by Soil Moisture, Inc.), 30 and 45 cm deep, were installed in the soil near the well 4-5 Mor located about 200 m upstream from the 2-5 Mor to take direct measurements of soil suction (Table C.3). Each device was filled with water consisted of a tube with a porous ceramic tip on the bottom, a vacuum gauge near the top, and a sealing cap. According to the principle of operation, as the soil dries, water moves out of the tensiometer through the porous tip; it creates a vacuum inside the tensiometer. If the soil is wet, moisture from the soil moves back into the tensiometer and the vacuum reduces. The dial gauge reading is then a direct measure of the force required to remove water from the soil. If the soil is completely saturated, the gauge reading on the tensiometer will drop to zero. A comparison the gauge reading between the two tensiometers allows determination of the direction of vertical movement of soil water.

The amount of water collected from soil water samplers, an indirect evidence of soil moisture content, was consistent with tensiometer readings. Soil horizon B contained more moisture than the A horizon over the extended dry periods, however soil A horizon was very wet specifically following the storm events. The deepest sampler installed in the C horizon remained dry during entire time of the experiment, even under the wet conditions, probably due to higher content of clay and pieces of bedrock in the soil. The volume of samples extracted from the upper two samplers was the highest in 7/7/10, 7/15/10, 8/17/10, and 11/13/10, i.e. within 1–4 days after significant storm events.

Table C.3. Soil suction measured with tensiometers. On 11/13/10, following the 41 mm storm event on 11/12/10, soil was completely saturated with water and the suction was equal to zero as expected after the heavy rain, while on 10/10/10, 25 days after the latest rainfall, the suction was high and moisture was moving up, in a direction of higher soil suction value, which is the evidence of evapotranspiration.

| Date | Suction (kPa) | | Note |
|---|---|---|---|
| | depth - 30 cm | depth - 45 cm | |
| 9/12/10 | 60 | n. d. | |
| 10/10/10 | 55 | 24 | very dry |
| 11/13/10, morning | 0 | 0 | after the storm on 11/12/10 |
| 11/13/10, afternoon | 0-1 | 0 | |

# Appendix D. Geochemical data

Table D.1. Concentration and isotopic composition of the soil air $CO_2$.

| Soil horizon | Date / Time | $CO_2$, % | $\delta^{13}C$ VPDB (‰) | σ last 4 sample peaks | $\delta^{18}O$ VPDB (‰) | σ last 4 sample peaks |
|---|---|---|---|---|---|---|
| A | 7/7/10 10AM | 3.6 | -15.53 | 0.08 | -5.03 | 0.11 |
| | 7/7/10 12PM | 3.6 | -15.69 | 0.07 | -5.23 | 0.10 |
| | 7/7/10 3PM | 3.3 | -15.36 | 0.07 | -5.20 | 0.09 |
| | 7/15/10 5PM | 3.3 | -15.65 | 0.07 | -3.84 | 0.11 |
| | 7/15/10 6PM | 3.6 | -15.47 | 0.06 | -2.78 | 0.11 |
| | 7/29/10 3PM | 1.3 | -12.33 | 0.03 | -4.49 | 0.03 |
| | 8/17/10 11AM | 1.7 | -13.87 | 0.04 | -5.06 | 0.11 |
| | 8/21/10 11AM | 1.1 | -16.81 | 0.02 | -4.90 | 0.06 |
| | 9/12/10 10AM | 0.58 | -15.83 | 0.02 | -5.61 | 0.22 |
| | 10/10/10 10AM | 0.47 | -14.47 | 0.04 | -6.20 | 0.41 |
| | 10/10/10 5PM | 0.45 | -13.22 | 0.04 | -5.02 | 0.02 |
| | 11/13/10 12PM | 0.51 | -17.18 | 0.07 | -7.47 | 0.15 |
| | 11/13/10 4PM | 0.59 | -17.06 | 0.06 | -7.28 | 0.09 |
| | 1/15/11 11AM | 0.25 | -14.34 | 0.11 | -6.97 | 0.05 |
| | 3/12/11 11AM | 0.24 | -19.47 | 0.04 | -6.26 | 0.13 |
| B | 7/7/10 10AM | 6.1 | n.d. | n.d. | n.d. | n.d. |
| | 7/7/10 12PM | 7.2 | n.d. | n.d. | n.d. | n.d. |
| | 7/7/10 3PM | 6.2 | n.d. | n.d. | n.d. | n.d. |
| | 7/15/10 5PM | 6.9 | n.d. | n.d. | n.d. | n.d. |
| | 7/15/10 6PM | 7.0 | n.d. | n.d. | n.d. | n.d. |
| | 7/29/10 3PM | 7.3 | n.d. | n.d. | n.d. | n.d. |
| | 8/17/10 11AM | 1.9 | -12.86 | 0.06 | -4.53 | 0.08 |
| | 8/21/10 11AM | 1.5 | -13.86 | 0.03 | -4.98 | 0.08 |
| | 9/12/10 10AM | 1.2 | -14.08 | 0.02 | -5.34 | 0.11 |
| | 10/10/10 10AM | 1.4 | -13.46 | 0.02 | -5.76 | 0.12 |
| | 10/10/10 5PM | 1.3 | -12.93 | 0.03 | -4.80 | 0.10 |
| | 11/13/10 12PM | 1.1 | -14.90 | 0.03 | -7.02 | 0.05 |
| | 11/13/10 4PM | 1.0 | -13.57 | 0.03 | -7.11 | 0.31 |
| | 1/15/11 11AM | 0.79 | -13.85 | n.d. | -6.69 | n.d. |
| | 3/12/11 11AM | 0.33 | -19.70 | 0.03 | -5.98 | 0.07 |
| C | 7/10/10 10AM | 6.7 | n.d. | n.d. | n.d. | n.d. |
| | 7/10/10 11AM | 6.5 | n.d. | n.d. | n.d. | n.d. |
| | 7/15/10 5PM | 6.7 | n.d. | n.d. | n.d. | n.d. |
| | 7/15/10 6PM | 6.4 | n.d. | n.d. | n.d. | n.d. |
| | 8/17/10 11AM | 7.2 | n.d. | n.d. | n.d. | n.d. |
| | 8/21/10 11AM | 6.6 | n.d. | n.d. | n.d. | n.d. |
| | 9/12/10 10AM | 3.9 | n.d. | n.d. | n.d. | n.d. |
| | 10/10/10 10AM | 2.6 | -13.40 | 0.07 | -5.84 | 0.08 |
| | 10/10/10 5PM | 2.4 | -13.36 | 0.06 | -4.93 | 0.08 |
| | 11/13/10 12PM | 2.3 | -14.47 | 0.17 | -10.04 | 0.47 |
| | 11/13/10 4PM | 2.1 | -14.44 | 0.04 | -7.00 | 0.17 |
| | 1/15/11 11AM | 1.1 | -13.82 | 0.00 | -6.63 | 0.06 |
| | 3/12/11 11AM | 0.50 | -15.90 | 0.02 | -5.38 | 0.06 |

Table D.2. Chemical composition of groundwater from 2-5 Mor and 2-4 Mor.
Concentrations are given in ppm.

| Well | Date, time | Alk. ($HCO_3^-$) | $SO_4$ | Cl | $NO_3$-N | $HPO_4$-P | Si | Mg | Sr | Ca | Na | K | TDS |
|---|---|---|---|---|---|---|---|---|---|---|---|---|---|
| 2-5 Mor | 3/6/10 3PM | 259 | 13.7 | 1.14 | 0.16 | <0.1 | 0.8 | 21.8 | n.d. | 44.5 | 7.4 | 0.52 | 218 |
| | 5/17/10 3PM | 362 | 12.2 | 0.82 | 0.09 | <0.1 | 8.0 | 19.8 | 0.89 | 77.4 | 13 | 1.11 | 320 |
| | 6/12/10 2PM | 377 | 11.1 | 0.86 | 0.07 | <0.1 | 7.4 | 20.8 | 0.86 | 73.6 | 8.8 | 0.94 | 318 |
| | 7/7/10 12PM | 398 | 9.2 | 21.5 | 0.17 | <0.1 | 7.9 | 20.5 | 0.93 | 94.1 | 10 | 8.15 | 378 |
| | 7/7/10 5PM | 423 | 9.2 | 19.7 | 0.18 | <0.1 | 7.6 | 20.2 | 0.96 | 101 | 13 | 9.09 | 397 |
| | 7/15/10 5PM | 326 | 9.8 | 12.4 | 0.15 | <0.1 | 9.0 | 20.6 | 0.86 | 64.1 | 10 | 5.84 | 303 |
| | 7/29/10 4PM | 378 | 10.2 | 9.27 | 0.14 | <0.1 | 8.7 | 21.4 | 0.96 | 80.9 | 12 | 4.68 | 344 |
| | 8/17/10 12PM | 396 | 10.4 | 6.36 | 0.10 | <0.1 | 9.2 | 23.1 | 1.04 | 83.0 | 12 | 3.75 | 354 |
| | 8/17/10 3PM | 355 | 10.5 | 6.69 | 0.20 | <0.1 | n.d. | n.d. | n.d. | n.d. | n.d. | n.d. | n.d. |
| | 8/21/10 1PM | 468 | 10.3 | 5.68 | 0.14 | <0.1 | 9.0 | 23.3 | 1.04 | 95.8 | 13 | 3.59 | 402 |
| | 9/12/10 11AM | 473 | 10.5 | 4.69 | 0.11 | <0.1 | 8.5 | 23.3 | 1.24 | 103 | 12 | 3.60 | 409 |
| | 10/10/10 12PM | 470 | 11.1 | 4.31 | 0.09 | <0.1 | 9.3 | 24.0 | 1.00 | 104 | 13 | 3.14 | 412 |
| | 11/13/10 3PM | 459 | 11.2 | 3.76 | 0.09 | <0.1 | 8.4 | 25.2 | 1.05 | 105 | 3.1 | 0.16 | 393 |
| | 12/22/10 2PM | 456 | 11.2 | 3.01 | <0.05 | <0.1 | 8.3 | 24.7 | 1.02 | 98.5 | 9.0 | 1.71 | 391 |
| | 1/15/11 3PM | 441 | 11.8 | 2.88 | 0.06 | <0.1 | 7.9 | 24.6 | 1.03 | 97.9 | 8.7 | 1.65 | 382 |
| | 2/12/11 2PM | 430 | 11.9 | 2.97 | 0.06 | <0.1 | 7.7 | 24.6 | 0.99 | 93.7 | 8.4 | 1.48 | 372 |
| | 3/12/11 12PM | 434 | 12.0 | 2.73 | 0.08 | <0.1 | 9.3 | 24.9 | 0.99 | 96.0 | 8.6 | 1.52 | 380 |
| 2-4 Mor | 7/10/10 5PM | 711 | 0.70 | 1.41 | 0.10 | n.d. | 9.1 | 40.9 | 2.16 | 121 | 13 | 12.4 | 561 |
| | 7/15/10 5PM | 544 | 90.9 | 2.99 | 3.4 | <0.1 | 5.0 | 37.6 | 2.10 | 123 | 10 | 12.9 | 561 |
| | 7/29/10 4PM | 545 | 57.1 | 2.39 | 1.3 | <0.1 | 5.6 | 34.1 | 1.75 | 115 | 8.5 | 12.4 | 512 |
| | 8/17/10 12PM | 591 | 43.1 | 2.12 | 0.61 | <0.1 | 6.0 | 35.9 | 2.01 | 122 | 8.8 | 12.6 | 531 |
| | 8/21/10 2PM | 690 | 22.3 | 2.90 | 1.1 | 0.23 | 8.6 | 44.4 | 2.07 | 127 | 10 | 9.85 | 579 |
| | 9/12/10 1PM | 462 | 79.5 | 2.24 | <0.05 | <0.1 | 4.8 | 35.2 | 1.89 | 124 | 8.0 | 11.4 | 500 |
| | 10/10/10 1PM | 465 | 52.5 | 2.44 | 4.4 | <0.1 | 5.1 | 29.4 | 1.48 | 111 | 6.9 | 7.79 | 455 |
| | 10/10/10 7PM | 576 | 42.6 | 2.58 | 0.88 | <0.1 | 5.9 | 38.3 | 1.91 | 115 | 7.6 | 8.11 | 513 |
| | 11/13/10 2PM | 487 | 31.8 | 1.98 | 0.79 | <0.1 | 5.9 | 30.8 | 1.47 | 106 | 5.5 | 5.24 | 435 |
| | 11/13/10 5PM | 401 | 21.2 | 2.03 | 0.14 | <0.1 | 5.8 | 23.5 | 1.14 | 90.8 | 3.9 | 3.09 | 355 |
| | 1/15/11 3PM | 514 | 26.2 | 2.31 | 2.1 | <0.1 | 5.7 | 34.5 | 1.56 | 107 | 6.7 | 5.32 | 451 |
| | 3/12/11 10AM | 435 | 38.0 | 2.40 | 1.7 | <0.1 | 3.8 | 29.4 | 1.39 | 98.0 | 5.0 | 3.99 | 402 |
| | 3/12/11 2PM | 498 | 26.8 | 2.47 | 0.22 | <0.1 | 4.7 | 33.8 | 1.63 | 97.8 | 6.1 | 1.78 | 425 |

Table D.3. Soil water chemistry collected from the samplers in the soil horizons A and B. Concentrations are given in ppm.

| Horizon | Date and time | Alk. ($HCO_3^-$) | $SO_4$ | Cl | $NO_3$-N | $HPO_4$-P | Si | Mg | Sr | Ca | Na | K | TDS |
|---|---|---|---|---|---|---|---|---|---|---|---|---|---|
| A | 7/7/10 2PM | 106 | 362 | 61.6 | 0.34 | 4.1 | 23.5 | 18.0 | 1.06 | 127 | 78 | 15.5 | 779 |
| | 7/7/10 5PM | 85 | 501 | 52.8 | 0.35 | 1.8 | 18.9 | 18.9 | 0.97 | 135 | 103 | 17.0 | 917 |
| | 7/10/10 11AM | 85 | 717 | 38.2 | 0.64 | 0.51 | 17.8 | 21.1 | 1.01 | 154 | 166 | 20.3 | 1200 |
| | 7/15/10 3PM | 42 | 704 | 26.8 | 0.29 | <0.1 | 18.1 | 20.6 | 0.81 | 139 | 145 | 19.9 | 1116 |
| | 7/15/10 6PM | 37 | 617 | 17.8 | 0.23 | <0.1 | n.d. | n.d. | n.d. | n.d. | n.d. | n.d. | n.d. |
| | 7/29/10 2PM | 80 | 668 | 11.6 | <0.05 | <0.1 | 18.1 | 17.5 | n.d. | 113 | 165 | 17.1 | 1069 |
| | 8/17/10 3PM | n.d | 408 | 3.12 | 0.36 | 2.9 | 17.7 | 8.18 | 0.34 | 52.2 | 103 | 9.97 | n.d. |
| | 8/21/10 10AM | n.d | 378 | 3.36 | 0.33 | <0.1 | 16.9 | 7.6 | 0.19 | 49.8 | 95 | 8.64 | n.d. |
| | 10/10/10 7PM | n.d. | 258 | 10.8 | 0.18 | <0.1 | n.d | n.d. | n.d | n.d. | n.d | n.d. | n.d. |
| | 11/13/10 10AM | 30 | 224 | 10.4 | 0.27 | 2.2 | n.d. | 4.68 | n.d. | 28.7 | 73 | 5.64 | 369 |
| | 11/13/10 5PM | 24 | 208 | 11.7 | 0.09 | <0.1 | n.d. | 5.27 | n.d. | 31.1 | 77 | 6.01 | 351 |
| | 3/12/11 1PM | 15 | 157 | 8.54 | <0.05 | <0.1 | n.d. | 3.43 | n.d. | 21.7 | 53 | 4.79 | 255 |
| B | 7/7/10 2PM | 342 | 1206 | 55.0 | 0.68 | <0.1 | 22.1 | 21.7 | n.d. | 150 | 531 | 9.90 | 2190 |
| | 7/7/10 5PM | 324 | 1238 | 56.5 | 0.74 | <0.1 | n.d. | n.d. | n.d. | n.d. | n.d. | n.d. | n.d. |
| | 7/10/10 11AM | 368 | 1793 | 41.0 | 1.0 | <0.1 | 19.4 | 29.9 | 1.33 | 212 | 642 | 8.19 | 2950 |
| | 7/15/10 3PM | 334 | 1537 | 36.0 | 0.70 | <0.1 | 18.8 | 27.3 | n.d. | 196 | 530 | 8.36 | 2540 |
| | 7/15/10 6PM | 338 | 1568 | 33.8 | 0.75 | <0.1 | 17.4 | 26.5 | n.d. | 194 | 567 | 7.31 | 2600 |
| | 7/29/10 2PM | 322 | 1101 | 17.8 | 0.89 | <0.1 | 18.0 | 19.6 | 0.85 | 132 | 411 | 5.34 | 1886 |
| | 8/17/10 10AM | 286 | 878 | 8.20 | 0.64 | 0.37 | 16.6 | 16.7 | 0.69 | 113 | 328 | 3.51 | 1526 |
| | 8/17/10 3PM | n.d | 874 | 9.07 | 0.66 | 0.42 | 17.4 | 16.1 | 0.71 | 117 | 345 | 4.05 | n.d. |
| | 8/21/10 10AM | 275 | 848 | 6.84 | 0.26 | <0.1 | n.d. | n.d. | n.d. | n.d. | n.d. | n.d. | n.d. |
| | 10/10/10 11AM | 153 | 496 | 6.80 | 0.38 | <0.1 | 14.2 | 9.14 | 0.30 | 69.1 | 186 | 2.08 | 876 |
| | 10/10/10 6PM | 155 | 494 | 5.95 | 0.13 | <0.1 | n.d | n.d. | n.d | n.d. | n.d | n.d. | n.d. |
| | 1/15/11 10AM | 96 | 574 | 2.95 | <0.05 | <0.1 | n.d. | 13.4 | n.d. | 98.0 | 172 | 2.02 | 909 |
| | 1/15/11 3PM | n.d. | 565 | 2.91 | <0.05 | <0.1 | n.d | n.d. | n.d | n.d. | n.d. | n.d. | n.d. |
| | 3/12/11 12PM | n.d | 345 | 5.60 | <0.05 | <0.1 | n.d. | 13.4 | n.d. | 100 | 159 | 1.45 | n.d. |

Table D.4. Stable isotope composition of DIC ($\delta^{13}C_{DIC}$, $\delta^{18}O_{DIC}$) and water ($\delta^{18}O$) measured in precipitation, soil water, streamwater, and groundwater samples.

| Horizon | Date and time | $\delta^{13}C_{DIC}$ VPDB (‰) | σ | $\delta^{18}O_{DIC}$ VPDB (‰) | σ | $\delta^{18}O$* VSMOW (‰) | σ | $\delta^{18}O$** VSMOW (‰) | σ | δD** VSMOW (‰) | σ |
|---|---|---|---|---|---|---|---|---|---|---|---|
| 2-5 Mor | 3/6/10 3PM | n.d. | n.d. | n.d. | n.d. | -6.57 | 0.05 | | | | |
| | 5/17/10 3PM | n.d. | n.d. | n.d. | n.d. | n.d. | n.d. | -6.72 | 0.20 | -42.13 | 0.71 |
| | 7/7/10 12PM | n.d. | n.d. | n.d. | n.d. | -6.74 | 0.05 | -6.82 | 0.21 | -42.40 | 0.75 |
| | 7/15/10 5PM | -4.72 | 0.02 | -6.94 | 0.02 | -6.58 | 0.04 | -6.51 | 0.19 | -41.43 | 0.73 |
| | 7/29/10 4PM | -4.96 | 0.02 | -7.17 | 0.03 | -6.75 | 0.03 | -5.91 | 0.22 | -39.71 | 0.78 |
| | 8/17/10 12PM | -5.05 | 0.02 | -7.09 | 0.04 | -6.75 | 0.04 | n.d. | n.d. | n.d. | n.d. |
| | 8/21/10 1PM | -5.83 | 0.03 | -6.91 | 0.03 | -6.77 | 0.03 | -6.15 | 0.22 | -40.16 | 0.78 |
| | 9/12/10 11AM | -6.36 | 0.01 | -6.95 | 0.02 | -6.78 | 0.04 | -6.37 | 0.22 | -40.77 | 0.75 |
| | 10/10/10 12PM | -6.36 | 0.02 | -6.90 | 0.03 | -6.77 | 0.03 | -6.13 | 0.23 | -40.31 | 0.76 |
| | 11/13/10 3PM | 0.10 | 0.05 | -6.91 | 0.09 | -6.48 | 0.04 | n.d. | n.d. | n.d. | n.d. |
| | 12/22/10 2PM | -6.15 | 0.08 | -8.07 | 0.24 | -6.93 | 0.07 | -6.56 | 0.19 | -41.37 | 0.74 |
| | 1/15/11 3PM | -5.78 | 0.05 | -8.04 | 0.19 | -5.91 | 0.09 | -5.44 | 0.21 | -38.76 | 0.65 |
| | 2/12/11 2PM | -5.46 | 0.02 | -7.28 | 0.01 | n.d. | n.d. | -6.40 | 0.21 | -41.35 | 0.77 |
| | 3/12/11 12PM | -5.61 | 0.01 | -7.28 | 0.02 | -6.08 | 0.04 | -6.10 | 0.22 | -40.44 | 0.77 |
| | 4/12/11 12PM | n.d. | n.d. | n.d. | n.d. | n.d. | n.d. | -6.41 | 0.20 | -41.14 | 0.68 |
| 2-4 Mor | 7/10/10 5PM | n.d. | n.d. | n.d. | n.d. | -6.04 | 0.08 | n.d. | n.d. | n.d. | n.d. |
| | 7/15/10 5PM | -5.53 | 0.04 | -6.63 | 0.04 | -6.25 | 0.04 | n.d. | n.d. | n.d. | n.d. |
| | 7/29/10 4PM | -6.83 | 0.01 | -6.74 | 0.02 | -6.50 | 0.03 | -6.39 | 0.22 | -39.29 | 0.73 |
| | 8/17/10 12PM | -6.00 | 0.01 | -6.75 | 0.02 | -6.31 | 0.02 | -5.63 | 0.22 | -37.15 | 0.68 |
| | 8/21/10 2PM | -1.86 | 0.02 | -6.84 | 0.02 | -6.48 | 0.03 | -6.32 | 0.21 | -38.87 | 0.74 |
| | 9/12/10 1PM | -9.00 | 0.02 | -6.77 | 0.01 | -6.53 | 0.03 | -5.81 | 0.21 | -38.06 | 0.82 |
| | 10/10/10 1PM | -10.06 | 0.04 | -6.74 | 0.03 | -6.49 | 0.02 | -5.78 | 0.19 | -37.79 | 0.74 |
| | 10/10/10 7PM | -6.50 | 0.03 | -7.15 | 0.02 | -6.45 | 0.07 | -6.35 | 0.21 | -38.93 | 0.71 |
| | 11/13/10 2PM | -8.68 | 0.04 | -7.62 | 0.20 | -6.14 | 0.07 | -5.94 | 0.21 | -37.53 | 0.74 |
| | 11/13/10 5PM | -10.19 | 0.05 | -7.26 | 0.24 | -5.85 | 0.05 | -5.71 | 0.22 | -36.30 | 0.77 |
| | 1/15/11 3PM | -6.75 | 0.08 | -7.82 | 0.28 | -5.89 | 0.09 | -5.61 | 0.20 | -36.60 | 0.75 |
| | 3/12/11 10AM | -7.05 | 0.00 | -6.92 | 0.03 | -6.27 | 0.06 | -6.16 | 0.21 | -38.65 | 0.79 |

Table D.4. (Continued).

| Horizon | Date and time | $\delta^{13}C_{DIC}$ VPDB (‰) | σ | $\delta^{18}O_{DIC}$ VPDB (‰) | σ | $\delta^{18}O$* VSMOW (‰) | σ | $\delta^{18}O$** VSMOW (‰) | σ | δD** VSMOW (‰) | σ |
|---|---|---|---|---|---|---|---|---|---|---|---|
| 3-5 Mor | 11/13/10 5PM | -9.96 | 0.05 | -7.35 | 0.21 | n.d. | n.d. | -6.21 | 0.21 | -37.84 | 0.77 |
| 3-1 Stream | 11/13/10 5PM | -7.44 | 0.06 | -7.11 | 0.17 | -6.27 | 0.03 | -5.99 | 0.19 | -37.68 | 0.79 |
| A | 7/7/10 2PM | n.d. | n.d. | n.d. | n.d. | -5.03 | 0.03 | -5.18 | 0.21 | -32.58 | 0.81 |
| | 7/15/10 3PM | -6.47 | 0.03 | -6.90 | 0.06 | -6.18 | 0.04 | -6.04 | 0.21 | -40.10 | 0.76 |
| | 7/15/10 6PM | -8.14 | 0.04 | -6.97 | 0.14 | n.d. | n.d. | n.d. | n.d. | n.d. | n.d. |
| | 7/29/10 2PM | -6.85 | 0.05 | -6.52 | 0.06 | -5.89 | 0.02 | -5.88 | 0.22 | -37.18 | 0.78 |
| | 11/13/10 10AM | -9.35 | 0.01 | -4.51 | 0.11 | -4.16 | 0.07 | -3.90 | 0.23 | -23.69 | 0.77 |
| | 11/13/10 5PM | -9.46 | 0.06 | -4.32 | 0.07 | n.d. | n.d. | n.d. | n.d. | n.d. | n.d. |
| | 3/12/11 1PM | -7.17 | 0.02 | -6.85 | 0.05 | n.d. | n.d. | n.d. | n.d. | n.d. | n.d. |
| B | 7/15/10 3PM | -4.40 | 0.01 | -6.25 | 0.02 | -5.87 | 0.03 | -5.77 | 0.21 | -34.94 | 0.71 |
| | 7/15/10 6PM | -4.61 | 0.02 | -6.22 | 0.01 | n.d. | n.d. | n.d. | n.d. | n.d. | n.d. |
| | 7/29/10 2PM | -5.42 | 0.01 | -6.19 | 0.02 | -5.79 | 0.02 | -5.36 | 0.22 | -33.49 | 0.75 |
| | 8/17/10 10AM | -4.91 | 0.03 | -6.23 | 0.01 | -5.93 | 0.02 | -5.43 | 0.21 | -33.66 | 0.76 |
| | 10/10/10 11AM | -6.65 | 0.03 | -6.07 | 0.05 | -5.96 | 0.05 | n.d. | n.d. | n.d. | n.d. |
| | 1/15/11 10AM | -0.79 | 0.04 | -6.37 | 0.19 | n.d. | n.d. | n.d. | n.d. | n.d. | n.d. |
| Rain | 11/13/10 10AM | n.d. | n.d. | n.d. | n.d. | -13.21 | 0.06 | -12.91 | 0.23 | -88.70 | 0.80 |
| Snow | 2/12/11 12PM | n.d. | n.d. | n.d. | n.d. | n.d. | n.d. | -26.26 | 0.23 | -200.40 | 0.84 |

* – measured with Gas Bench II coupled to MAT 253 mass spectrometer integrated with ThermoFinnigan Temperature Conversion Elemental Analyzers (TC/EA) (isotope-ratio mass spectrometry);

** – measured with Picarro® L1102-i Water Isotope Ratio analyzer (cavity ring down spectroscopy).

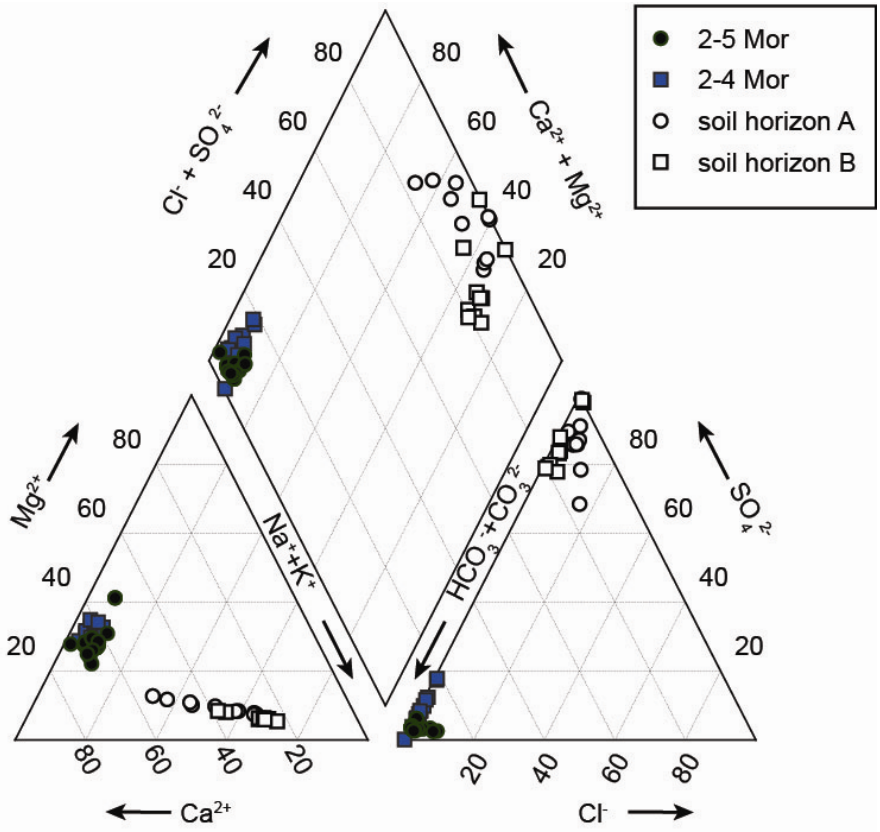


Figure D.1. Piper diagrams of groundwater from the Morrill aquifer and soil water. Groundwater had relatively stable composition with $HCO_3^-$ being the most abundant anion and $Ca^{2+}$ with $Mg^{2+}$ being dominant cations. Points for soil water are plotted along the mixing line between groundwater and bentonite clay with high $Na^+$ and $SO_4^{2-}$ content.

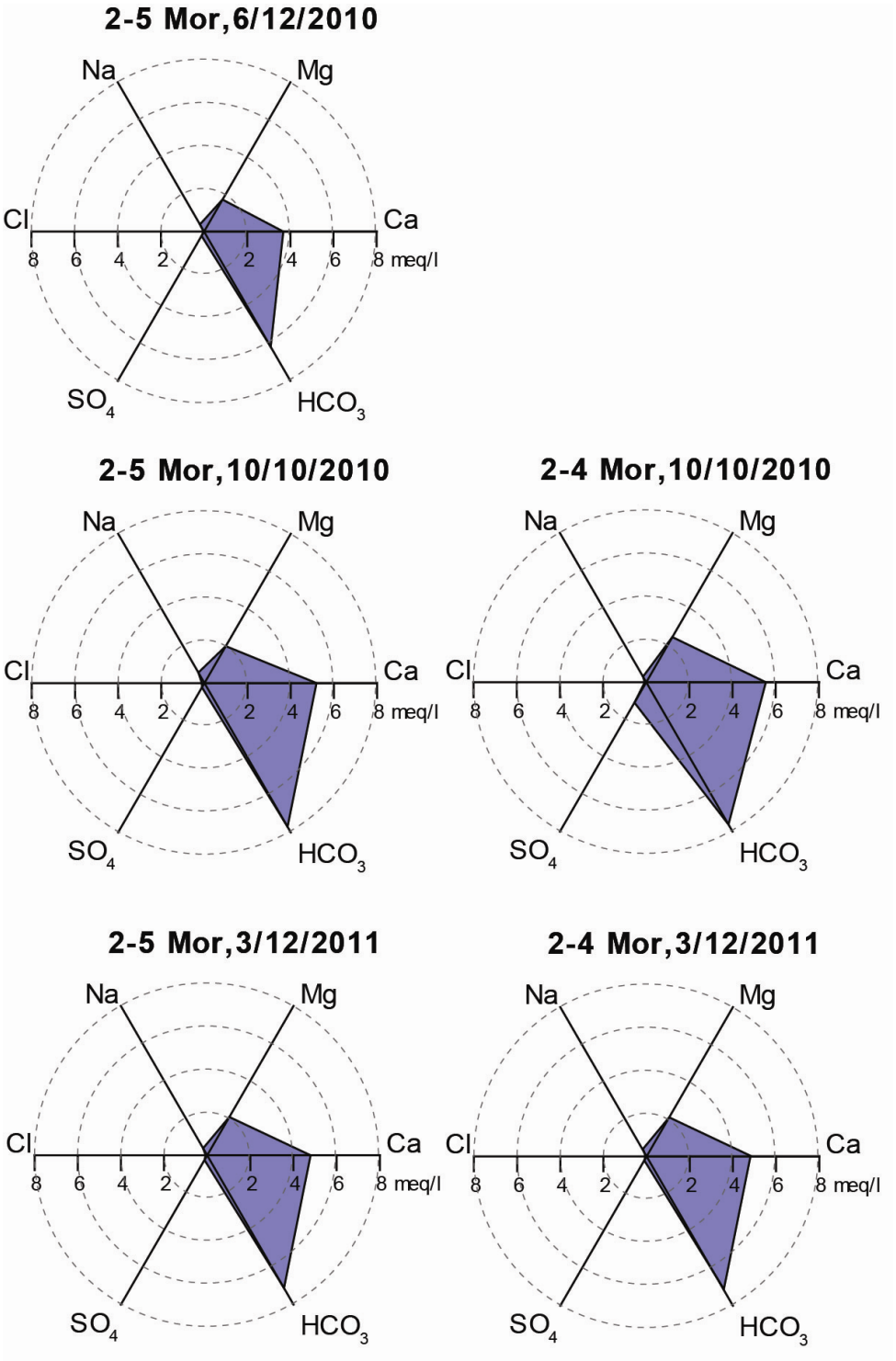


Figure D.2. Radial plots showing seasonal changes in $Ca^{2+}$ and $HCO_3^-$ concentration with the maximum in the late growing season and the minimum in the early spring. Note higher $SO_4^{2-}$ content in 2-4 Mor on 10/10/10.

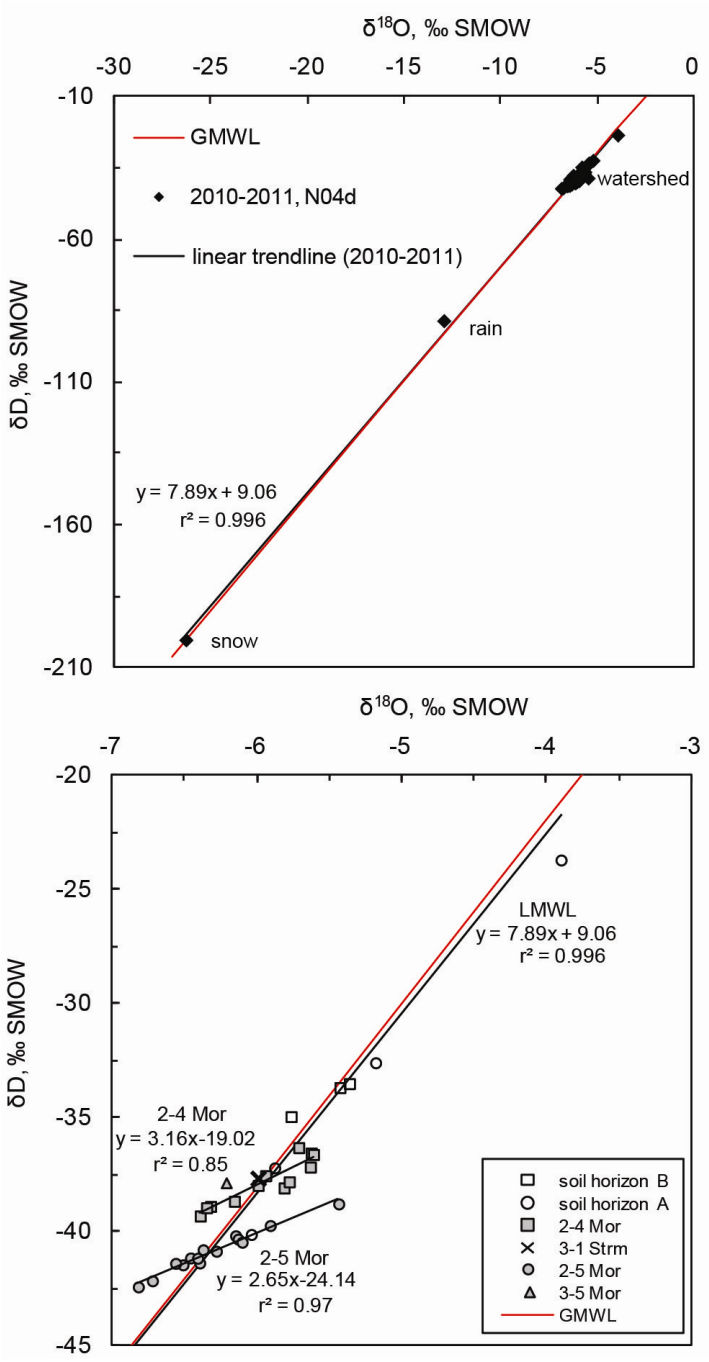


Figure D.3. Stable isotope composition of water collected at N04d watershed (a) and divided into groups (b). Linear trendline for all collected samples is very similar to the Global Meteoric Water Line (GMWL – Craig, 1961), suggesting that meteoric water is the main source of the recharge. Groundwater from 2-4 Mor and 2-5 Mor exhibit analogous deviation from the meteoric water line. 2-4 Mor, as a shallower well, has higher δD and $\delta^{18}O$ and is closely linked to streamwater. Soil water is typically heavier because of the near-surface evaporative effect and varies on a greater range along the LMWL being more sensitive to changes in precipitation composition.

## Appendix E. Soil air $CO_2$

In September 2010, water level in the wells increased following a precipitation event. However there was no change in groundwater chemistry and no dilution was detected during the closest sampling event (Table C.2). This might be explained by recharge of the water with similar chemistry from the lower soil or Lisse effect that represents the water-level increase in a well driven by airflow induced by an advancing wetting front during intensive storm events (Guo et al., 2008). One of the implications of a wetting front is entrapped air that causes the rapid rise of water level. Seasonal water-table fluctuations or water-level elevation due to long-term recharge, as well as capillary fringe rise, can cause groundwater to rise closer to the depth of root respiration or active microbial biodegradation and accumulate $CO_2$.

During the winter, it has been shown that frozen soil or wet snow pack reduces the ability of $CO_2$ to migrate from the unsaturated zone to the atmosphere (Solomon and Cerling, 1987; Sommerfeld et al., 1996), preventing escape of $CO_2$ and thereby increasing $CO_2$ in the saturated zone. However, at the study site constant decrease of $CO_2$ concentration during the winter suggests that the migration of $CO_2$ to the atmosphere was not obstructed by a frozen layer or wet snow pack (Fig. E.1). The winter of 2010-2011 was mild: precipitation in the form of snow was about 40 cm and the snowpack was on the ground for no more than 10 days, with the maximum depth of 13 cm (Ft. Riley).

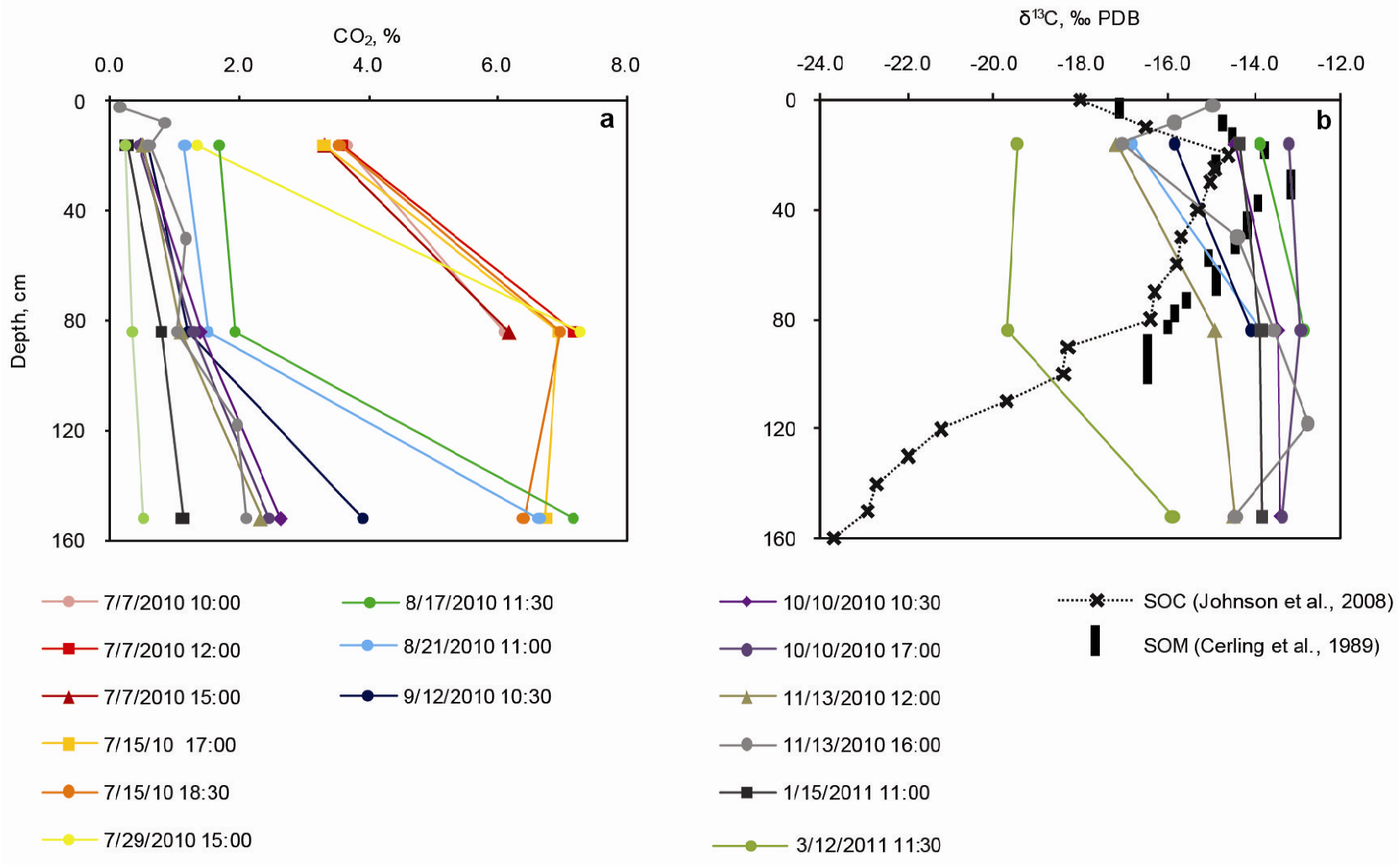


Figure E.1. Variations in (a) soil air $CO_2$ concentration and (b) $\delta^{13}C_{CO2}$ through the vertical profile. There is a downward concentration gradient between soil and groundwater from July until mid-August.

## Soil air pressure and suction

One pressure transducer was submerged in the soil water sampler 84 cm deep with a crack in the ceramic cup in order to monitor changes in the barometric pressure in soil (Fig. E.2) and soil temperature in July of 2010. The sampler pipe was isolated from the atmosphere with a stopper, thus it only communicated with the soil environment.

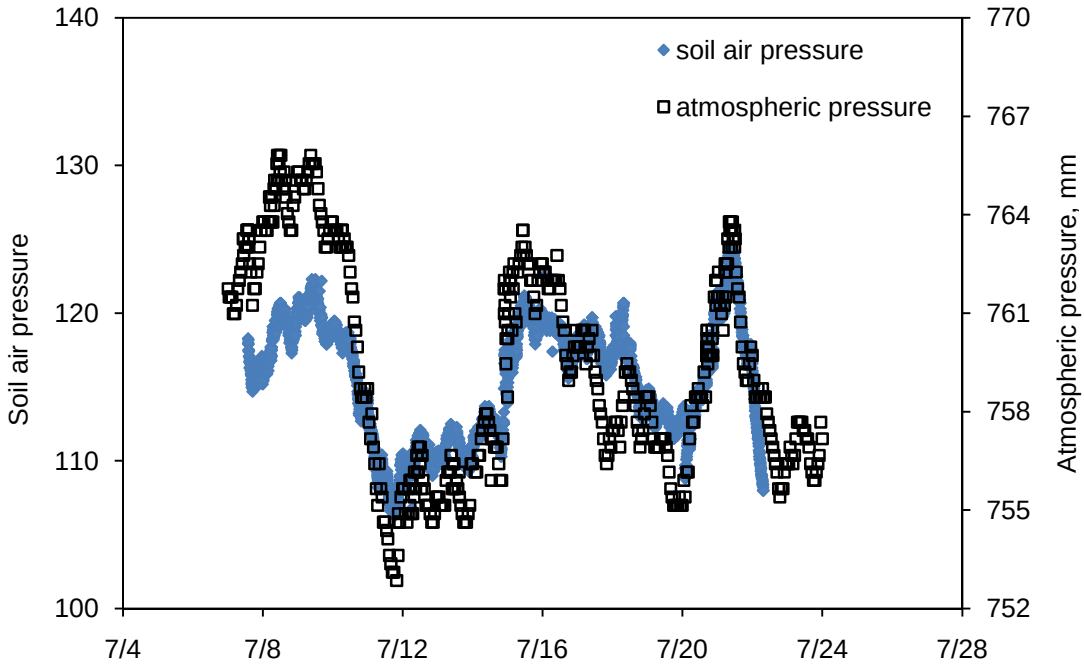


Figure E.2. Soil air pressure at the depth of 50 cm below the surface recorded with pressure transducer shows similar behavior to the atmospheric pressure on a daily scale.

## Appendix F. Carbonate equilibrium and isotopic fractionation

In aquatic systems carbon is present as dissolved organic C (DOC), dissolved inorganic C (DIC), free $CO_2/CH_4$ or particulate organic C (POC) (Dinsmore et al., 2009). DIC consists of four aqueous species: $H_2CO_3$, $CO_{2(aq)}$, $HCO_3^-$, $CO_3^{2-}$ distribution of which is controlled by chemical equilibria with gaseous $CO_2$ and/or carbonate minerals.

Initially, carbon dioxide dissolves in water until equilibrium is reached:

$$CO_{2(g)} \Leftrightarrow CO_{2(aq)}. \quad K_{CO2} = ([CO_2]/pCO_2). \tag{F.1}$$

Aqueous carbon dioxide reacts with water to form carbonic acid:

$$CO_{2(aq)} + H_2O \Leftrightarrow H_2CO_3. \tag{F.2}$$

Eq. (F.1) and Eq. (F.2) are usually combined (Stumm and Morgan, 1996):

$$CO_{2(g)} + H_2O \Leftrightarrow H_2CO_3^* \qquad K_{CO2} = ([H_2CO_3^*] / pCO_2) = 10^{1.47} \tag{F.3}$$

Two steps of carbonic acid association are the following:

$$H^+ + HCO_3^- \Leftrightarrow H_2CO_3^* \qquad K_1 = [H_2CO_3^*] / [HCO_3^-] [H^+] = 10^{6.35} \tag{F.4}$$

$$H^+ + CO_3^{2-} \Leftrightarrow HCO_3^- \qquad K_2 = [HCO_3^-] / [CO_3^{2-}] [H^+] = 10^{10.33} \tag{F.5}$$

Carbonic acid formed in the reaction with $CO_2$ in Eq (F.3) also enhances the dissolution of calcite (Fig. F.1):

$$H_2CO_3 + CaCO_{3(s)} \Leftrightarrow Ca^{2+} + 2HCO_3^-. \tag{F.6}$$

According to the net dissolution reaction

$$CO_{2(g)} + H_2O + CaCO_{3(s)} \Leftrightarrow Ca^{2+} + 2HCO_3^-, \tag{F.7}$$

in the two moles of bicarbonate, one originates from calcite and one from $CO_2$.

The knowledge of accurate pH values in water is required for calculation of carbonate speciation, $pCO_2$, saturation indexes, and carbon isotope fractionation (Fig. F.2). Direct field pH measurements were taken with Fisher Scientific Accumet 1003 pH meter. An estimation of groundwater pH, $pCO_2$ and DIC for 2-5 Mor was made imposing equilibrium with calcite and using measured alkalinity. In PHREEQC Interactive 2.17.4799 (Parkhurst and Appelo, 1999) pH, adjusted to achieve calcite saturation, was used to model carbonate speciation and related chemical reactions. Another estimation of pH was obtained using $pCO_2$ measured for the lowest layer of the soil zone, where $CO_2$ is presumably in equilibrium with shallow groundwater. pH values measured in the lab were approximately 1 unit higher than field / modeled values because of the sample degassing and equilibration with $CO_2$ in the atmosphere. For all methods of

estimating pH, groundwater changed from slightly alkaline values during late non-growing - early growing seasons to neutral and slightly acidic values during the late growing - early non-growing seasons. Due to uncertainty in pH values, the estimation of DIC (based on alkalinity values) has a possible error of up to ±15%.

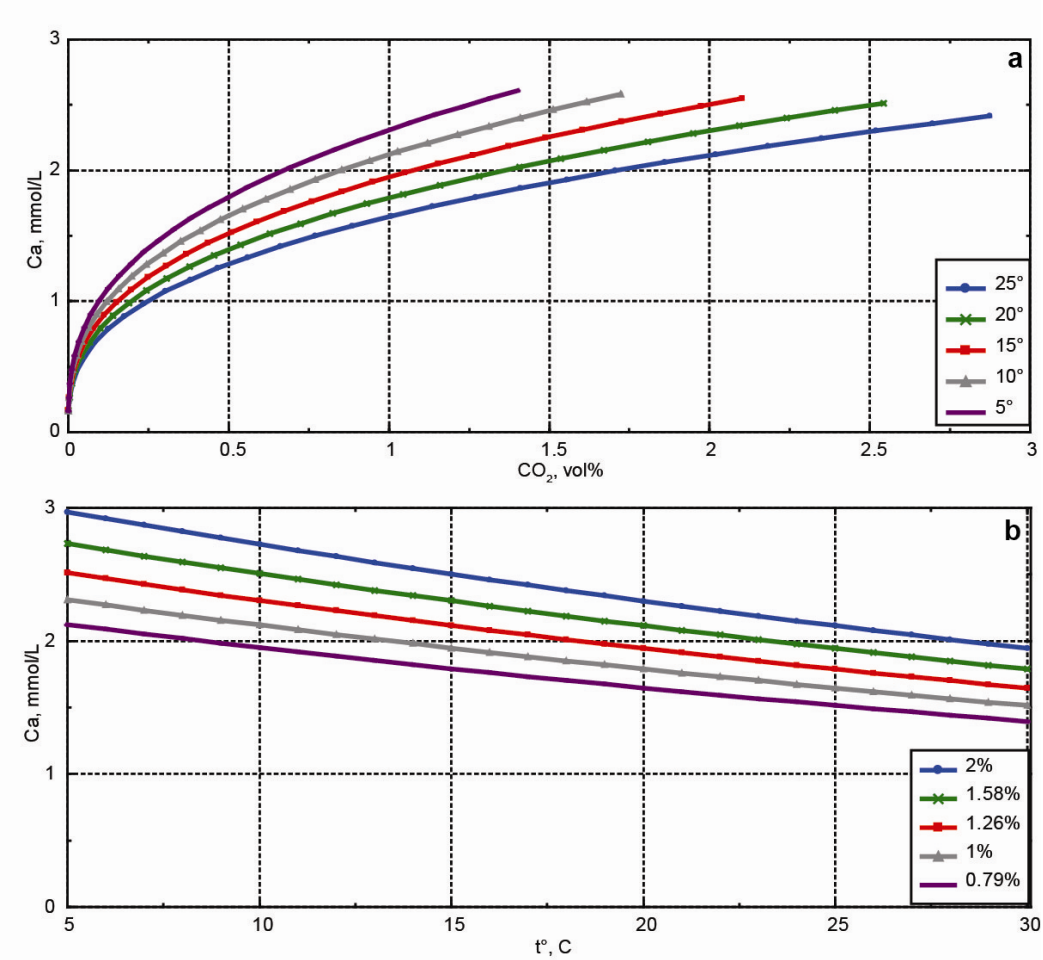


Figure F.1. Equilibrium between calcite and pure water for various temperatures that span the range of likely soil and groundwater temperatures (a) and $CO_2$ spanning the range of measured $CO_2$ at the field site (b), showing the opposite effect of those variables. Calcite saturation is more sensitive to $pCO_2$ than temperature.

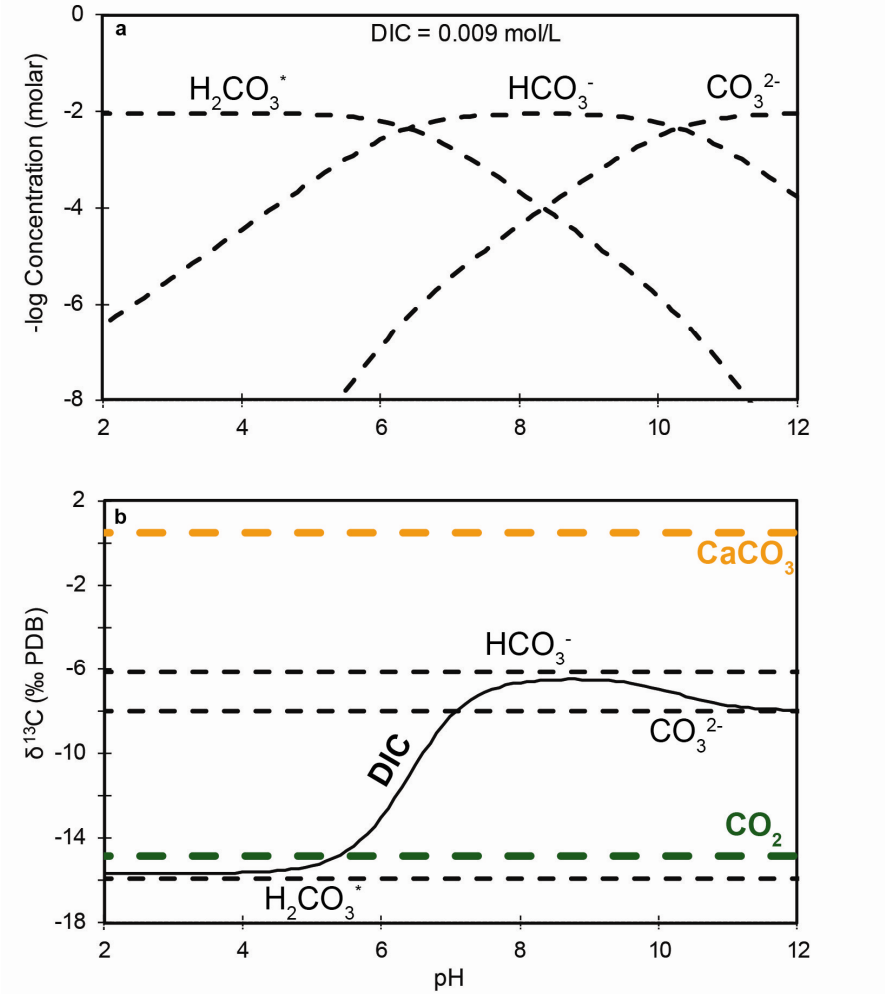


Figure F.2. Calculation of $\delta^{13}C$ of dissolved carbonate species in equilibrium with $CO_2$ gas. First, molar concentration of aqueous species were found for the average measured DIC of 0.009 mol/L (a). Fractionation factors from Clark and Fritz (1997) and initial conditions, $\delta^{13}C_{CO2}$=−14.8‰; t°=+17°C, were then used to predict $\delta^{13}C$ for each of the species (black dashed lines) (b). Resulting curve for DIC summarizes isotopic composition with changing pH, which affects molar fractions of $H_2CO_3$*, $HCO_3^-$, and $CO_3^{2-}$. The composition of $CaCO_3$ is shown for reference, although in an open system, calcite will not alter $\delta^{13}C_{DIC}$.

## Appendix G. Sources of groundwater DIC

Dissolution of the carbonate minerals is the main source of bicarbonate-ion in the aquifer. Sources outside of the aquifer, shown on Figure G.1, include:

1. Downward movement of gaseous $CO_2$, then equilibration with groundwater at the water table in July-August.

2. Soil $CO_2$ or DIC from dissolved pedogenic carbonate with diffuse flow of recharge during the growing season.

3. Recharge from the stream in May-June with net C loss from baseflow.

4. Focused flow following storm events in the growing season; the main effect of such rapid recharge is groundwater dilution.

On Figure G.2, the sampling points can by divided into three groups:

1. A negative trend between $\delta^{13}C_{DIC}$ and alkalinity / $Ca^{2+}$ and heavier carbon isotopes: wells 3-5 Mor, 4-6 Mor, and 3-5-1 Mor, and streamwater.

2. A negative trend between $\delta^{13}C_{DIC}$ and alkalinity / $Ca^{2+}$ and lighter carbon isotopes: well 2-5 Mor.

3. A positive trend between $\delta^{13}C_{DIC}$ and alkalinity / $Ca^{2+}$: well 2-4Mor.

The difference between (1) and (2) is proposed to be the result of different $CO_2$ isotopic composition. Wells 3-5 Mor, 4-6 Mor, 3-5-1 Mor and the stream are situated in or adjacent to the riparian zones, where some $C_3$ woody species are growing along with $C_4$ grasses, while 2-5 Mor is surrounded by $C_4$ grasses only. $C_3$ plants have average $\delta^{13}C$ values about 10–16‰ lower than $C_4$ grasses (O'Leary, 1988) and the contribution of $C_3$ plants to root respiration should make carbon in soil $CO_2$ and, consequently, in DIC lighter (Still et al., 2003). The local character of this link suggests that at least some recharge occurs near the groundwater sampling point.

2-4 Mor is also situated in the riparian zone, and $\delta^{13}C$ values are similar to the group 1. The higher alkalinity is proposed to be the result of oxidation of organic matter with dissolved oxygen of freshly recharged groundwater or by sulphate reduction (Mook, 2000):

$$2CH_2O + SO_4^{2-} = H_2S + 2HCO_3^-.$$

Evidence for this process includes murky water and a rotten smell prior to bailing, and uncharacteristically low measured $SO_4^{2-}$ (Fig. G.4) and high measured alkalinity (11.65 mmol/L), when the well was sampled for the first time after a long break.

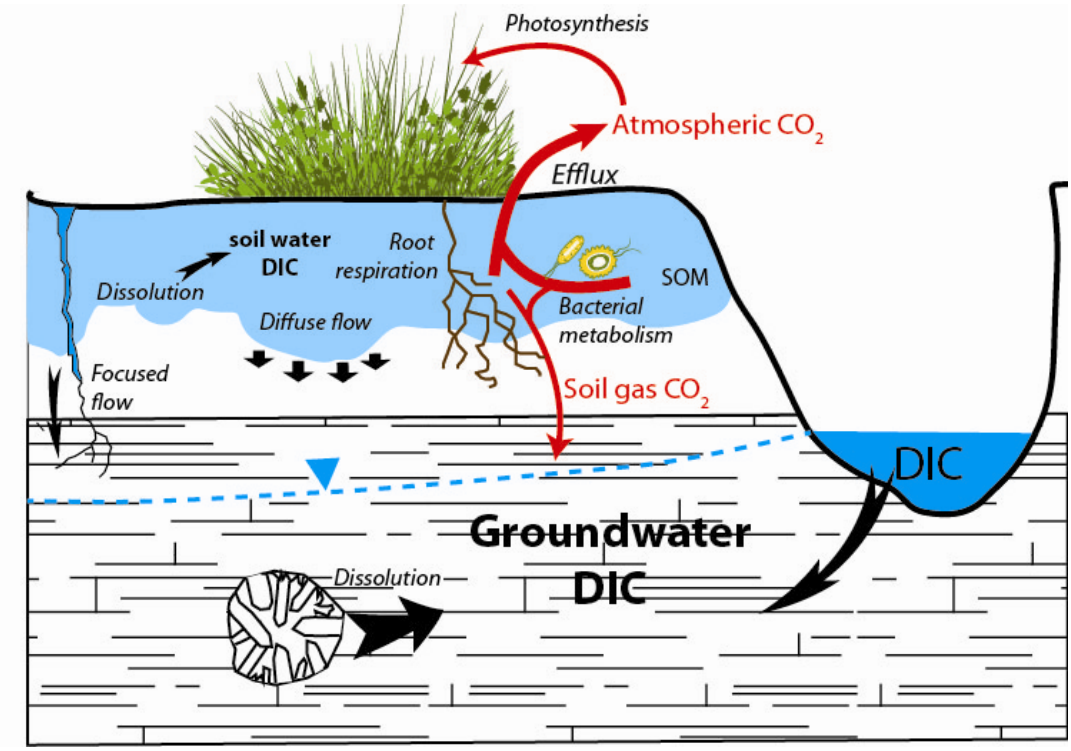


Figure G.1. Fluxes and sources of groundwater DIC in the Morrill aquifer.
Arrows show paths of inorganic carbon in the dissolved (black) or gaseous (red) form.

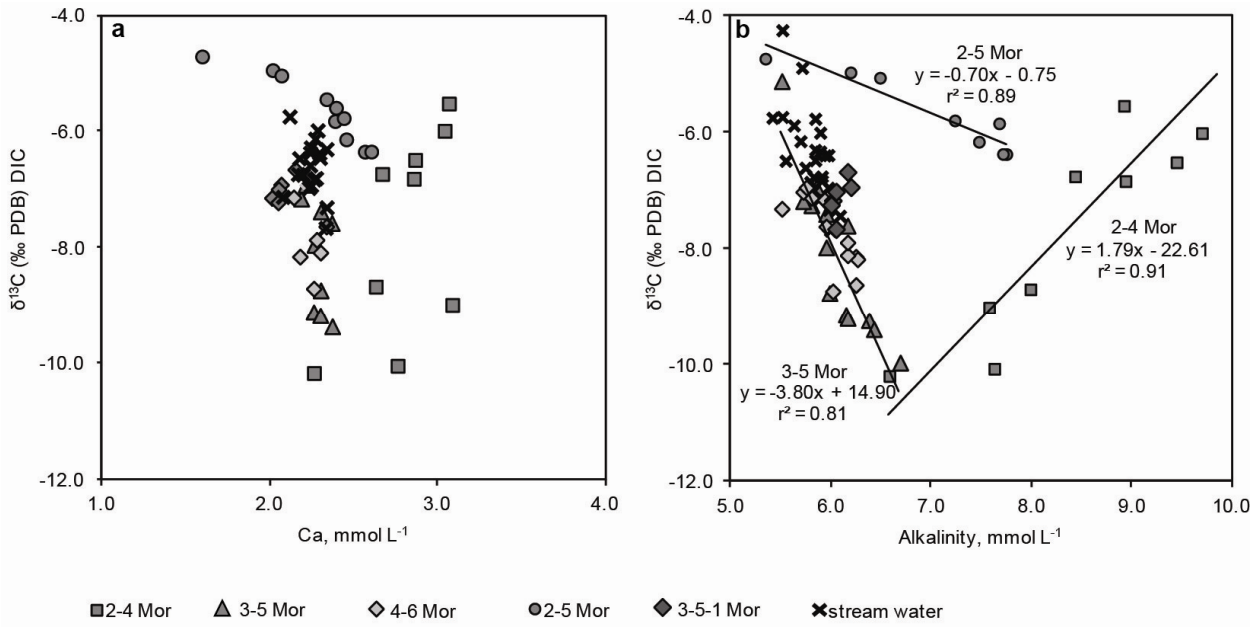


Figure G.2. $\delta^{13}C_{DIC}$ of groundwater and streamwater collected in 2008-2009 (Macpherson, unpublished data) and 2010-2011 (this study) plotted against (a) calcium concentration and (b) alkalinity.

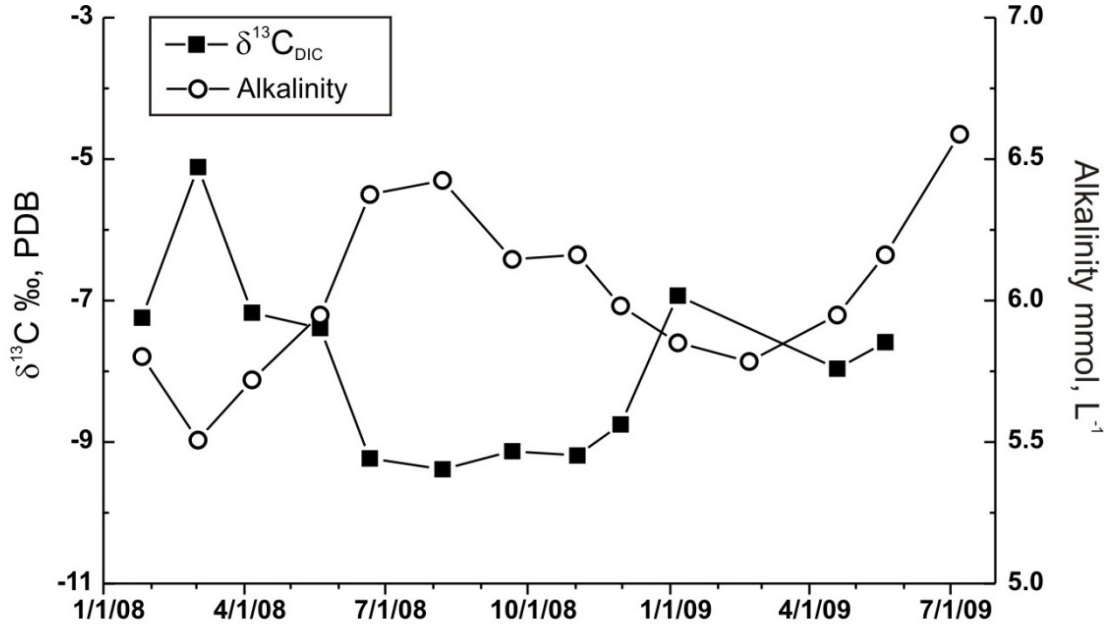


Figure G.3. $\delta^{13}C_{DIC}$ and alkalinity of groundwater from 3-5 Mor collected in 2008-2009 (Macpherson, unpublished data). The peak of alkalinity in the August of 2008 corresponds to lightest $\delta^{13}C_{DIC}$ value, which is in agreement with present study measurements for 2-5 Mor.

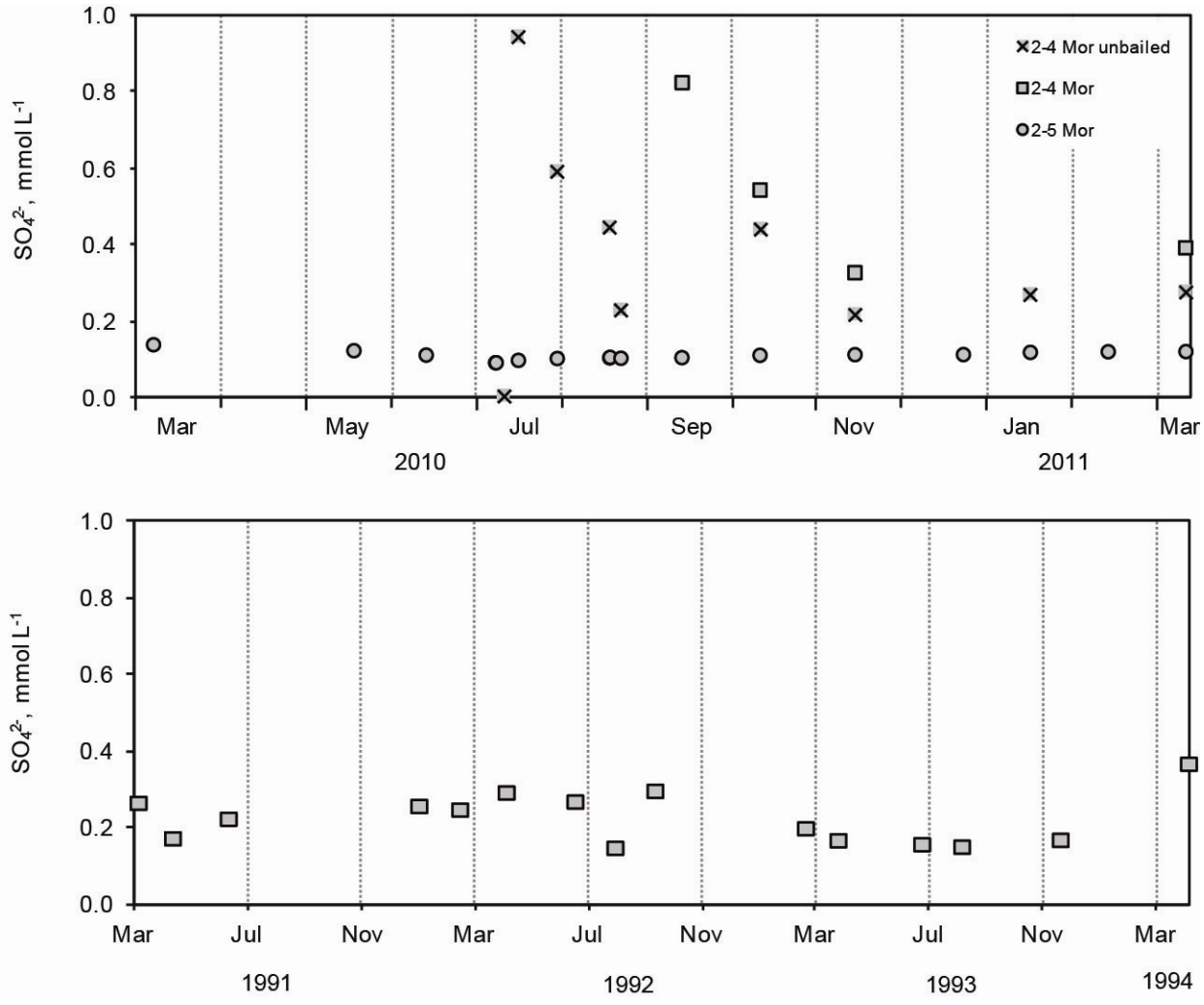


Figure G.4. Concentration of the sulfate ion in the wells 2-4 Mor and 2-5 Mor over the study period (a) and historical data for 2-4 Mor (Macpherson, unpublished data) (b). Note uncharacteristically low $SO_4^{2-}$ content in 2-4 Mor in the early July of 2010 (0.01 mmol/L).

Table G.1. Hypotheses on reasons of increasing belowground $CO_2$ at a tallgrass prairie.

| | **Hypothesis** | **Reference** |
|---|---|---|
| 1 | Increasing groundwater residence time due to drought, that allowing more reaction time between water and limestone, which increases carbonate mineral weathering and produces more DIC | Macpherson et al., 2008 |
| 2 | Increased atmospheric nitrogen loading increases rates of soil organic matter breakdown, thereby increasing the soil $CO_2$ that drives increased weathering | Macpherson et al., 2008 |
| 3 | Reforestation of prairie areas, that increases $CO_2$ production in the soil zone | Liu et el., 2008, Huff, 2009 |
| 4 | Increasing mean air temperature could stimulate organic matter decomposition, increasing soil respiration and soil $CO_2$ | Bond-Lamberty and Thomson, 2010; Davidson and Janssens, 2006; Macpherson et al., 2008 |

## References


Bond-Lamberty, B., Thomson, A., 2010. Temperature-associated increases in the global soil respiration record. Nature 464, 579-582.

Cerling, T.E., Quade, J., Wang, Y., Bowman, J.R., 1989. Carbon isotopes in soils and palaeosols as ecology and palaeoecology indicators. Nature 341, 138-139.

Clark, I., Fritz, P., 1997. Environmental Isotopes in Hydrogeology. Lewis Publishers, Boca Raton.

Cochran, P.H., Marion, G.M., Leaf, A.L., 1970. Variations in Tension Lysimeter Leachate Volumes. Soil Sci. Soc. Am. J. 34, 309-311.

Craig, H., 1961. Isotopic Variations in Meteoric Waters. Science 133, 1702-1703.

Davidson, E.A., Janssens, I.A., 2006. Temperature sensitivity of soil carbon decomposition and feedbacks to climate change. Nature 440, 165-173.

Dinsmore, K.J., Billett, M.F., Moore, T.R., 2009. Transfer of carbon dioxide and methane through the soil-water-atmosphere system at Mer Bleue peatland, Canada. Hydrological Processes 23, 330-341.

Guo, H., Jiao, J.J., Weeks, E.P., 2008. Rain-induced subsurface airflow and Lisse effect. Water Resour. Res. 44, W07409.

Hayden, B., 1998. Regional climate and the distribution of tallgrass prairie, in: Knapp, A.K., Briggs, J.M., Hartnett, D.C., Collins, S.L. (Eds.), Grassland Dynamics—Long-Term Ecological Research in Tallgrass Prairie Oxford University Press, New York, pp. 19–34.

Huff, B.L., 2009. Reforestation or response to rising atmospheric $CO_2$: investigating two possible mechanisms for the increase in groundwater $CO_2$ at the Konza Prairie, Northeastern Kansas, Geological Society of America Abstracts with Programs, p. 664.

Johnson, W.C., Willey, K.L., Macpherson, G.L., 2007. Carbon isotope variation in modern soils of the tallgrass prairie: Analogues for the interpretation of isotopic records derived from paleosols. Quaternary International 162-163, 3-20.

Lamb, H.H., 1972. Climate: Present, Past and Future. Vol. 1: Fundamentals and Climate Now. Methuen, London.

Litaor, M.I., 1988. Review of soil solution samplers. Water Resour. Res. 24, 727-733.

Liu, Z., Dreybrodt, W., Wang, H., 2008. A possible important $CO_2$ sink by the global water cycle. Chinese Science Bulletin 53, 402-407.

Macpherson, G.L., 1996. Hydrogeology of thin limestones: the Konza Prairie Long-Term Ecological Research Site, Northeastern Kansas. Journal of Hydrology 186, 191-228.

Mook, W.G., 2000. Environmental isotopes in the hydrological cycle principles and applications, Vol. I: Introduction - Theory, Methods, Review. UNESCO/IAEA, Paris.

O'Leary, M.H., 1988. Carbon Isotopes in Photosynthesis. BioScience 38, 328-336.

Parkhurst, D.L., Appelo, C.A.J., 1999. User's guide to PHREEQC (Version 2)—A computer program for speciation, batch-reaction, one-dimensional transport, and inverse geochemical calculations: U.S. Geological Survey Water-Resources Investigations Report 99-4259, p. 310.

Pomes, M.L., 1995. A study of the aquatic humic substances and hydrogeology in a prairie watershed, use of humic material as a tracer of recharge through soils. Ph.D. thesis, University of Kansas, p. 296.

Schulmeister, M.K., Butler, J.J., Healey, J.M., Zheng, L., Wysocki, D.A., McCall, G.W., 2003. Direct-Push Electrical Conductivity Logging for High-Resolution Hydrostratigraphic Characterization. Ground Water Monitoring & Remediation 23, 52-62.

Solomon, D.K., Cerling, T.E., 1987. The annual carbon dioxide cycle in a montane soil: Observations, modeling, and implications for weathering. Water Resour. Res. 23, 2257-2265.

Sommerfeld, R.A., Massman, W.J., Musselman, R.C., Mosier, A.R., 1996. Diffusional flux of $CO_2$ through snow: Spatial and temporal variability among alpine-subalpine sites. Global Biogeochem. Cycles 10, 473-482.

Still, C.J., Berry, J.A., Ribas-Carbo, M., Helliker, B.R., 2003. The contribution of $C_3$ and $C_4$ plants to the carbon cycle of a tallgrass prairie: an isotopic approach. Oecologia 136, 347-359.

Stumm, W., Morgan, J.J., 1995. Aquatic Chemistry: Chemical Equilibria and Rates in Natural Waters. Wiley-Interscience, New York.

Wehmueller, W.A., Campbell, H.V., Hamilton, V.L., Graber, S.P., 2005. Soil survey of Geary County, Kansas: U.S. Dept. of Agriculture, Natural Resources Conservation Service, p. 230.

Winston, R.B., 2000. Graphical User Interface for MODFLOW, Version 4: U.S. Geological Survey Open-File Report 00-315, p. 27.

Zeller, D.E., ed., 1968. The stratigraphic succession in Kansas: Kansas Geol. Survey Bull. 189, p. 81.

USDA-NRCS, 2007. U.S. Department of Agriculture, National Resources Conservation Service (USDA-NRCS) http://websoilsurvey.nrcs.usda.gov/app/WebSoilSurvey.aspx.